LARS Technical Report 053183

SPECTRAL CHARACTERIZATION OF IRON OXIDE AND ORGANIC MATTER IN ERODED SOILS

S. E. Pazar
G. E. VanScoyoc
R. A. Weismiller
M. F. Baumgardner

Agronomy Department
Laboratory for Applications of Remote Sensing
Purdue University
West Lafayette, Indiana 47907 USA

May 1983

Pages i-iv are blanks

TABLE OF CONTENTS

LIST OF TABLES

LIST OF FIGURES

ABSTRACT

Recent advances in providing spectral reflectance data of soils indicate that remote sensing techniques may be an excellent tool for delineating and monitoring soil erosion. The accurate classification of multispectral data requires that the classes of interest be spectrally, or otherwise separable. The goal of classifying soil erosion rests on our ability to define and understand the nature and degree of separability between classes of erosion. The results of previous research efforts are testimony to the extreme complexity of the interactions of many variables in determining a soil's reflectance characteristics. This complexity within soils themselves coupled with the often localized nature of soil erosion makes the accurate delineation of eroded areas with remote sensing techniques a challenging objective.

The study of simulated erosion profiles has lead to the development of an approach for examining the relationship between soil reflectance properties and erosion. The most important factors affecting the spectral response of soils in this study appear to be

iron oxide and organic matter contents. The interactions of these two factors within an eroded soil has a significant effect on the shape of the overall spectral response, and thus determines the degree of separability between erosion classes.

The following equations are proposed as a model to predict iron oxide and organic matter contents from soil reflectance.

$$\% \, Fe_2O_3 = b_1(R_{560}) + b_2(R_{485})$$

$$\% \, OM = b_3(R_{660}P + b_4[b_1(R_{560}) + b_2(R_{485})]$$

where:

$b_1 = 0.2690$

$b_2 = -0.2924$

$b_3 = 0.0768$

$b_4 = -1.4786$

R_{485} = Reflectance at 485 nm

R_{560} = Reflectance at 560 nm

R_{660} = Reflectance at 660 nm

Testing this model on naturally eroded soil and soil samples simulating erosion classes resulted in r^2 values of 0.94 for organic matter, 0.96 for iron oxide, and 0.92 for organic matter/iron oxide ratio prediction. This degree of accuracy confirms the view that classes of soil erosion are spectrally separable, and that the separability is significant for the soils examined. To truly assess the significance and applicability of this result, it must be tested in a field mapping study of soil erosion with remote sensing techniques.

INTRODUCTION

Soil is a finite natural resource. Protection of this resource from degradation is essential for the maintenance of its productive capacity. New scientific agricultural methods and technologies have enabled man to produce unprecedented amounts of food and fiber. However, while fertilizers, pesticides, and improved crop varieties have extended the limits of soil productivity they have also masked damage to the land. Soil degradation in the form of accelerated soil erosion threatens our ability to sustain the productive capacity of our soil resource.

Many approaches to the study of soil erosion have been developed in an effort to provide quantitative information on the cost of erosion. The Universal Soil Loss Equation is one tool which has proved very useful for erosion prediction and conservation design (Morgan, 1980). Several methods of mapping soil erosion to help evaluate erosion risks have also been developed. One problem, however, is that few of these mapping surveys contain any data on measured rates of soil loss (Morgan, 1978). Recent advances in providing multispectral scanner data on soils has prompted questions regarding the use of remote sensing in the mapping of soil erosion. Can remote sensing technology provide the researcher and land manager with quantitative information on soil erosion?

A consensus on questions involving soil erosion and remote sensing is not easily reported. The complexity within the soil itself, coupled with the variability of soil erosion, makes generalizations about the spectral response of eroded soils almost meaningless. Remote sensing is often viewed in a global perspective, but soil spectral responses and soil erosion are both localized phenomena and must be studied as such.

How then, using the knowledge already at hand about remote sensing, the spectral reflectance of soils, and soil erosion, can these interactions be studied so that meaningful results may be put to use?

The answer may lie in an approach described by Young (1978). He suggests we be less ambitious with respect to scale in mapping soil erosion, and prefers a practice employed in Yugoslavia and the United Kingdom. "Go to where the erosion is, and find out why it is there." He goes on to say that from studies of this kind, areas of high erosion risk can be identified.

A similar approach could be developed to implement remote sensing techniques. Go to where erosion is, and find out why a soil has a particular spectral response. By studying the complex interactions within an eroded soil, or group of soils, we may learn how to identify characteristics of eroded soils through their multispectral responses. Detailed study of eroded soils will provide answers to the questions of whether or not, and to what degree, soils are spectrally separable. Only from this basic information can one assess the ultimate goal of accurately delineating, monitoring, and quantifying soil erosion with remote sensing techniques.

The research presented in this thesis will seek to establish the feasibility of, and examine methods for, the following:

1.) determination of the optimal spectral bands for erosion studies of a soil, or soils.

2.) development of methods for defining the interaction of organic matter and iron oxides in the visible and near infrared wavelengths.

3.) formation of a soil erosion model to be applied to remotely sensed data for quantitatively delineating stages and monitoring rates of erosion.

In addition to the general objectives above a similar evaluation will be made on the use of the Cary spectrophotometer for the following:

1.) use of the Cary spectrophotometer in soil reflectance studies.

2.) evaluation of the second derivative of the spectral response as a tool for studying and/or quantifying a soil's reflectance with its physiochemical properties.

LITERATURE REVIEW

Iron Oxide

The types and distribution of iron oxides or hydroxides within a soil profile determines the color of many soils (Schwertmann and Taylor, 1977). Goethite ($\alpha FeOOH$) and hematite (αFe_2O_3) are the most common forms of iron oxides occurring in soils and both have high pigmenting power even at low concentrations.

Schwertmann and Taylor (1977) present an excellent discussion of the chemical and physical properties of iron oxides in the soil environment. Geothite is reported as having the greatest thermodynamic stability under most soil conditions and as being responsible for the yellowish-brown color in soils. High concentrations of geothite may assume dark brown or even black colors. Synthetic geothite usually has an acircular structure while in soils its needle-like crystals are often poorly developed.

Hematite is the second most frequently occurring iron oxide and is associated with goethite in many reddish soils. The pigmenting effect of hematite is greater than that of geothite in that even low concentrations will change the hue of geothitic soils to 5YR or redder. The structure of hematite in soils is usually weakly expressed as crystal plates of a hexagonal shape.

The influence of climate on the types of iron oxides formed is discussed by Schwertmann and Taylor (1977). In general warm climates favor hematite formation but hematite and goethite are found closely associated in many regions with goethite located in wetter and/or cooler areas. Hematite formation is inhibited by high concentrations of organic compounds which complex iron as it is released via weathering of primary rocks. This complexation prevents the formation of ferrihydrite, which is a necessary precursor of hematite, and thus results in geothite formation. If ferrihydrite is formed low temperatures suppress its dehydration which favors transformation of ferrihydrite via solution to goethite. Ferrihydrite and eventually hematite, will form over goethite in areas where the amount of organic matter available to complex with iron is limited. High temperatureas then accelerate the dehydration of ferrihydrite to hematite (Torrent et al., 1980). These results concerning the formation of goethite and hematite are generally accepted and confirmed in studies by Walker (1967), Schwertmann (1971), Davey et al. (1975), Duchaufour and Souchier (1978), and Torrent et al. (1980). In addition to climate and organic matter influencing the formation of iron oxides other factors such as aluminum substitution have been noted to change their structure and color (Davey et al. (1975), Konama and Schnitzer (1977), Torrent et al. (1980)).

The color imparted to a material, such as iron oxide, in the visible range of the spectrum may be due to specific absorptions in this region, or intense absorptions in the ultraviolet and/or near-infrared regions (Hunt and Salisbury, 1970). For iron oxides these

absorptions are the result of electron transitions within the unfilled d-orbitals of the iron ions. The theoretical explanation for these effects has been established through crystal or ligand field theory (Ballhausen, 1962; McClure, 1959; and Burns, 1970). White and Keester (1966), and Burns (1970) provide excellent discussions of crystal field theory and use it to predict and explain the absorption bands of iron ions.

Although the iron in soil iron oxide is found in the ferric (Fe^{3+}) state a review of the literature concerning both ferric and ferrous (Fe^{2+}) iron absorption is presented as much of the early work discussed both forms. Also agreement concerning the absorption properties of ferric iron is relatively recent compared with that of ferrous iron and this recent data warrants detailed review.

An early study by McClure (1962), as reported by Lehmann and Harder (1970), presented polarized absorption spectra of ferric iron but the absorption bands within the spectra were too weak to be accurately assigned to specific electron transitions. White and Keester (1966) studied crystals containing ferrous and ferric iron and correlated absorption bands with the form of iron found in the sample. Ferrous iron gave rise to a single intense absorption band at 1100 nm while the spectrum of ferric iron was poorly explained due to the weak expressions of its absorption bands. In this report the diffuse reflectance spectra of finely ground mineral powders were also presented. The slight absorption in epidote at approximately 600 nm (Figure 1) was attributed to the ferric ion while the more intense absorption band at 1100 nm was attributed to ferrous iron. Ferrous iron absorption also predominates the spectra

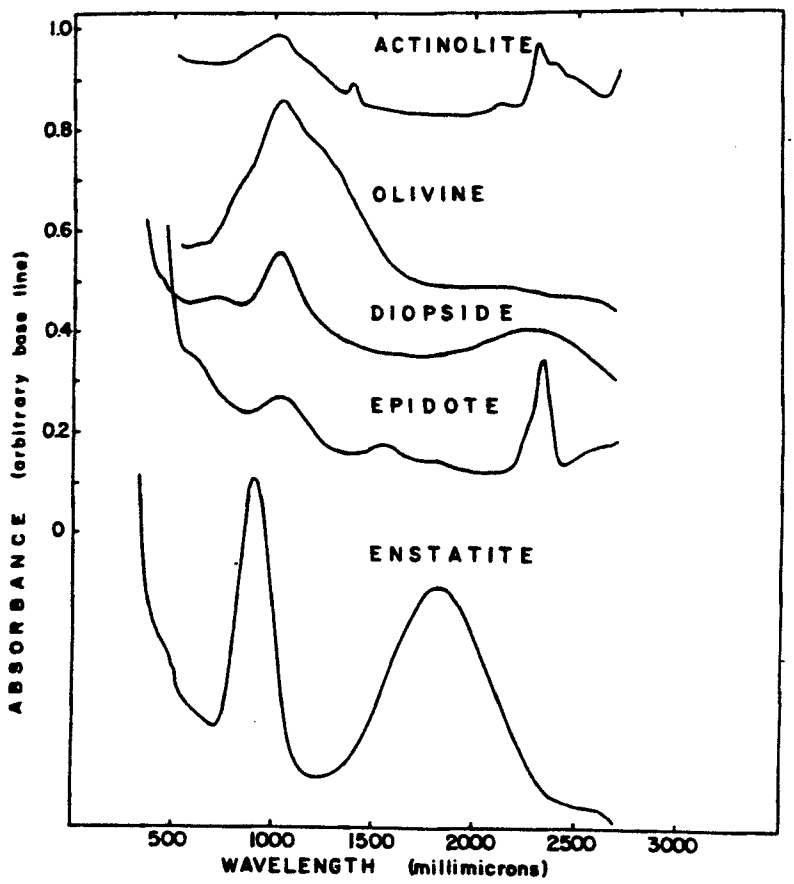

Figure 1. Diffuse reflectance spectra of iron-containing silicate minerals at 300°K, (from White and Keester, 1966).

of the other iron containing silicate minerals studied (Figure 1).

In the early 1970's several researchers investigated the optical spectra of ferric and ferrous iron (Lehmann and Harder, 1970; Burns, 1970; Faye, 1971; and Lehmann, 1971). All of these writings present results which indicate the presence of relatively weak ferric absorption bands in the near-infrared region while the sharpest bands occur in the 300-600 nm wavelength region. Typical examples are the spectra for ferric and ferrous iron presented by Burns (1970)). The polarized absorption spectra of epidote which contains 0.8864 Fe^{3+} ions per formula unit is presented in Figure 2. The inset is the spectrum of iron (III) in ferric ammonium sulphate solution and is characterized by broad absorption bands at approximately 550 and 800 nm, and sharper absorption peaks at approximately 400 and 430 nm. By comparison the absorption spectrum of aqueous Fe^{2+} in a solution of iron (II) ammonium sulphate (Figure 3) shows a strong absorption at 1000 nm due to the ferrous ion. Note that the scale on the y-axis of the ferrous plot indicated a higher magnitude of absorption for ferrous iron. These spectra illustrate the range of absorption levels which occur in the visible and near-infrared wavelength regions for ferric and ferrous iron.

In addition to studies of the optical properties of iron ions of various crystals several researchers have examined goethite and hematite iron oxides (Hunt and Salisbury, 1970; Hunt, Salisbury and Lenhoff, 1971; and Marusak, Messier and White, 1980).

Hunt, Salisbury and Lenhoff (1971) recorded the spectra of mineral and rock samples using a Cary 14 spectrophotometer fitted with a specially constructed bi-directional reflectance attachment.

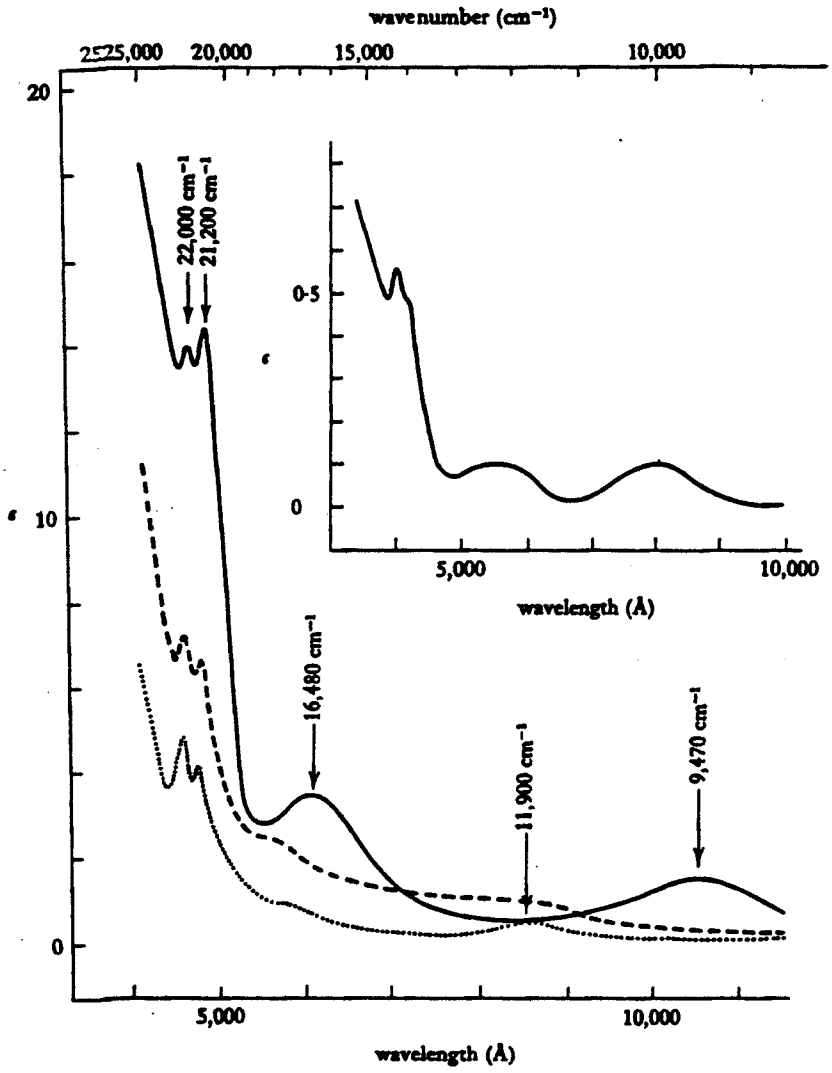

Figure 2. Polarized absorption spectra of epidote .... α spectrum; ---- β spectrum; —— γ spectrum. The epidote contains 0.864 Fe^{3+} ions per formula unit (optic orientation: α : c = 10°; β = b; γ : a = 35°). Inset: absorption spectrum of iron (III) in ferric ammonium sulphate solution, (from Burns, 1970).

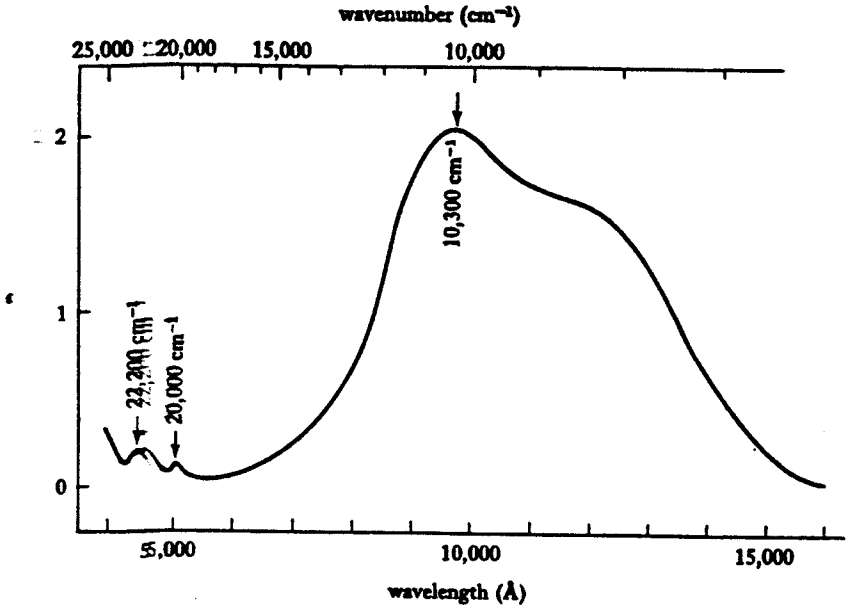

Figure 3. Absorption spectrum of the aqueous Fe^{2+} ion in a solution of iron (II) ammonium sulphate, (from Burns, 1970).

Percent reflection relative to a magnesium oxide standard was measured. Four spectra each of goethite and hematite of various size fractions are presented in Figures 4, 5 and 6.

The explanations for the features of these spectra are described by Hunt and Salisbury (1970) and are interpreted from the writings of White and Keester (1966, 1967). In particular Hunt and Salisbury note that the spectrum of ferric iron is less well known than that of ferrous iron but that White and Keester did assign five absorption bands for ferric iron in chlorite. These bands are all transitions from the $^6A_{1g}$ ground state to $^4T_{1g}$ at ~0.87μ; to $^4T_{2g}$ at ~0.7μ (this is noted as the strongest Fe^{3+} band); to A_{2g} and $^2T_{1g}$ at ~0.49μ and 0.45μ; and to either the $^4A_{1g}$ or ^4E_g level at about 0.4μ. It may be noted that the diffuse reflectance spectrum of the chlorite sample was not obtained by White and Keester (1966) and therefore was unavailable for comparison in Figure 1. However, from these assignments Hunt, Salisbury, and Lenhoff explained the reflectance changes which occurred in the spectra of goethite and hematite. The ferric ion was described as producing a feature near 0.9 μ and a fall-off short of 0.55μ due to the presence of a conduction band with a quite well resolved absorption edge. The absence of the "strongest" absorption band, as reported by White and Keester (1966), at ~0.7μ was not discussed.

Hunt et al. (1971) also present three spectra of Limonite ($2Fe_2O_3 \cdot 3H_2O$) (Figure 6). Limonite is described as a poorly characterized ferric oxide material with a typical water content of 12-14% by weight. The band near 0.9μ is reportedly due to ferric iron while the bands at 1.4μ and 1.9μ arise from water of hydration

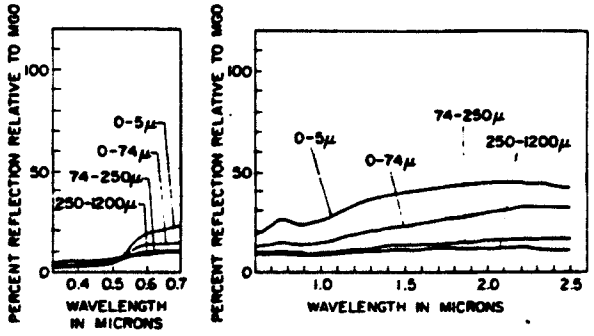

Figure 4. Spectral reflectance of Goethite 36 Biwabik, Minn. (from Hunt et al., 1971).

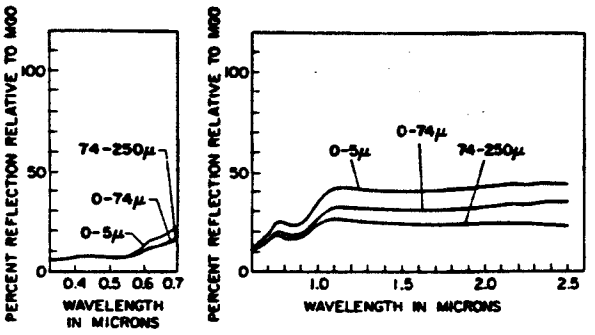

Figure 5. Spectral reflectance of Hematite 45 Irontown, Minn. (from Hunt et al., 1971).

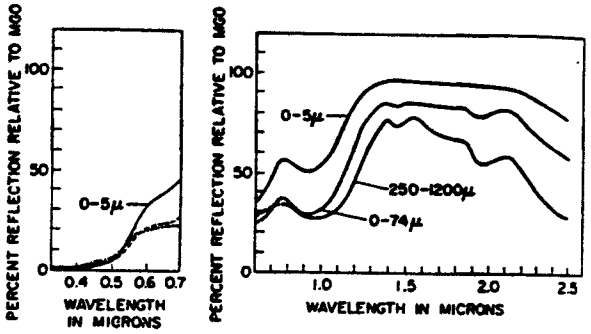

Figure 6. Spectral reflectance of Limonite 41 Tuscaloosa Co., Alabama, (from Hunt et al., 1971).

and are quite clear at the larger particle sizes. It should be noted that the intensity of the ferric iron band does not diminish with increased particle size as is the case for the unhydrated oxides shown in the goethite and hematite spectra. This lack of decreased intensity, and slight shift in the 250-1200μ size fraction spectrum to a higher wavelength, at ~0.9μ to 1.0μ may be due to the influence of absorption bands for the water molecule at 0.942μ and 1.135μ. This possibility was not discussed by Hunt et al. (1971) who attributed the apparently more highly resolved features to a more transparent sample.

In their report on the optical absorption spectra of hematite Marusak, Messier and White (1980) review the previous works and optical transition assignments of Bailey (1960), Tandon and Gupta (1970), and Tossel et al. (1973). Table 1 summarized the transitions and assignments reported by various researchers as well as the calculated transitions obtained from energy-level diagrams as presented by Marusak et al. (1980).

The optical absorption spectrum of hematite (Marusak et al., 1980) (Figure 7), can be divided into three regions. The bands at ~12000, 16670 and 18690 cm^{-1} arise from spin-forbidden ligand or crystal field transformations and have been reported by Bailey (1960), and Tandon and Gupta (1970). The bands at 20408 and 23800 cm^{-1} are considered to arise from spin-flip transitions among the $2t_g$ and $3e_g$ states. The bands at 26670, 31750, 38900, and 44840 cm^{-1} arise from O^{2-} to Fe^{3+} charge transfers between the 02p nonbonding orbitals and the $2t_{2g}$ and/or $3e_g$ orbitals. Agreements between the observed bands and those calculated by Tossell et al.

Table 1. Observed transitions and assignments of the absorption bands in αFe_2O_3 (from Marusak et al., 1980).

This work (cm^{-1})	Calculated (Tossell)	Assignment	Tandon & Gupta	Bailey
11,560		$^6A_1 \rightarrow {}^4A_2$ (11,580)	11,630	12,000
12,900		$^6A_1 \rightarrow {}^4E$ (11,850)		
16,670		$^6A_1 \rightarrow {}^4A_1$ (16,100)		16,000
18,690		$^6A_1 \rightarrow {}^4E$ (18,530)		18,250
20,408	21,050	$2t_{2g}^{\uparrow} \rightarrow 2t_{2g}^{\downarrow}$	21,500	
23,800	24,040	$3e_g^{\uparrow} \rightarrow 3e_g^{\downarrow}$		24,500
26,670	25,330	$6t_{1u}^{\downarrow} \rightarrow 2t_{2g}^{\downarrow}$		
31,750	29,380	$1t_{1u}^{\downarrow} \rightarrow 2t_{2g}^{\downarrow}$	28,570	
38,900	35,750	$1t_{1g}^{\downarrow} \rightarrow 3e_g^{\downarrow}$	34,480	
44,840	42,860	$6t_{1u}^{\downarrow} \rightarrow 3e_g^{\downarrow}$	43,290	

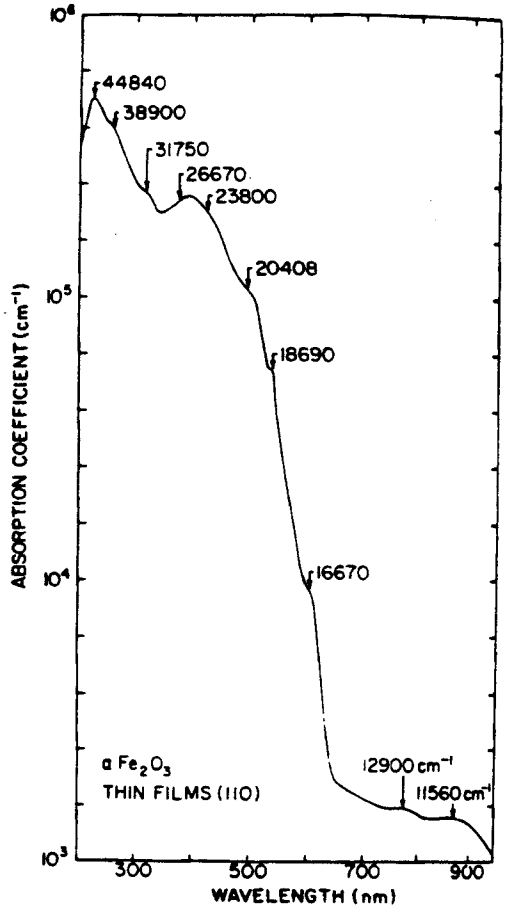

Figure 7. Absorption coefficient as a function of wavelength for αFe_2O_3 at 298 K, (from Marusak et al., 1980).

(1973) (Table 1), are excellent. From this data Marusak et al. (1980) attribute the strong absorbing characteristics of hematite in the visible and ultraviolet regions of the optical spectrum to allowed transitions which are either spin flip or charge transfer in origin, and place little emphasis on spin-forbidden ligand field transformations in determining the color of hematite.

Although no attempt was made to assign transitions to absorption bands Bryant (1981) obtained diffuse reflectance spectra of goethite and hematite samples. The spectra were recorded on a Cary 17D spectrophotometer in the range from 380 to 800 nm relative to a magnesium carbonate standard (Figure 8). Since no strict moisture equilibration was attempted Bryant (1981) accounted for variation in moisture content by normalizing the spectra of hematite-geothite mixutres at a point of minimal absorption (800 nm). With the exception of the 100% hematite or goethite samples there was a regular increase in absorption near 480 nm with increasing goethite content and near 565 nm with increasing hematite content. A comparison of the spectra of these mixutres with those of soil samples showed that the absorptions were much less distinct in a natural soil system.

The effects of iron oxides on the spectral reflectance properties of natural soil samples has been observed in several early studies (Obukhov and Orlov (1964); Orlov et al. (1966); Karmanov and Rozhkov (1972); Mathews et al. (1973); and Leger et al. (1979)).

Obukhov and Orlov (1964) determined that iron oxides were responsible for the hue of soils and produce a characteristic

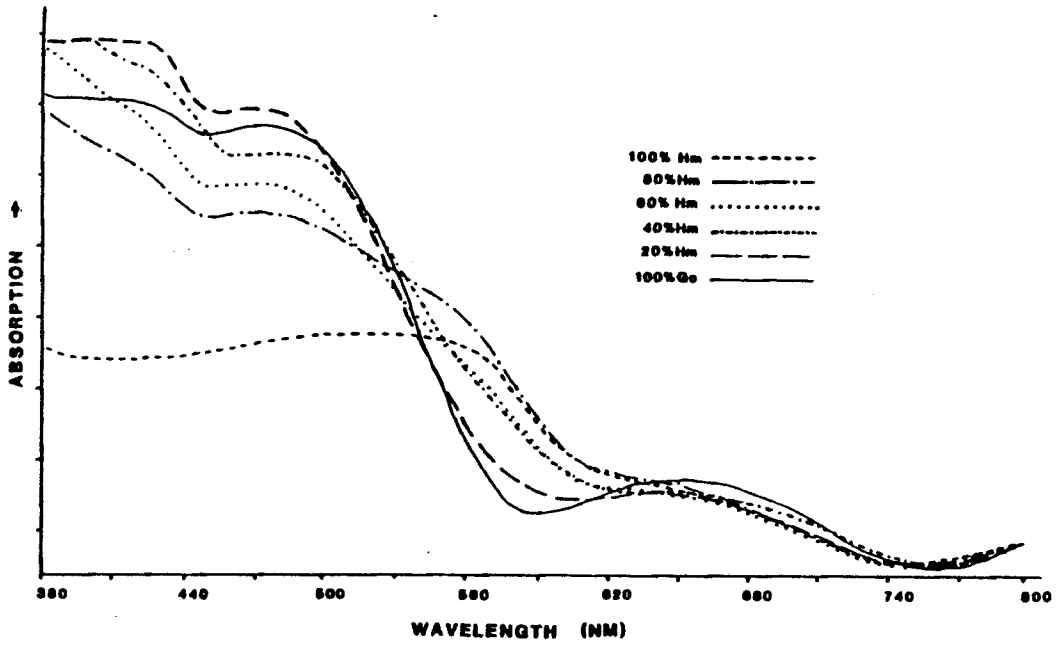

Figure 8. Normalized absorption curves for hematite - goethite mixtures in the range 380 to 800 nm, (from Bryant, 1981).

inflection in the spectral curve at 530-580 nm. The intensity of the reflection in the 500-640 nm region was inversely proportional to the iron content and a straight line equation for artificial mixtures of SiO_2-Fe_2O_3 with an iron oxide content from 2-9% was developed. Percent reflection is represented by R, and C is the percent Fe_2O_3 content.

$$R(\%) = 85 - (4.9)C$$

In another measure Obukhov and Orlov (1964) used the value of reflectance at 450 nm subtracted from that at 650 nm to quantify iron content for specific soil groups:

$$R_{650} - R_{450} = A + K \cdot C$$

A and K are coefficient constants which vary with each soil group. The proportionality coefficient K is almost the same for all soils studied but the general reflectivity, expressed by constant A, differed noticeably with soil group (Table 2).

Karmanov (1970, 1972) did extensive studies into the use of computing the chromaticity of soils and also examined the effect of different degrees of hydration upon iron oxide reflectance in soils. The reflection intensity of iron hydroxides containing little water and having a dark brown-red color increased most strongly in the wavelength interval from approximately 554 to 596 nm. Iron oxides containing a large amount of water had the greatest increase in reflection intensity in the wavelength range from approximately 500 to 540 nm. The total reflection intensity of the highly hydrated oxides was markedly higher than that of oxides containing little water.

Table 2. Quantification of iron content for specific soil groups as a function of soil reflectivity (Obukhov and Orlov, 1964).

Parameters of equation $R_{550} - R_{450} = A + K \cdot C$ for various soils

Soil	Range of Fe_2O_3 content, %	A	K
Thick podzol	2-6	12.0	2.6
Gray forest	2-6	15.5	3.0
Ordinary chernozem	2-6	8.5	2.7
Weakly podzolic red earth	6.5-10	11.5	2.6

Mathews et al. (1973) found that the spectrum of a Hagerstown silt loam (Typic Hapludalf) had a significant increase in reflectance in the visible range and also a decrease in the degree of absorption at 0.9μm after free iron removal by the sodium dithionite-citrate-bicarbonate procedure of Mehra and Jackson (1960) (Figure 9). Leger et al. (1979) also removed free iron via the same procedure and found the largest change in reflectance occurred in the 450 to 570 nm region.

In a more recent study of soil reflectance properties Stoner and Baumgardner (1980) measured the bidirectional reflectance factor of over 240 different soil series and compared spectral characteristics with physicochemical properties. The wavelength range measure extended from 0.52μm to 2.32μm and therefore excluded some of the visible region. Ferric iron absorption bands are observed and discussed with reference being made to the writings of Hunt et al. (1970, 1971). An absorption band at ~0.87μm was described as a sharp, well defined ferric band and was noted in samples with only small amounts of iron oxide (Figure 10). This absorption band due to ferric iron at ~0.9μm has been observed as a rather weak, broad absorption in previously discussed studies. A sharp ferric iron absorption band was noted in the Leon sand (Figure 11), even though only a trace of free iron oxides was measurable (Stoner and Baumgardner, 1980). A similar observation was made for the ferrous iron absorption band near 1.0μm which was frequently noted by Hunt et al. (1970, 1971). Stoner and Baumgardner (1980) state that this band was more difficult to identify in the soil samples studied but did suggest evidence of its occurrence in

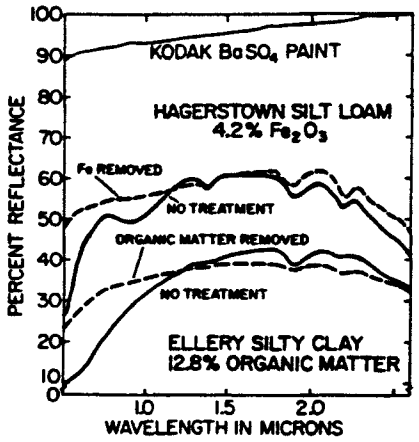

Figure 9. Reflectance curves illustrating the effect of free iron oxide and organic matter on reflectance intensity (Hagerstown curve from the B21t horizon, sample No. 564 Pa 14-5-2; Ellery curve from the Ap horizon, sample no. 567 Pa 48-36-1), (from Mathews et al., 1973).

TOQUOP(NV)

Typic Torripsamment
mixed, thermic
arid zone
deep sandy alluvium
Clark Co.

A1 horizon	A1 horizon
A slope	A slope
excessively drained	excessively drained
fine sand	fine sand
92%S 5%Si 3%C	94%S 3%Si 3%C
5YR 6/6 (moist)	7.5YR 5/6 (moist)
7.5YR 7/6 (dry)	7.5YR 7/6 (dry)
0.0% O.M.	0.23% O.M.
9.0 meq/100g CEC	4.9 meq/100g CEC
0.20% Fe_2O_3	0.30% Fe_2O_3

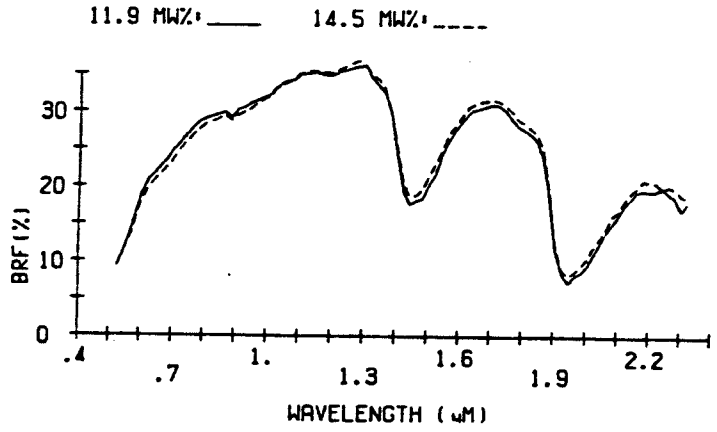

Figure 10. Reflectance curves, soil analyses and site characteristics of duplicate samples of the Toquop soil series, (from Stoner and Baumgardner, 1980).

several more poorly drained soils. The Leon sand shown in Figure 11 is one example presented of the slight ferrous absorption band at 1.0μm. However, the presence of a ferrous absorption band in soils is not consistent with present knowledge of soil iron. Buol et al. (1973) state that the free iron contents of soils decrease with increasingly poor natural drainage. This is a result of the translocation of ferrous or reduced iron from the soil profile. Therefore these absorptions noted as being due to iron in the ferrous form are unlikely to occur in soils. A possible explanation for these sharp bands in the near-infrared, either ferric or ferrous, could be related to the water content of the soil samples. Specifically the expression of overtones or combination tones of the fundamental vibrational frequencies of the isolated water molecule which occur at 0.942 and 1.135μm (Hunt and Salisbury, 1970).

Latz et al. (1981), using methods similar to Stoner and Baumgardner (1980), studied the reflectance of eroded and depositional soils of various toposequences. Simulated Landsat reflectance curves showed an increasingly convex appearance as the degree of erosion increased (Figure 12). Increased iron oxide content was highly correlated with the a decrease in slope between Landsat Bands 3 and 4 (0.75 to 0.9μm).

Organic Matter

Soil organic matter may be separated into two major groups based largely on the state of decompositon of organic debris (Kononova, 1966):

1) Unaltered materials, which include fresh debris and non-transformed components of older debris.

LEON(FL)

Aeric Haplaquod
sandy, siliceous, thermic
humid zone
acid marine sands
Bay Co.

———	———
A1-A21 horizon	A1-A21 horizon
A slope	A slope
poorly drained	poorly drained
sand	sand
97%S 2%Si 1%C	99%S 0%Si 1%C
7.5YR 4/1 (moist)	10YR 5/1 (moist)
10YR 7/1 (dry)	10YR 6/1 (dry)
0.85% O.M.	1.07% O.M.
2.1 meq/100g CEC	3.4 meq/100g CEC
trace Fe_2O_3	trace Fe_2O_3
12.1 MW% ———	16.8 MW% ----

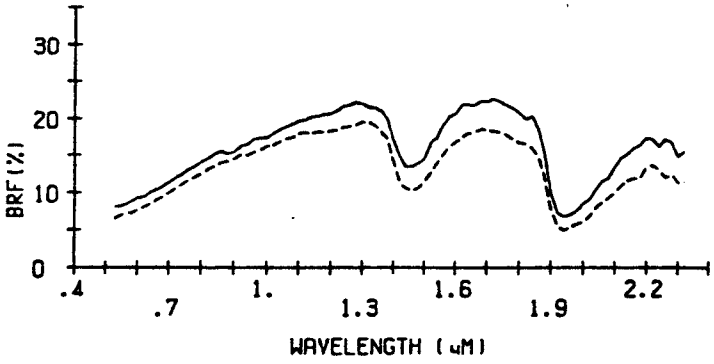

Figure 11. Reflectance curves, soil analyses and site characteristics of duplicate samples of the Leon soil series, (from Stoner and Baumgardner, 1980).

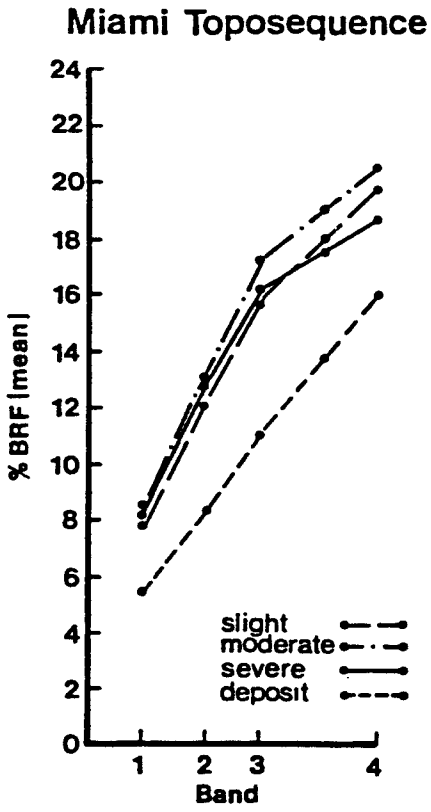

Figure 12. Simulated Landsat reflectance curves for an eroded Miami toposequence, (from Latz, 1981).

2) Transformed products, or humus, bearing no morphological resemblance to the structures from which they were derived.

The transformed products, or humus, can be subdivided as follows:

2a) Amorphous, polymeric, brown colored humic substances which are differentiated on the basis of solubility properties into humic acids, fulvic acids, and humins.

2b) Compounds belonging to recognizable classes, such as polysaccharides, polypeptides, altered lignins, etc. These can be synthesized by microorganisms or can arise from modifications of similar compounds in the original debris.

Of these materials which we classify as organic matter the humic substances (primarily humic and fulvic acids), have the strongest influence on the reflectivity and color of soils (Obukhov and Orlov, 1964). In an early study Obukhov and Orlov (1964) provide an excellent discussion of the effects of humic substances on soil reflectance. They state that pure humic acid absorbs light very strongly and that the total amount of light reflected by dried humic acids extracted from a thick chernozem (Mollisol) hardly reaches 2%. Powered humic acid is practically achromatic, or absorbs light evenly along the entire spectrum, while fulvic acid has a somewhat higher reflection coefficient in the green wavelength and red wavelength regions of the spectrum. They also provide an explanation as to why it is easier to detect the effect of humic substances in the red region of the spectrum. From 700-750 nm the reflection coefficients of soils are high, reaching 50-60%, while in the blue-violet region 380-450 nm they rarely exceed 20-25%. For this reason a uniform effect of reflectance due to the humus content is more easily detected in the red region of the spectrum.

The exact nature of humic substances is still a subject of much research and debate. Studies indicate the presence of phenolic, various aromatic, and possibly aliphatic functional groups which act as chromophores in the ultraviolet and visible regions of the spectrum (Hayes and Swift, 1978). The visible spectra of humic substances are nearly featureless with some materials expressing shoulders or inflections which may indicate the presence of particularly strong or abundant chromophores. As a rule reflectance increases gradually with increasing wavelength.

Although the visible spectra of humic substances are featureless attempts have been made to characterize differences in their color or hue by describing changes in the gradient of the spectral response (Kononova, 1966; Orlov, 1972; Chen, Senesi and Schnitzer, 1977; Ghosh and Schnitzer, 1979). The E_4/E_6 ratio is the optical density or absorbance of dilute aqueous solutions of humic substances measured at 465 and 655 nm, and is used as a measure of the gradient of the spectrum. Kononova (1966) found the ratio to be independent of concentration and believes that its magnitude is related to the condensation of aromatic humic constituents. Chen et al. (1977) tested this hypothesis and found that the magnitude of the ratio is goverened by the particle sizes and weights of the materials. They also found secondary relationships between the ratio and pH, free radical concentration, and total acidity but could not find any direct relationship to the concentration of condensed aromatic rings. Although changes in the magnitude of the E_4/E_6 ratio are not fully understood Hayes and Swift (1978) note that red-brown materials have higher ratios than grey-brown

materials and believe this is related to the degree of oxidation and/or molecular weight of the humic substances.

In more recent attempts to characterize humic substances Ghosh and Schnitzer (1980) studied the fluorescence excitation spectra of both humic and fulvic acids and identified well defined bands at 465 nm. They concluded that humic substances have characteristic absorption bands near 465 nm but that these bands cannot be detected in absorption spectra because of excessive overlapping by neighboring bands.

The influence of organic matter on the reflectance of whole soil samples has been studied by many researchers(Obukhov and Orlov, 1964; Bowers and Hanks, 1965; Orlov, 1966; Shields et al., 1968; Hoffer and Johannsen, 1969; Al-Abbas et al., 1972; Mathews et al., 1973; Leger et al., 1979; Krishnan et al., 1980; Stoner and Baumgardner, 1980.). The results of these works are inconsistent with respect to conclusions about the accurate measurement of organic matter contents of soils. Variations in other factors affecting soil reflectance make it difficult to quantify the influence of organic matter on reflectance properties. Several general observations concerning soil reflectance and organic matter have been widely accepted:

1) As organic matter content increases soil reflectance decreases throughout the visible and near-infrared wavelength region (Hoffer and Johannsen, 1969).

2) The visible wavelength region provides better information than the near infrared wavelength region for determining organic matter content (Krishnan et al., 1980).

3) Organic matter plays a dominant role in bestowing spectral properties on soils when its content exceeds 2.0%. As organic matter drops below 2.0% it becomes less effective

in masking out the effects of other soil constituents on the spectral response (Baumgardner, et al., 1970).

Soil Moisture

The interaction of radiant energy and the water associated with soils is a complex phenomenon. The basis of this interaction can be explained through an understanding of the absorptive properties of water itself.

Hunt and Salisbury (1970) provide a detailed explanation of common water absorption bands associated with the spectra of rocks and minerals. The water molecule has three fundamental vibrational modes: ν_1, the symmetric OH stretch; ν_2, the H-O-H bend; and ν_3, the asymmetric OH stretch. All of these are infrared active and their positions shifts depending of the state (gas, liquid, or solid) of the water. In the near-infrared water absorption bands are due to overtones or combination tones of these fundamental vibrational modes. In the case of the isolated water molecule the five bands which appear relatively strong are the $(\nu_2 + \nu_3)$ at ~1.875 , $(2\nu_2 + \nu_3)$ at 1.454 , $(\nu_1 + \nu_3)$ at 1.379 , $(\nu_1 + \nu_2 + \nu_3)$ at 1.135, and $(2\nu_1 + \nu_3)$ at 0.942μm. Water present in rocks and minerals produces two characteristic bands. One appears at 1.4μm due to $2\nu_3$, and the other appears at 1.9μm due to $\nu_2 + \nu_3$. According to Hunt and Salisbury (1970) the shape of these bands indicates the location of the water. Sharp bands usually indicate that the water molecules are located in well defined ordered sites, while broad bands indicate relatively unordered sites and/or that more than one site is occupied by the water molecule. The presence of both bands is indicative of undissociated water molecules in the structure, as in

water of hydration or water trapped in the lattice, but the appearance of the 1.4μm band without the 1.9μm band means that OH groups other than those associated with the water molecule are present.

Moisture content was one of the first factors influencing reflectance of soils to be studied quantitatively. Angstrom (1925), as reported by Planet (1970), measured soil reflectance under wet and dry conditions from the visible to 4.0 μm wavelength region. His study attempts to define the reason for the decrease in reflectance of natural soils after they have been wetted. Angstrom proposed that the reduction in reflectance was due to the internal total reflections of the thin water layer covering the soil, surface, in that a portion of the reflected energy is not reflected out into space but is rereflected to the surface itself. He then developed an equation relating reflectance of wet and dry soils to the index of refraction of the liquid. Planet (1970) supports Angstrom's explanation that the observed darkening is due to the optical effects of a thin layer of water on the surface of the soil.

The presence of water in the soil affects the level of reflectance and also influences the overall shape of the spectral response. Lindberg and Snyder (1972) demonstrated how hydration state changes the reflectance spectra of montmorillonite (Figure 13). In addition to strong water absorption bands at 1.45μm and 1.92μm, Lindberg and Snyder (1972) also observed very weak bands at 0.97μm, 1.19μm and 1.78μm.

Several researchers have used diffuse reflectance techniques to show the effect of moisture on soil reflectance. Obukhov and Orlov

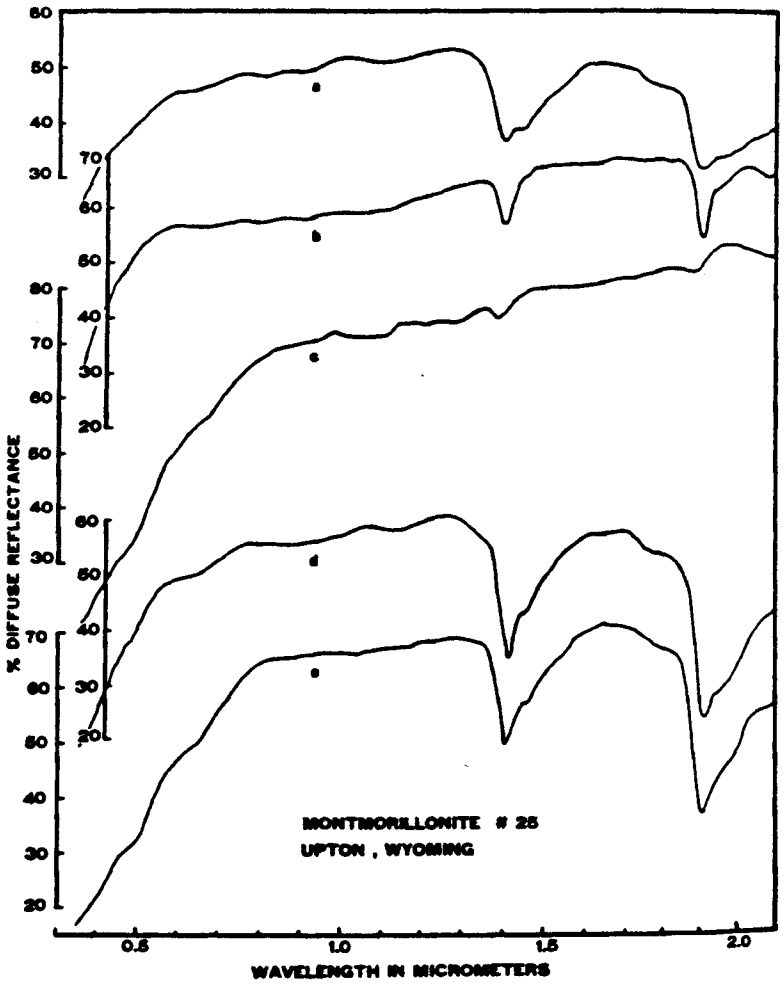

Figure 13. Changes in the reflectance spectra of montmorillonite as a result of changes in hydration state. Curve (a) original sample; (b) sample after heating to 120° C; (c) sample after heating to 600°C; (d) sample from curve b after humidification for two weeks; (e) sample from curve c after humidification for two weeks, (from Lindburg and Snyder, 1972).

(1964) demonstrated that reflectivity decreases very strongly when soils are wetted but the spectral curve does not change its appearance on wetting nor when various fractions are measured. In addition the ratio of the reflectivity of moist to that of dry soils remains practically constant in the entire visible portion of the spectrum. The effect of moisture content on soil color was studied by Shields et al. (1968). Using spectrophotometric techniques they concluded that moisture had no significant effect on the hue or chroma of Chernozemic and Gray Wooded Soils but the addition of moisture caused a decrease of 1.1 to 2.0 Munsell value units. Bowers and Hanks (1965) determined that at all wavelengths measured, on all samples, reflectance decreased and absorbance increased as moisture content increased. Data for the Newtonia Silt Loam (Figure 14) represents six moisture contents and illustrates the effect of increased moisture content on percent reflectance. Hoffer and Johannsen (1969) and Condit (1970) also using diffuse reflectance techniques present similar general results and conclusions concerning moisture content and reflectance of soils.

In an effort to explain how water influenced the shape of reflectance spectra Bowers and Hanks (1965) identified three absorption bands located at approximately 1440 nm, 1900 nm, and 2200 nm (Figure 14). The first two bands centered on wavelengths strongly absorbed by water and specifically represent overtones of the fundamental frequencies at which water molecules vibrate. Hunt and Salisbury (1970) attributed the band noted but unidentified by Bowers and Hanks (1965) at 2200 nm (Figure 11) to the stretching

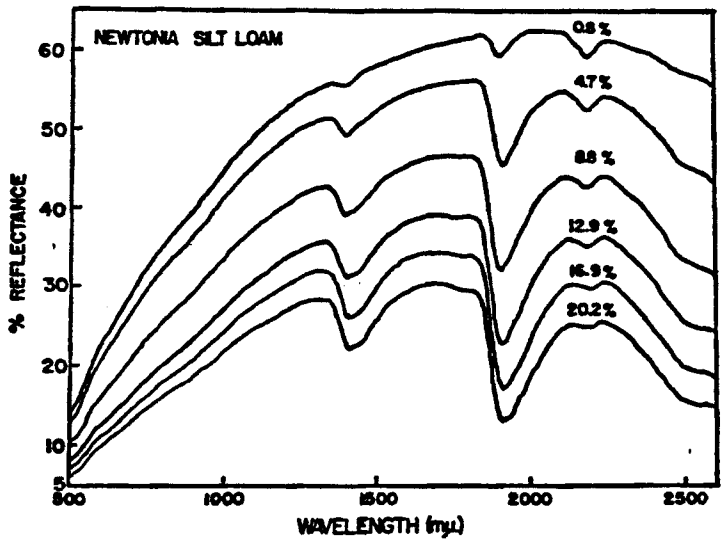

Figure 14. Percent reflectance vs. wavelength of incident radiation at various moisture contents (moisture contents indicated directly above each curve) (from Bowers and Hanks, 1965).

mode of the hydroxyl ion. The exact position of this band depends on the site in which the OH is located.

The control of the moisture variable in soil refectance studies has received considerable attention. Recent research has found that maintaining a uniform moisture tension between samples yields repeatable results (Shields et al., 1968; Mathews et al., 1973; Beck et al., 1975; Leger et al., 1979; Stoner and Baumgardner, 1980).

Particle Size

Particle size is a significant factor influencing reflectance from soil surfaces. Writings by Obukhov and Orlov (1964), Bowers and Hanks (1965), and Orlov (1966) provide excellent discussions on the effects of particle or aggregate size on reflectance.

Bowers and Hanks (1965) used clay minerals to study the effects of particle size on reflectance. The sieving of clay samples eliminated differences in mineralogy which could have occurred if soil samples of various size fractions were studied. Results at nearly all wavelengths indicate that the most noticeable increases in reflectance occur at sizes less than 400 μm (Figure 15). The changes in reflectance appeared to be a function of surface roughness.

Reinforcing the conclusions of Bowers and Hanks (1965), Orlov (1966) emphasized that the determining factor relating particle size and reflectance are the diameter of the aggregates and the form of their surface. Fine particles give a more even surface by filling a volume more completely. Coarse aggregates usually have an irregular

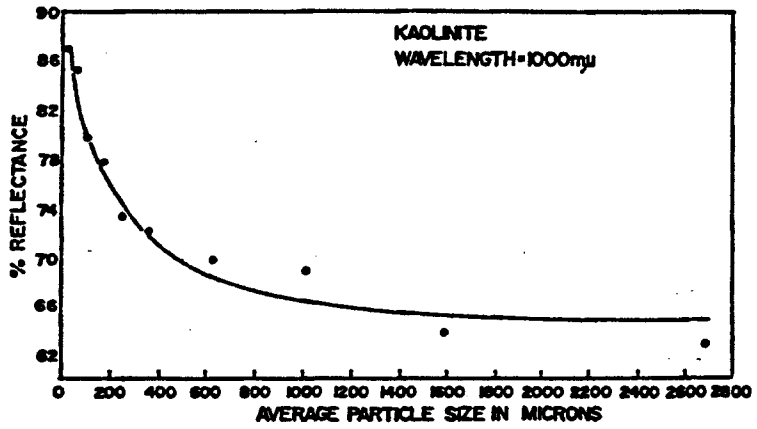

Figure 15. Percent reflectance vs. particle size for incident radiation of 1000 mμ wavelength, (from Bowers and Hanks, 1965).

shape with a large number of pores or cracks that act as light traps and reduce total reflectance.

Obukhov and Orlov (1964) determined that changes in the level of reflectance occur with differing diameters and shapes of particles but the energy distribution along the spectrum does not change. Fractions less than 0.25 mm in diameter had a maximum reflectance compared to a minimum response for the 5-10 mm fraction. The spectral response for undisturbed soil was found to coincide with the 1-2 mm and 2-3 mm size fractions.

METHODS AND MATERIALS

Soil Samples: Selection, Collection, and Preparation

Three sets of samples were used to aid examination of the effects of erosion on the spectral response of soils. The first set, designated as "simulated eroded" samples, was obtained through collection and mixing of soil cores for each of three common Indiana Typic Hapludalfs (Russell, Miami and Morley). The second set consisted of samples of an eroded Morley which were previously collected by the National Soil Erosion Laboratory for their study on soil productivity and erosion. The third set consisted of surface soil samples collected and classified by the Soil Conservation Service for the Purdue University Soil Characterization Laboratory (Russell, Miami, and Morley soils).

The Russell, Miami, and Morley soils were chosen because they have very similar properties and are commonly susceptable to erosion. Detailed descriptions of some of the sites and soils examined are presented in Appendices A and B. Those presented represent the range of properties found within any of the three soils and/or the family as a whole. The Russell soil collected at the Purdue Agronomy Farm characteristically is formed in 20-40 inches of loess over glacial loam till. A Miami soil collected in Montgomery County differs from the Russell in the depth of the loess (10-20 inches) over loamy glacial till. The Morley soil samples which were collected in

Whitley County typically have 10-20 inches of loess over clay loam glacial till.

Typically, as erosion proceeds, the A horizon is slowly removed, while with each successive pass of the plow more of the subsoil (E, BE or B horizons) is mixed into the Ap horizon. This sequence of events is the basis for differences in the appearance of eroded soils as compared to non-eroded or depressional soils. It is important to remember that differences seen in eroded soil classes are as unique as the original soil profiles themselves. For this reason this study focused on three soils of the taxonomic classification Typic Hapludalf.

For the "simulated eroded" samples of the Russell, Miami and Morley soils, four soil cores, 3 inches in diameter and 16 inches in depth, were collected for each soil. The cores were obtained from none-slightly eroded areas. These cores were then mixed in a manner which produced subsamples that simulated five different erosion classes. The uppermost 8 inches of the cores (<2 mm, dried and crushed) were mixed and a specific volume of this mixture was placed in a larger container. This initial total volume of soil will be referred to as a unit and represents a none-slightly eroded Ap horizon. From this volume 1/4 unit was removed to constitute the first sample or the none-slightly eroded soil. This left 3/4 of a unit in the container, to which a 1/4 unit volume of soil which represents the 8-10 inch section of the same set of cores was added. The total volume was mixed and a 1/4 unit subsample was removed to constitute the second or slightly eroded soil. This procedure was continued until the last sample represented a very severely eroded

soil. This dilution of the original surface "plow layer" with subsoil was used because it best represented the in situ condition of eroded cultivated soils. The rationale for this method lies in the fact that soils often erode slowly over a period of years, and that with each successive cultivation the plow layer is mixed, buffering any drastic changes one might observe in an undisturbed soil profile.

The second set of samples consisted of ten field samples of the Ap horizons of various Morley erosion classes. Samples were collected in Whitley County by staff from the National Soil Erosion Laboratory. (Note the core samples for the Morley simulated erosion samples were also obtained in Whitley County.) The physical and chemical data for these samples are found in Appendix A. Descriptions of the sampling sites are found in Appendix B.

The third set of samples consisted of an additional fourteen Ap horizon field samples representing various erosion classes of the Russell, Miami, and Morley soil series. These samples were obtained from the Purdue University Soil Characterization Laboratory. They were classified with respect to their degree of erosion by the Soil Conservation Service. Physical and chemical data are presented in Appendix A. Descriptions of the site locations for these soils are found in Appendix B. Samples of a Typic Argiaquoll (Brookston) and a Typic Paleudult (Frederick) collected for the Purdue University Soil Characterization Laboratory were also used for comparison.

Soil Samples: Chemical and Physical Analyses

Physical characterization of the soil samples consisted of crushing the air dry sample, collecting the fraction <2 mm, and then measuring the particle size distribution. Eight size fractions were

measured by the Soil Characterization Laboratory of the Department of Agronomy at Purdue University. The distribution was determined using the pipette method (Franzmeier et al., 1977).

Total carbon was determined on the Leco Carbon Determinator WR12. Organic matter content was computed by multiplying the percent total carbon by 1.724.

The citrate-bicarbonate-dithionite (CBD) method was used to determine the amount of total free iron in the soil samples. The extraction method was described by Franzmeier et al. (1977). However, the iron content was determined with an atomic absorption spectrophotometer and a nitrous oxide air-acetylene flame rather than a colorimeter. Also, organic matter was not removed from the sample used in the extraction.

Spectral Measurement of Soils

The spectral data collected in this study was obtained from the Cary 17D spectrophotometer. This unit was equipped with an integrating sphere and measured diffuse reflectance, in an absorbance mode, relative to a barium sulfate standard. A thin glass cover slide was placed over the sample port to prevent soil from falling into the sphere. A second glass cover slide was placed over the standard port to eliminate the effects of the sample port slide which protected the sphere. The spectral scan was from 1220 nm in the near-infrared to 380 nm in the visible wavelength region. A change from the lead sulfide detector to a photomultiplier tube took place at 650 nm. Since this region of the spectrum lacks any strong

absorption bands, the spectral response has a relatively constant slope suitable to such a detector change.

The preparation of soil samples for spectral measurement by the Cary spectrophotometer presented an interesting problem since mounts were held in a vertical position. Loose soil was lightly packed into a rubber stopple which had a hole in its base. Care was taken to provide a uniform "natural" surface between all samples in the stopple. The hole was filled with cotton to act as a wick. The stopple was placed in a tray of water allowing the sample to saturate and was then removed to air dry. This process produced an aggregated soil plug which could be removed from the stopple, placed in a sample holder, and mounted vertically on the sphere of the spectrophotometer.

Each soil sample was equilibrated in a desiccator at 77% relative humidity for six days to attain a uniform moisture tension. Samples were essentially air dry during the spectral measurement.

Digital data was collected by the Cary 17D spectrophotometer and recorded on tape by an HP 2645A computer terminal. This data was then shipped to files on the Agricultural Data Network and processed into its final form. Calculation of various plot files and derivatives was also done on the HP 2645A terminal through the Agricultural Data Network.

Second Derivative Spectroscopy

Second derivative spectroscopy was used to aid detection of subtle absorptions in the spectral response of soil. This method was introduced as early as 1955 as a means of extracting more information

from the spectral distribution (Giese and French, 1955). Derivative measurements can aid in determining quantitatively the position and intensity of a weak absorption band overlaid or obscured by another absorption band. To accomplish this measurement the first and second derivatives of the reflectance spectra were calculated as a function of wavelength. The result is a plot which quantifies the slope or curvature in the spectral response. Thus information can be gained by looking for more specific features in the spectral response (Hager, 1973). Detailed descriptions of the mathematical and application aspects of this technique have been published (Giese and French, 1955; Hager, 1973; Hawthorne and Thorngate, 1978; Whitbeck, 1981).

RESULTS AND DISCUSSION

Repeatability

To determine the repeatability of data collection, the spectrum of a Miami, very severely eroded, was obtained on five different occasions (Figure 16). All of the spectra were collected after samples were air dried and equilibrated in a desiccator at 77% relative humidity for a minimum of two days. The first four spectra were obtained over a three-day period while the fifth was obtained three weeks later. The consistency of these results indicate that the method of sample preparation and data collection provided excellent repeatability for quantitative soil reflectance studies.

Spectral Reflectance of Soil Components

In order to understand the effects of iron oxides and organic matter on soil reflectance the spectra of goethite, hematite, and humic acid were collected. The literature review illustrates many of the problems encountered when interpreting soil reflectance properties from studies of pure mineral samples. However, despite these complexities it was hoped that the study of samples similar to those of the major soil components affecting reflectance would provide a more complete explanation of their influence.

The reflectance spectra of two iron oxides (Figure 17) were obtained from the same samples used by Bryant (1981) (Figure 8).

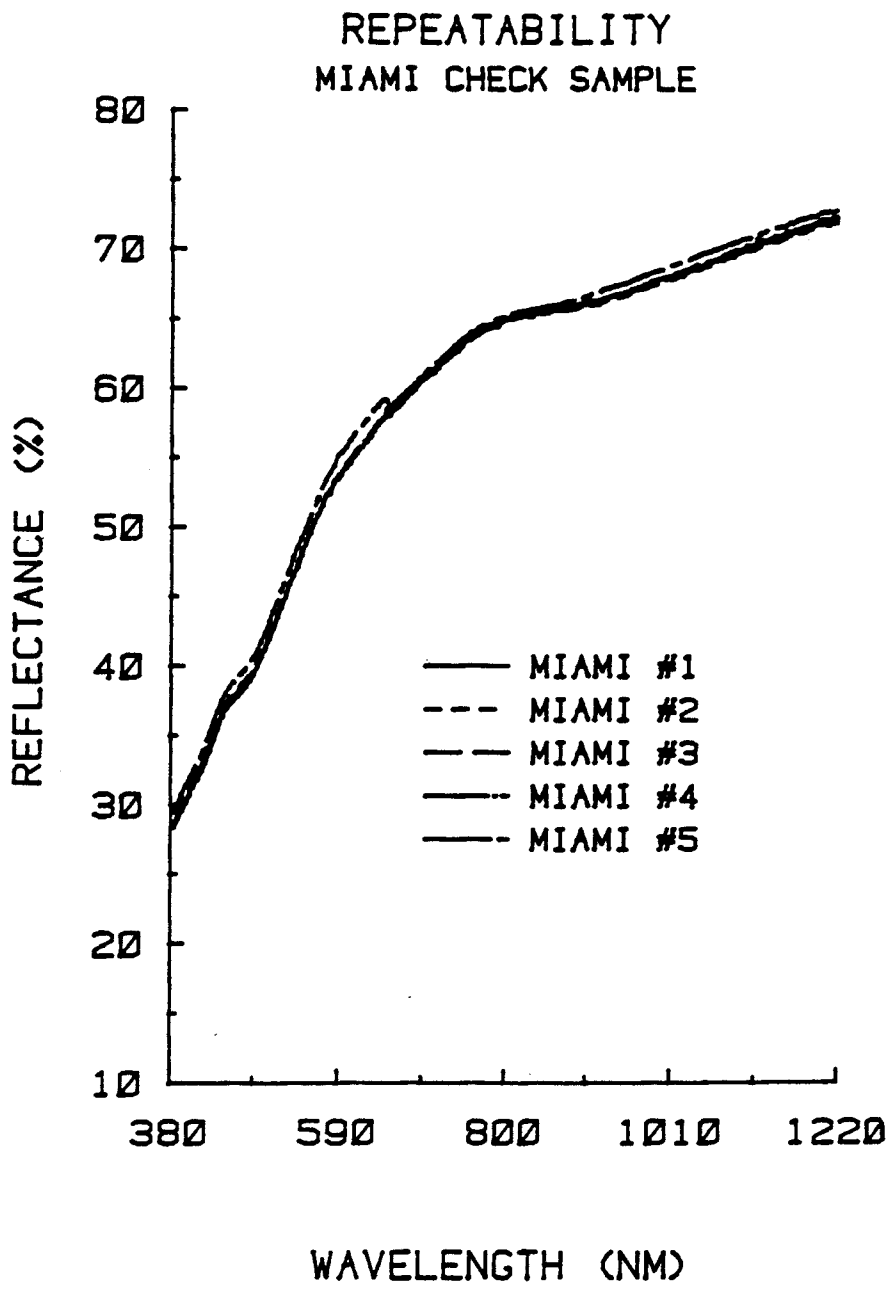

Figure 16. Reflectance spectra, repeatability of data collection, Miami very severely eroded check sample.

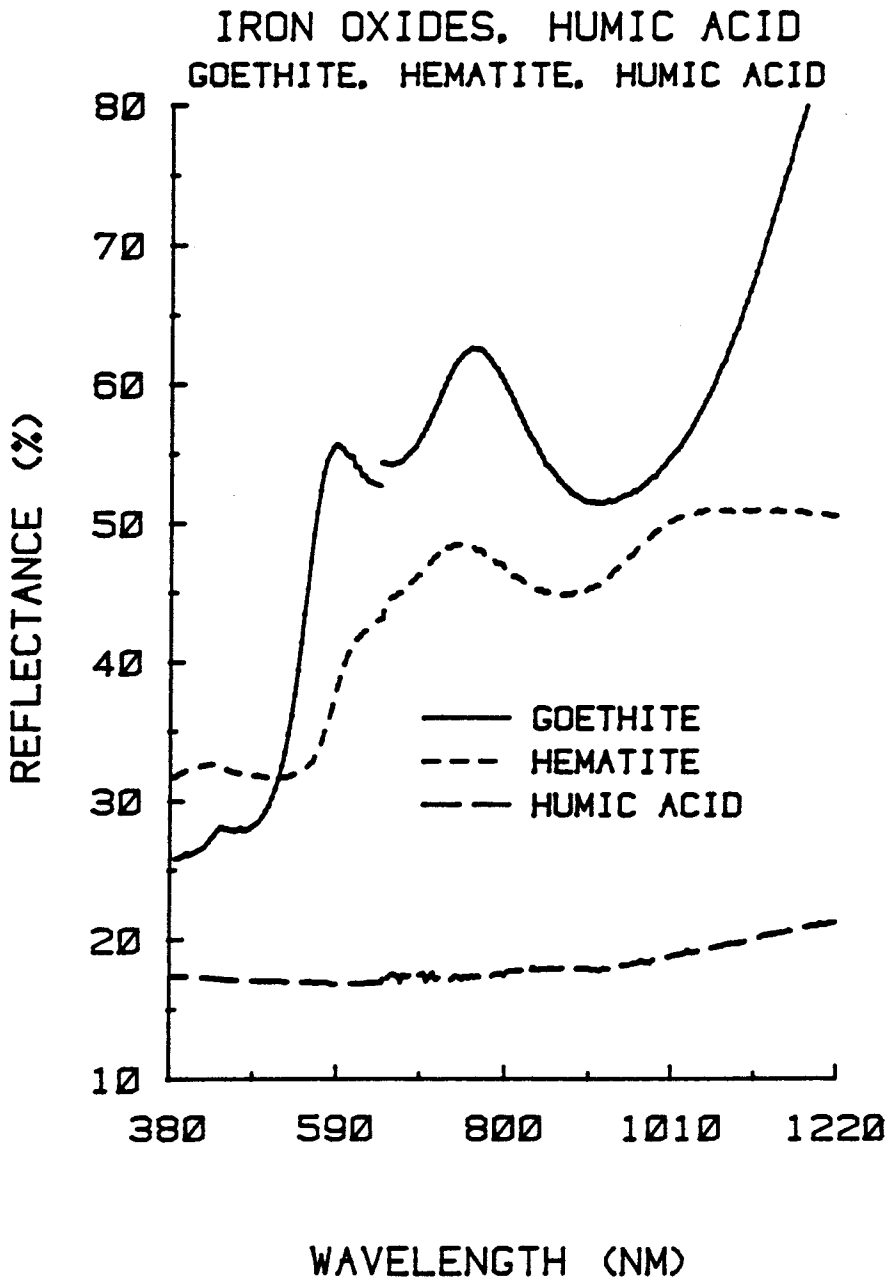

Figure 17. Reflectance spectra of iron oxides (Goethite, Hematite), and humic acid.

The goethite was synthetically prepared while the hematite was ground from a mineral sample. Curi (1982) characterized both samples with X-ray diffraction and described them as crystalline and pure with the exception of small amounts of chlorite contamination in the hematite sample. The small quantities of these samples available for study required that a thin sample mount be prepared for analysis.

An analysis of the goethite and hematite spectra with respect to their chemical composition and absorptive properties provides insight into how these iron oxides influence soil color. In the visible wavelength region (380-720 nm) the level of reflectance and shape of the spectra appear to be determined primarily by absorption bands within this visible region, rather than by absorptions in the ultraviolet or near infrared regions. The absorption band in the near infrared has little effect on the spectra in the visible region, as witnessed by the peaks in reflectance at approximately 750 nm.

The basic difference in the color of the two iron oxides is determined by the position and intensity of iron absorption bands in the visible region. The goethite sample has a strong iron absorption band at 520 nm and its reflectance increases sharply from 540 to 600 nm. There is a weaker absorption band centered at 650 nm. Note this is also the position of the change from the lead sulfide to the photomultiplier detector which causes the gap in the goethite spectrum. The reflectance of goethite is generally high in the green, yellow, and red regions of the spectrum. The hematite sample also has a strong absorption band in the visible region but

it is at a higher wavelength (560 nm) than that in goethite. In addition, the reflectance of hematite does not increase quite as quickly as that of goethite.

From these spectra it is clear why hematite has a higher pigmenting power in the soil than goethite. A soil which contains goethite as its predominant pigmenting agent will reflect light in a window spanning the green, yellow and red regions of the spectrum. This results in a bright brownish-yellow soil color. When even small amounts of hematite are present the green, and to a lesser degree, the yellow, wavelengths are absorbed very strongly. This narrows the window of highly reflected light to the red region of the spectrum and results in hematite expressing a bright orange-red color. Thus the presence of goethite is masked by hematite because of hematite's strong absorptive capacity in the green wavelength region of the spectrum. In other words, light which would have been reflected by goethite to yield a brownish-yellow color is strongly absorbed by hematite causing the soil to be redder in color.

The reflectance properties of goethite and hematite in the near infrared wavelength region are considered important in determining the shape of a soils spectral response. Previous research offers several different interpretations of the nature of iron oxide absorption in this region. The spectra collected in this study provide insight into the absorption characteristics of iron oxides. Although the explanation proposed may differ from that of previous researchers, it is consistent with the results they obtained.

In order to define the interactions and absorptions taking place in the near infrared region of the spectrum, the chemical

properties of the iron oxides under study must be understood. Goethite and hematite in their pure mineral form contain no water. However, when these iron oxides are formed in soil they occur in a hydrated state. Both goethite and hematite have the ability to tightly hold several layers of water through hydrogen bonding. Thus when discussing soil iron oxide it is understood that the hydroxide form will predominate. Water absorption bands at 940 nm and 1130 nm may be influencing the spectral response of iron oxides. The limonite sample presented by Hunt et al. (1971) (Figure 6) is one illustration of this interaction. Limonite (typically containing 12-14% water by weight) showed absorption bands assigned to water of hydration at 1.4 and 1.9 m in the largest particle size fraction sample. There was, however, a marked shift to higher wavelengths for the "iron absorption band" of this sample. Hunt et al. (1971) did not note this shift but attributed the increased intensity of absorption at 0.9 m to the transparent nature of the sample. In contrast the goethite and hematite spectra presented by Hunt et al. (1971) were obtained from ground mineral samples and contained little water.

The spectra of goethite and hematite presented (Figure 17) illustrate the influence of water of hydration on the reflectance spectra of iron oxides. As previously stated, the hematite sample was ground from a mineral and contains little or no hydrated water. It exhibits a characteristic iron absorption band at 870 nm. The goethite sample was synthetically prepared and contains hydrated water. Note the shift and broad nature of the absorption band at 940 nm. These results indicate that overtones of the fundamental

vibrational modes of the water molecule at 940 and 1130 nm are having a dramatic effect on the shape and magnitude of the reflectance spectrum of this synthetic goethite in the near infrared wavelength region.

This interaction may also help explain the results obtained by Stoner and Baumgardner who noted sharp absorption bands at 900 and 1000 nm in soils with only a trace of iron oxide. In these cases the two water absorption bands in the near infrared wavelength region may have had a pronounced effect on the reflectance spectra, particularly since the spectra of the soils were obtained at 0.1 bar moisture tension, or near field capacity.

The second derivatives of the goethite and hematite spectra help illustrate the position and intensity of some of the absorption bands found in their respective reflectance spectra (Figure 18). The slopes of the broad absorption bands in the near infrared wavelength region change so slowly that the second derivatives in this region do not contain detailed information on the shape of the spectral response. However, the second derivative does help to quantify the position and intensity of the stronger iron absorption bands in the visible wavelength region. Note that the gap in the second derivative at 650 nm is a result of the previously mentioned detector change.

A closer examination of the second derivative of the region from 380 to 620 nm yields specific information on the microstructure of the spectral responses of goethite and hematite (Figure 19). The peaks of the second derivative correspond to change in the slope of the spectral response. Specifically, the peak at 518 nm in the

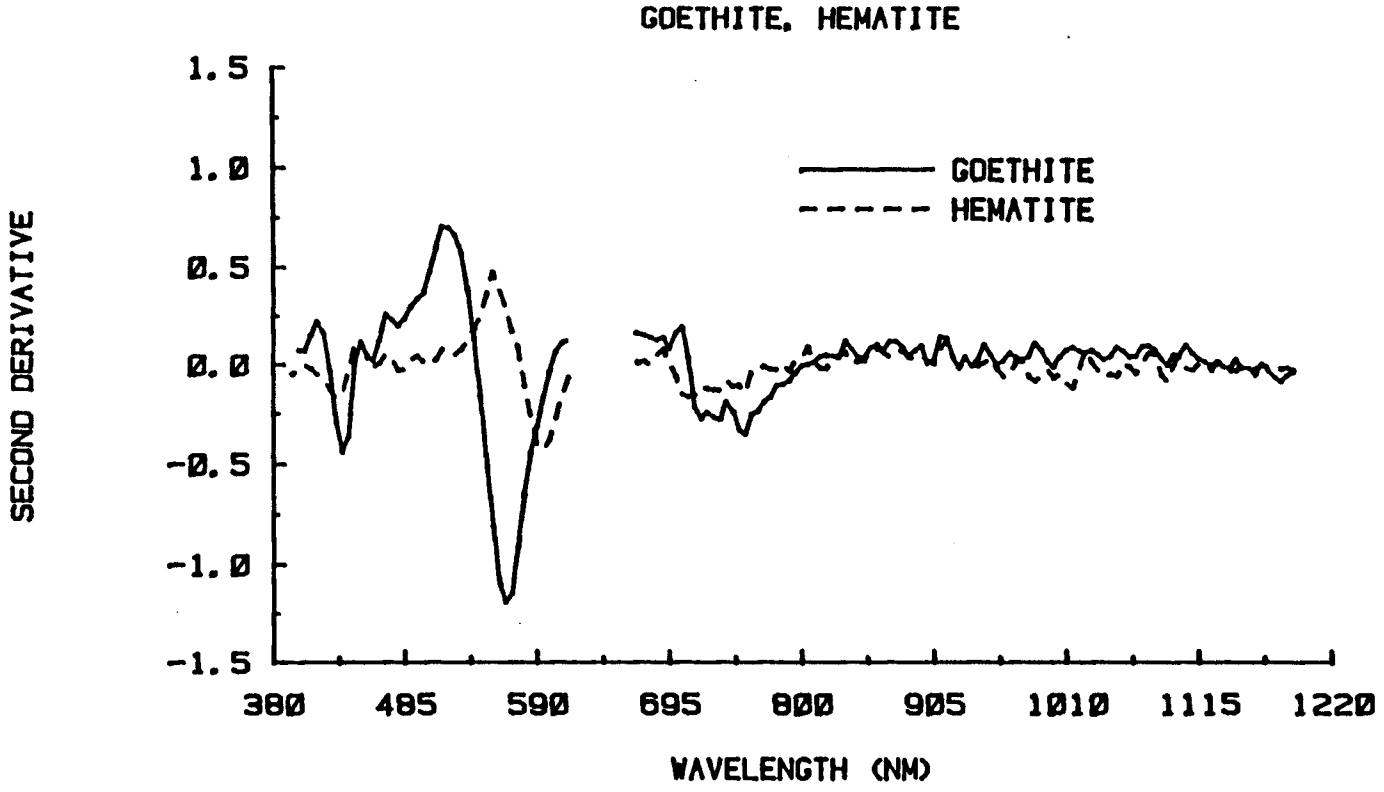

Figure 18. Second derivatives (380 - 1220 nm) of the reflectance spectra of goethite and hematite.

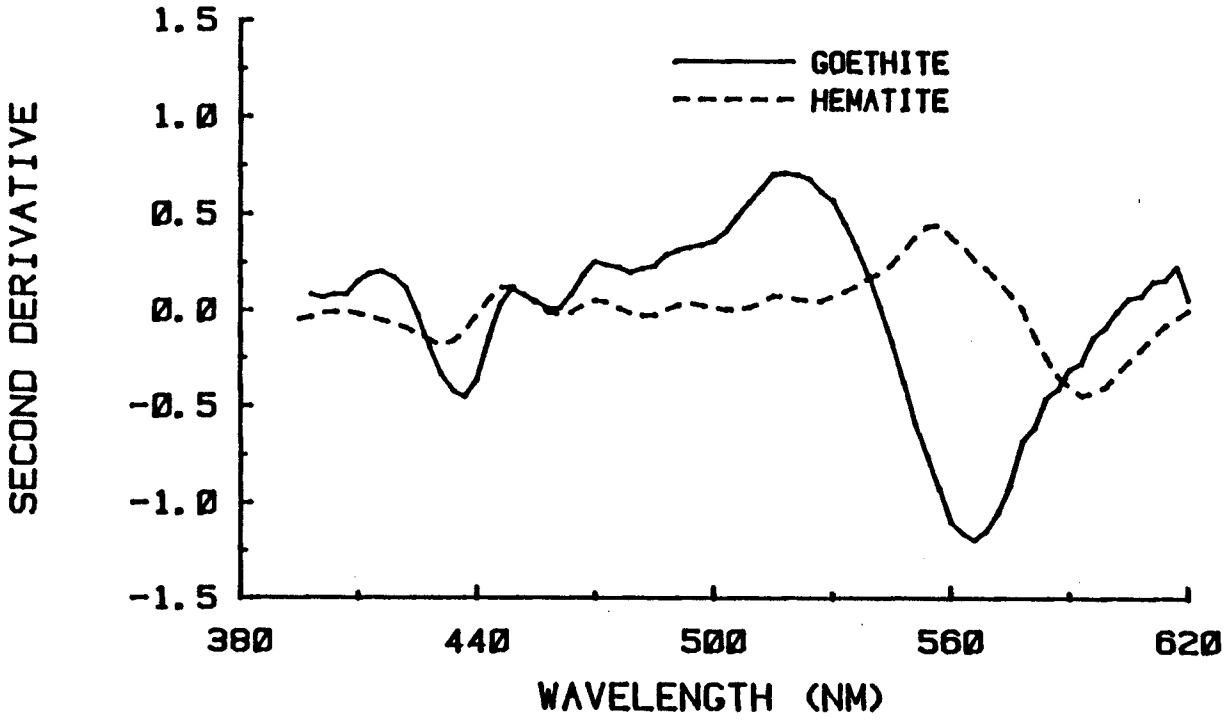

Figure 19. Second derivatives (380 - 620 nm) of the reflectance spectra of goethite and hematite.

goethite second derivative corresponds to the iron absorption band maximum seen in the reflectance spectrum (Figure 17). Similarly, the peak at 555 nm in the hematite second derivative corresponds to its iron absorption band maximum. The exact nature of the absorption maximum shift to a higher wavelength in the hematite sample is well illustrated in this comparative second derivative plot with the goethite sample. In addition, the height of these peaks is a measure of the intensity of the inflection in the reflectance spectra caused by a corresponding absorption.

The reflectance spectra of a humic acid sample extracted from a muck soil is also plotted for comparison in Figure 17. Its reflectance is typically low and featureless in all wavelength regions at the high concentration used.

Soil Spectral Reflectance Comparison

The knowledge obtained through the study of various soil components can be used to interpret the reflectance spectra of natural soils. Three soils with different colors and chemical properties (Table 3) were compared to determine the major factor or factors influencing the shape of their spectral response.

Figure 20 shows the reflectance spectra of the Frederick, Miami and Brookston soils. The Frederick and Miami soil samples have similar concentrations of organic matter and iron oxide. The slightly higher amounts of both of these constituents in the Frederick soil results in its lower level of reflectance. The shapes of these two spectra are also very similar except for differences in the region of strong iron absorption (460 to 560 nm).

Table 3. Selected chemical and physical data for soils used in a general soil reflectance comparison.

SOIL	SUBORDER	MUNSELL COLOR (HUE)	% OM	% Fe_2O_3
FREDERICK	Udult	5 YR	1.85	1.88
MIAMI	Udalf	10 YR	1.37	1.64
BROOKSTON	Aquoll	10 YR	5.40	1.21

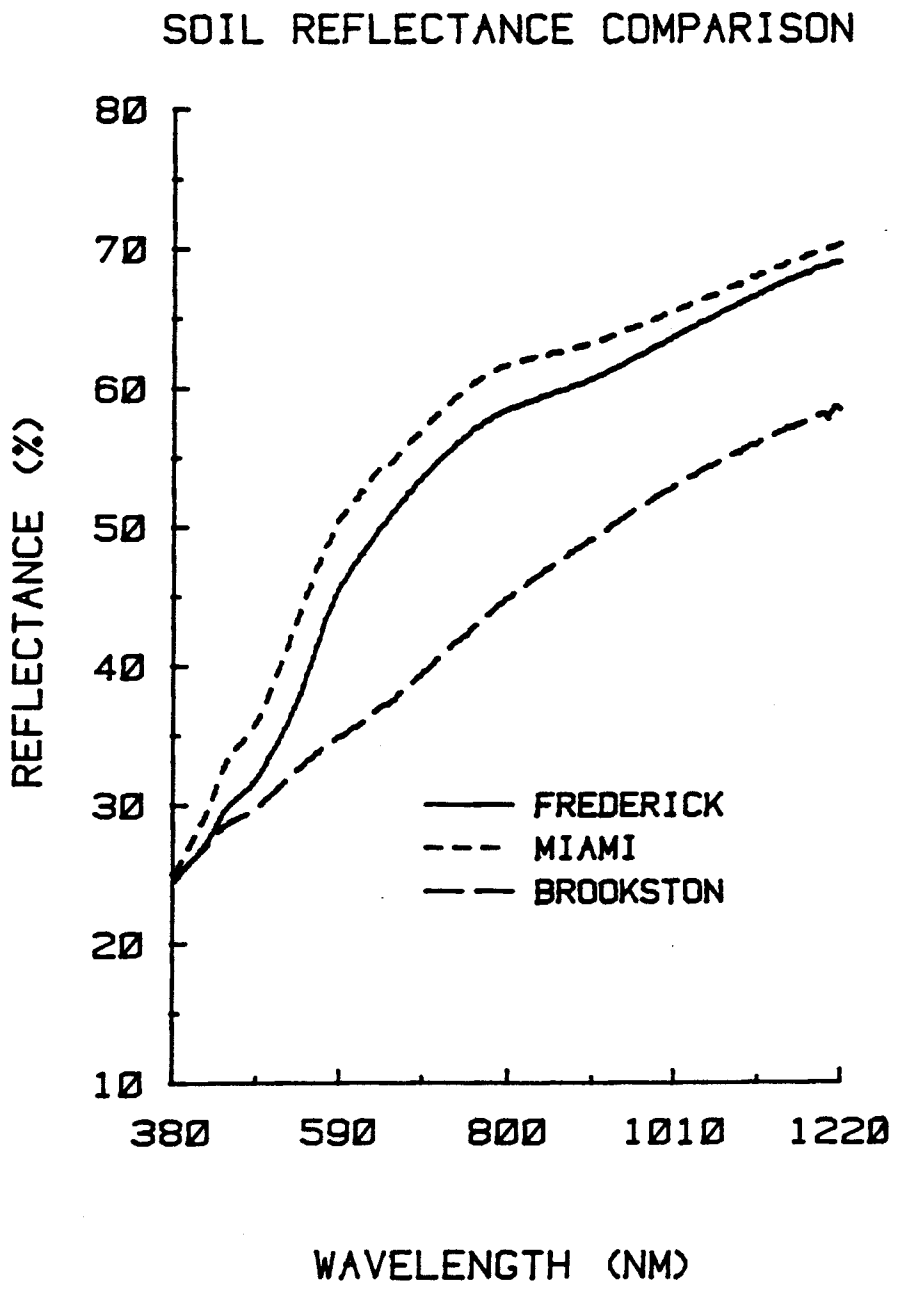

Figure 20. Soil reflectance comparison of the Frederick, Miami and Brookston soils.

To accurately describe the nature of these subtle changes from the reflectance spectra is a difficult task. However, a comparison of the second derivatives of the reflectance spectra provides valuable information on these subtle differences (Figure 21). The Frederick second derivative contains two major peaks, one at 476 nm, and a second at 538 nm. Note that the negative peak at 440 nm is the result of absorptions taking place at higher wavelengths, as stated in the discussion of the properties of the second derivative. The Miami second derivative contains one major peak at 476 nm. Comparison of this data with the reflectance spectra indicates the positions of absorptions caused by iron oxide compounds. The Frederick soil has two absorptions within its reflectance spectrum. One is in the same position as the major inflection of the Miami soil while the second is at a slightly higher wavelength.

A reason for this difference can be proposed by comparing the colors of the two soils. The Frederick soil was developed from limestone parent materials and is highly weathered. This favors the formation of hematite and thus a reddish soil color. The Miami soil was developed from glacial parent materials of Wisconsin age and is not highly weathered. This results in the brownish-yellow color which is typical of goethitic soils. The second derivatives indicate the presence of a major absorption in the green wavelength region for the Frederick soil while no such absorption is present in the Miami soil. This absorption in the green wavelength region by the Frederick soil results in a narrow window of reflected light and therefore a reddish color. The reflectance in the Miami increases sharply in this region resulting in a wider window of reflected

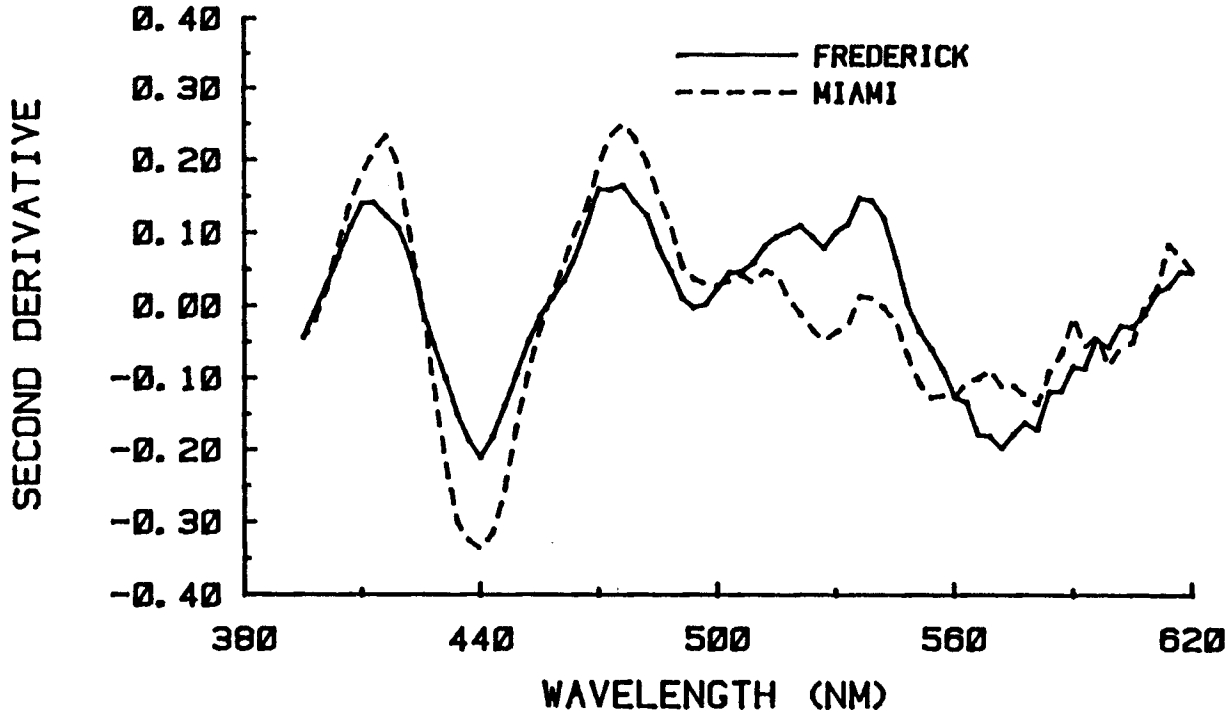

Figure 21. Second derivatives (380 - 620 nm) of the reflectance spectra of the Frederick and Miami soils.

light and its brownish-yellow color. A similar effect was described for the pure iron oxide samples of hematite and goethite. The fact that the Frederick soil contains a strong absorption in the same position as the Miami soil (476 nm) suggests that goethite is present in the Frederick soil but that its influence on soil color is being masked by hematite. This analysis, when supported by some knowledge of the types of iron oxides present, illustrates the power of the second derivative in detecting subtle differences in the reflectance spectra of soils.

It should be noted at this point that absorption bands in the near infrared wavelength region appeared only as weak broad features in all the soils examined in this study. The significant absorptions in this region found in the pure iron oxide samples are apparently masked and reduced when the iron oxides occur in the presence of other soil constituents. This result indicates that more information may be obtained about the iron oxides of soils by examination of the visible wavelength region.

The spectral reflectance of a Brookston soil with an organic matter content of 5.4%, is presented for comparison in Figure 20. The increase in organic matter results in a lower overall level of reflectance and a rather featureless spectrum. The second derivative, however, does provide some detailed information on the slight inflection in the visible wavelength region. Comparison of the Brookston and Miami second derivatives (Figure 22) shows the influence of iron oxide absorption on the reflectance spectrum of the Brookston soil. Use of the second derivative for this type of analysis should aid in determining the point at which one soil

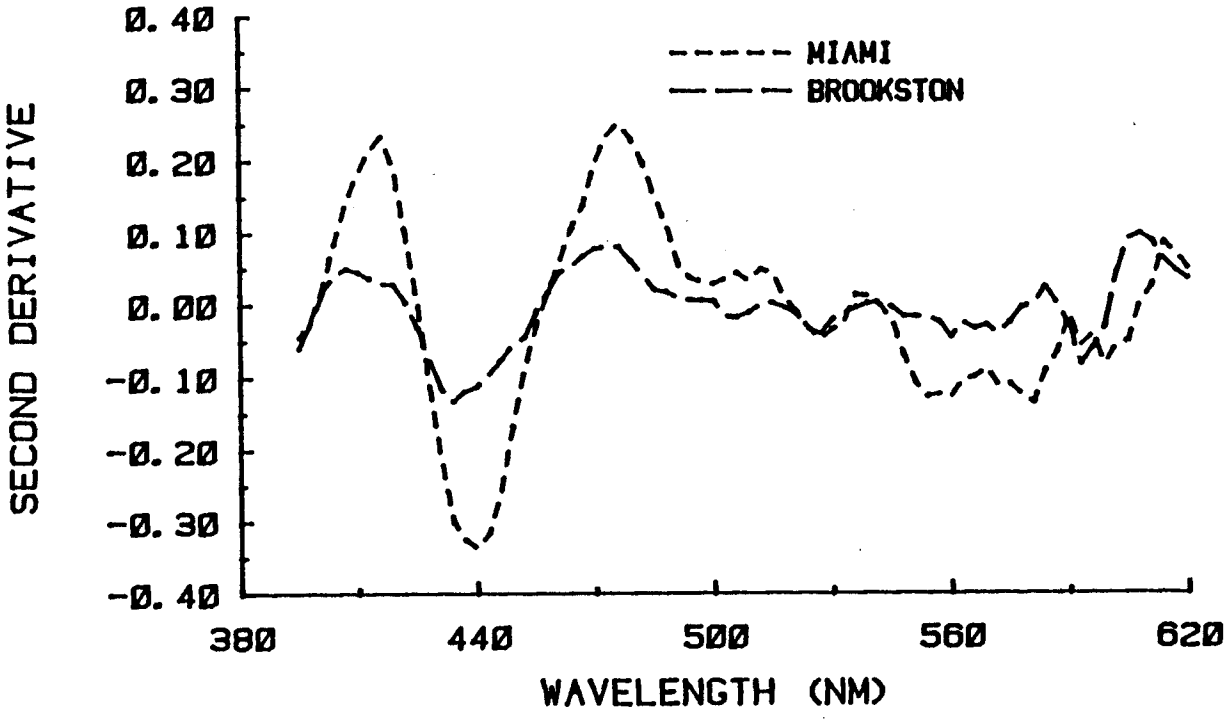

Figure 22. Second derivatives (380 - 620 nm) of the reflectance spectra of the Miami and Brookston soils.

constituent begins to mask the effect of another on soil reflectance.

To further illustrate the influence of organic matter on soil reflectance three Brookston soil samples are presented (Figure 23). The increase in organic matter content causes both a lowering of the level of reflectance and a change in the general overall shape of the spectral response from convex to concave. The second derivatives of these spectra (Figure 24) show how this increase in organic matter content masks the influence of iron oxides on the shape of the spectra in the visible wavelength region. The increase in organic matter content results in a decreased intensity of expression of the iron oxide absorptions. The influence of increased organic matter content on the second derivative near 440 nm suggests that the shape of the reflectance spectrum is affected by this soil component to some degree.

Soil Erosion Study

The development of a model from which basic questions about reflectance and soil erosion can be answered requires a detailed knowledge of the chemical and physical properties of the soils under study. The characterization of how these chemical and physical properties change as erosion progresses is also essential for accurate assessment of soil erosion.

This study examined three common Alfisols developed under forest vegetation on slightly different glacial parent materials. A detailed description of sample site selection and the method used to simulate erosion within these soils is presented in the methods and

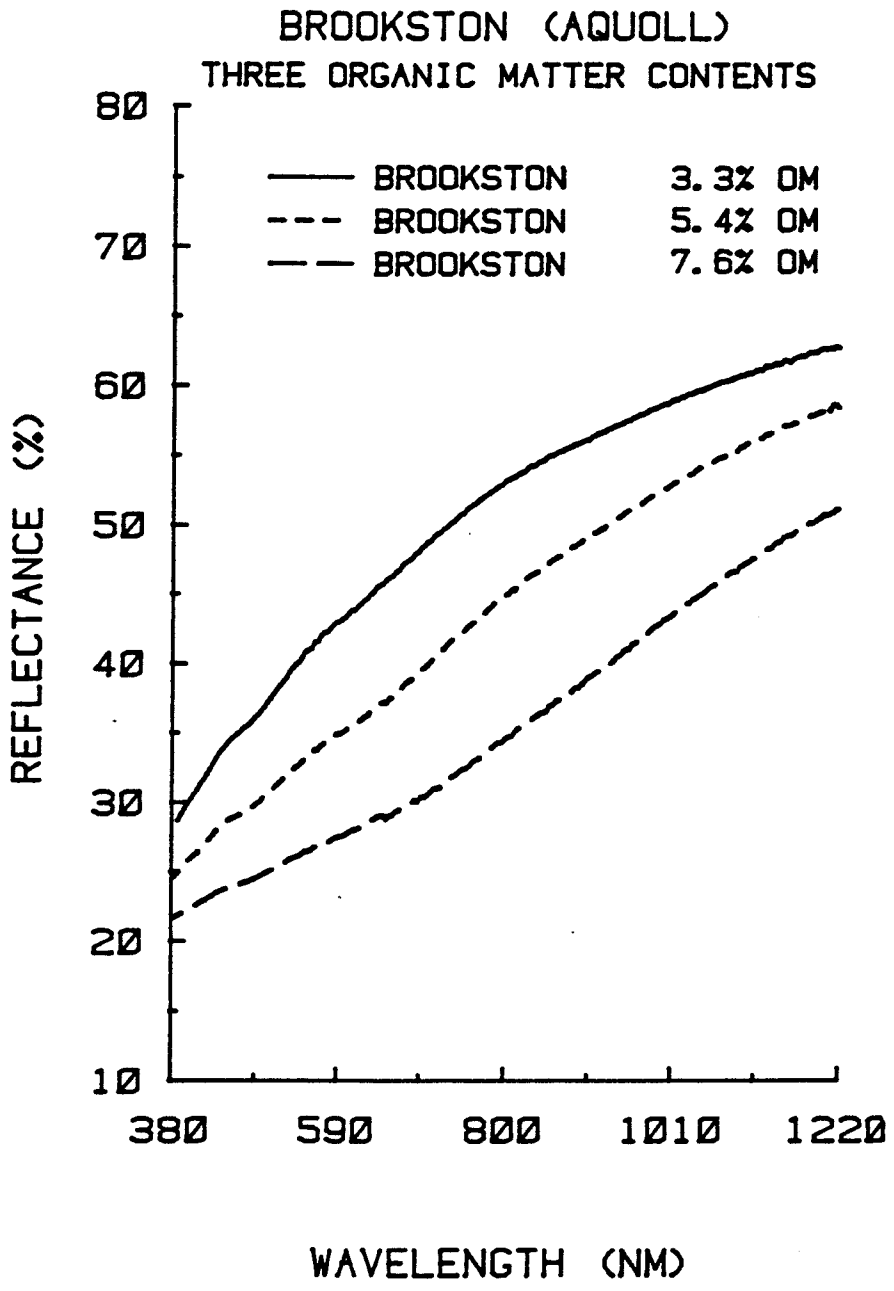

Figure 23. Reflectance spectra of Brookston soils: 3.3% OM, 5.4% OM, 7.6% OM.

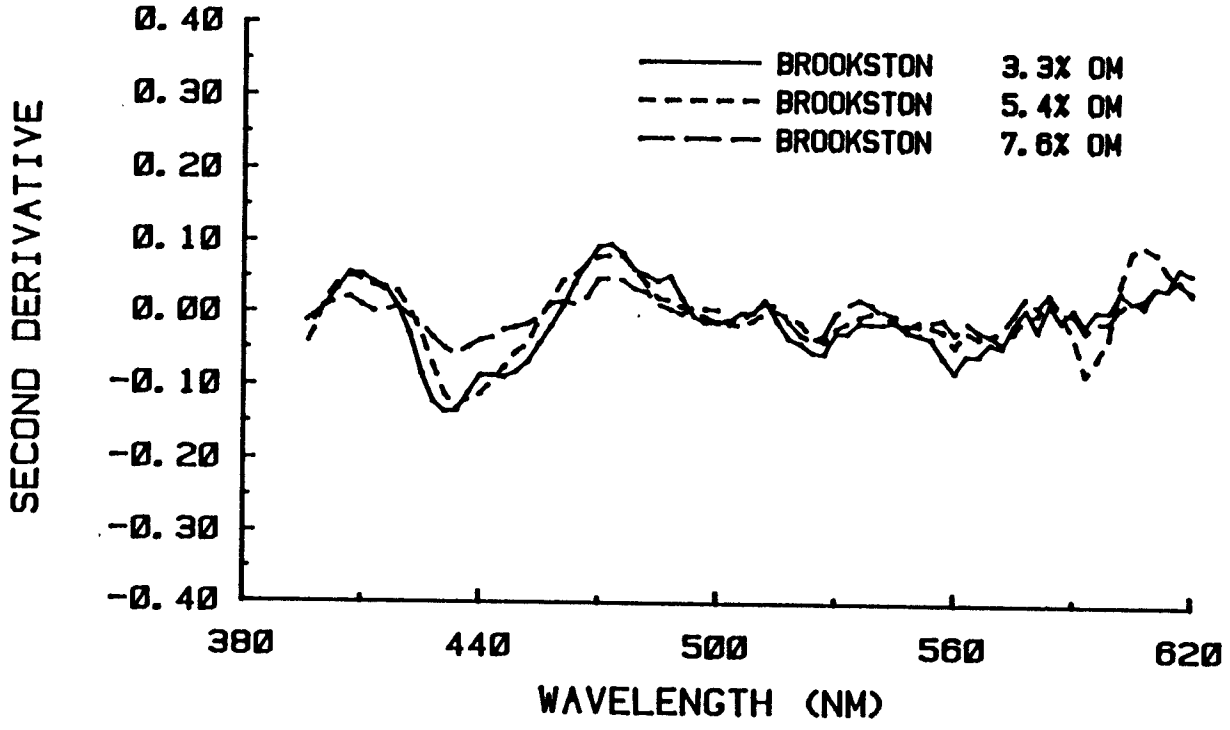

Figure 24. Second derivatives (380 - 620 nm) of the reflectance spectra of Brookston soils: 3.3% OM, 5.4% OM, 7.6% OM.

materials section. The important point with regards to the results obtained is that three very similar Alfisols were used to try to represent the range of soil properties most likely to occur in the field for any one of these three potentially erosive soils. The results of chemical and physical analyses are presented in Table 4. Two factors which strongly affect soil reflectance and are highly correlated with the degree of soil erosion are organic matter and iron oxide content. Chemical analysis showed that organic matter content decreased as the degree of erosion increased (Figure 25). Conversely the iron oxide content increased as the degree of erosion increased (Figure 26). Note that the range of organic matter contents for the three soils is much greater than the range of iron oxide contents. Also note that the range in either of these two factors is very small within a progression of erosion classes for any one soil.

Since these two factors, organic matter and iron oxide, are inversely related with respect to the degree of soil erosion, the ratio of organic matter to iron oxide content (OM/Fe oxide) is proposed as an aid in the classification of these eroded soils. This ratio helps to excentuate the differences between the erosion classes and should provide for a more accurate classification. The OM/Fe oxide ratios are plotted in Figure 27 for the three soils under study. The plot indicates that the OM/Fe oxide ratio for each soil decreases with an increase in the degree of soil erosion. The major objective in formulating a model for these soils is to determine how best to estimate this ratio from spectral reflectance data.

Table 4. Organic matter and iron oxide contents of the simulated erosion sequences.

Soil	Simulated Erosion Class	% OM	% Fe_2O_3
RUSSELL	None - Slight	3.17	0.96
	Slight	2.71	1.04
	Moderate	2.36	1.10
	Severe	2.09	1.17
	Very Severe	1.82	1.22
MORLEY	None - Slight	2.47	1.11
	Slight	2.20	1.14
	Moderate	2.03	1.21
	Severe	1.63	1.30
	Very Severe	1.44	1.43
MIAMI	None - Slight	1.60	1.25
	Slight	1.50	1.34
	Moderate	1.30	1.44
	Severe	1.11	1.51
	Very Severe	0.97	1.59

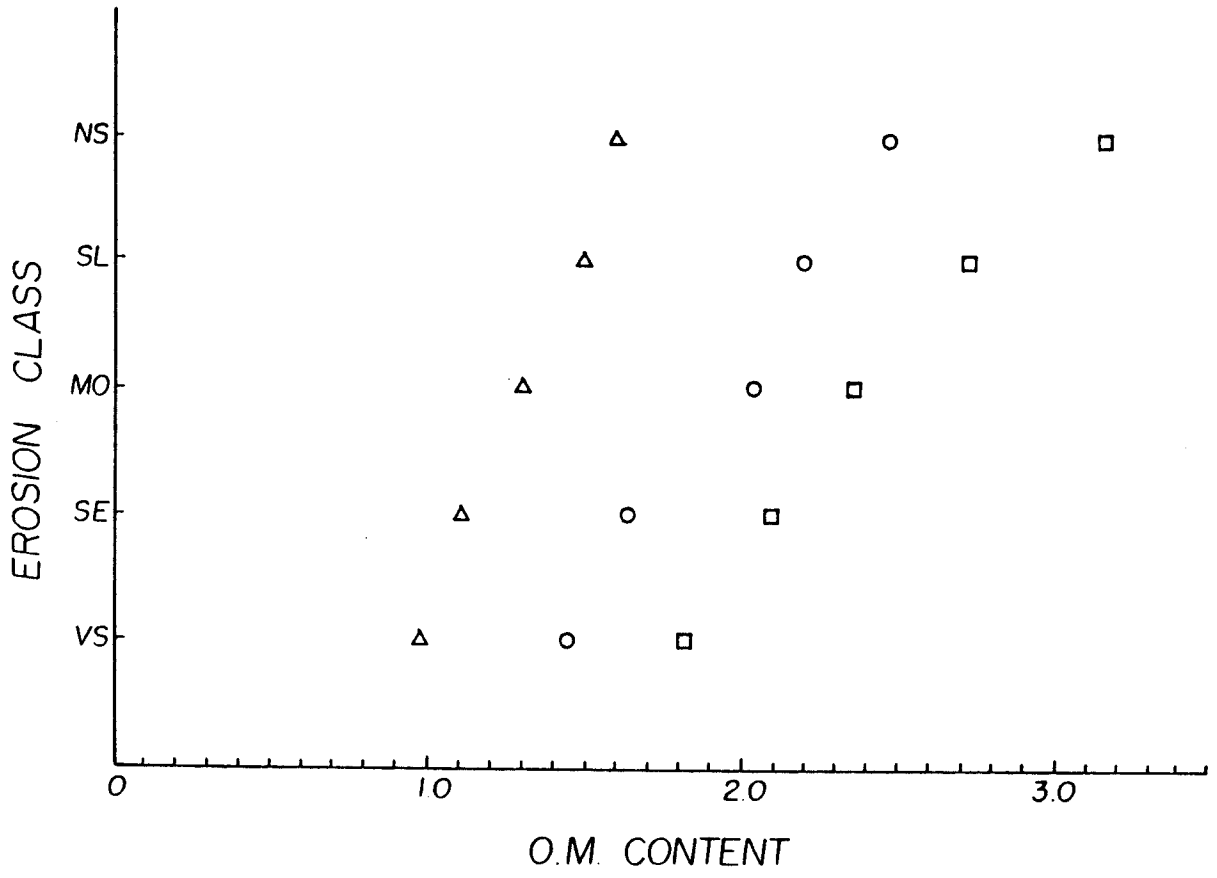

Figure 25. **Erosion class vs. organic matter content** for the simulated erosion sequences: Δ Miami, O Morley, □ Russell.

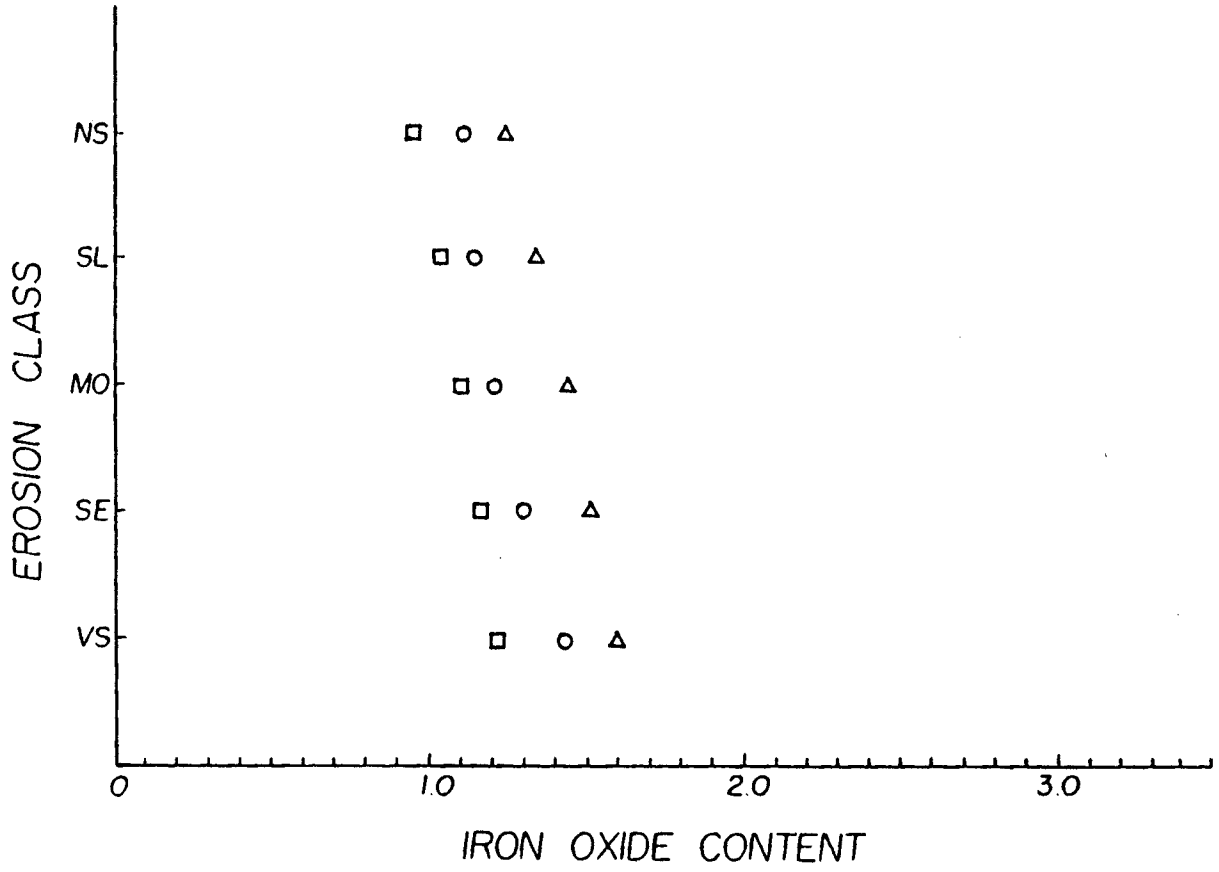

Figure 26. **Erosion class vs.** iron oxide content for the simulated erosion sequences: Δ Miami, O Morley, □ Russell.

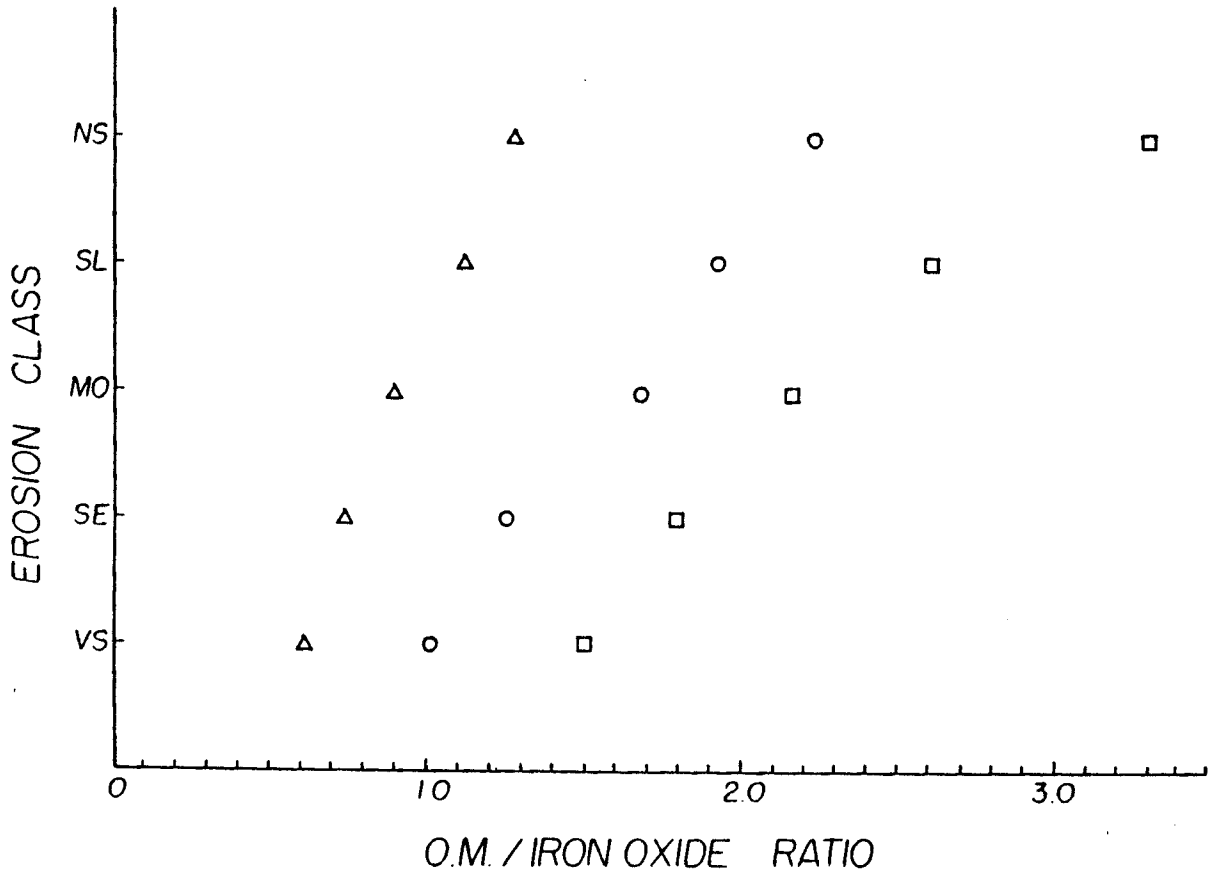

Figure 27. Erosion class vs. OM/Fe oxide ratio for the simulated erosion sequences: Δ Miami, O Morley, □ Russell.

The information obtained through the study of how various soil components affect the spectral response was utilized to determine the optimum wavelength bands for predicting soil organic matter and iron oxide contents. The spectral reflectance of three erosion classes of the Miami, Morley, and Russell soils are presented in Figures 28, 29 and 30. In these soils the level of reflectance generally increases as the severity of erosion increases. The comparison of pure soil components suggests that the shape of the spectral response may help to more accurately predict the content of a specific factor influencing reflectance. An examination of the second derivatives of these soils should determine if significant differences in the shape of the spectra do indeed exist. The Miami second derivatives (Figure 31) indicate that the shape of the spectral response changes only slightly in the 380-620 nm wavelength region regardless of the chemical analysis or erosion class. The Morley second derivatives (Figure 32) indicate that the intensity of the inflection at 476 nm increases as the severity of erosion increases. This coincides with an increase in the iron oxide content. A similar trend is observed in the Russell soil (Figure 33). The influence of organic matter on the shape of the Russell none-slightly eroded soil spectrum is suggested by the shoulder in the second derivative at 450 nm. The usefulness of the second derivative in evaluating the spectra of these soils is limited by a lack of information concerning the combined effects of iron oxide and organic matter on the absorption bands of the visible wavelength region. Although further study is needed in this regard the data presented above indicates that organic matter may be influencing the

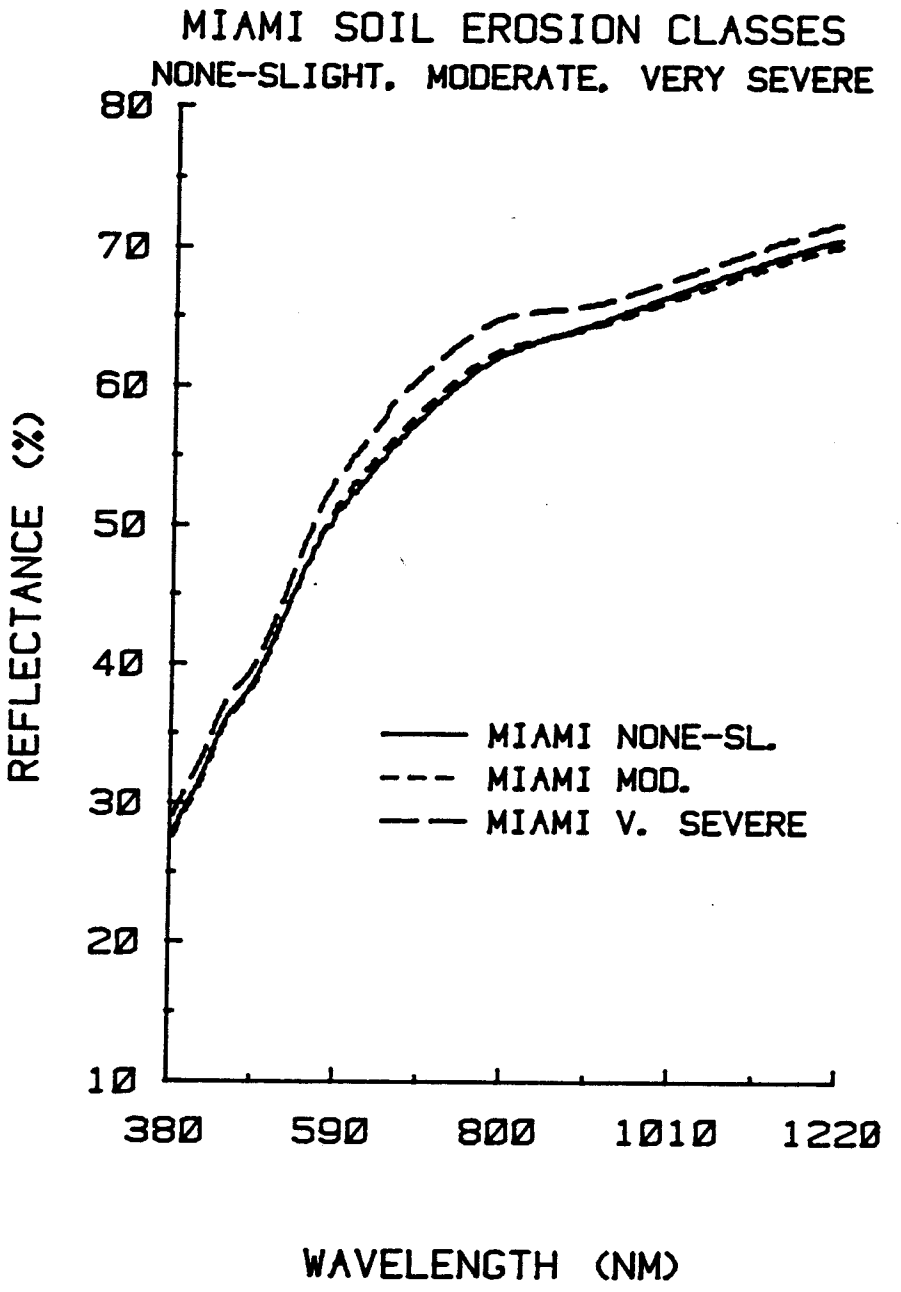

Figure 28. Reflectance spectra for the Miami soil erosion classes: none-slight, moderate, very severe.

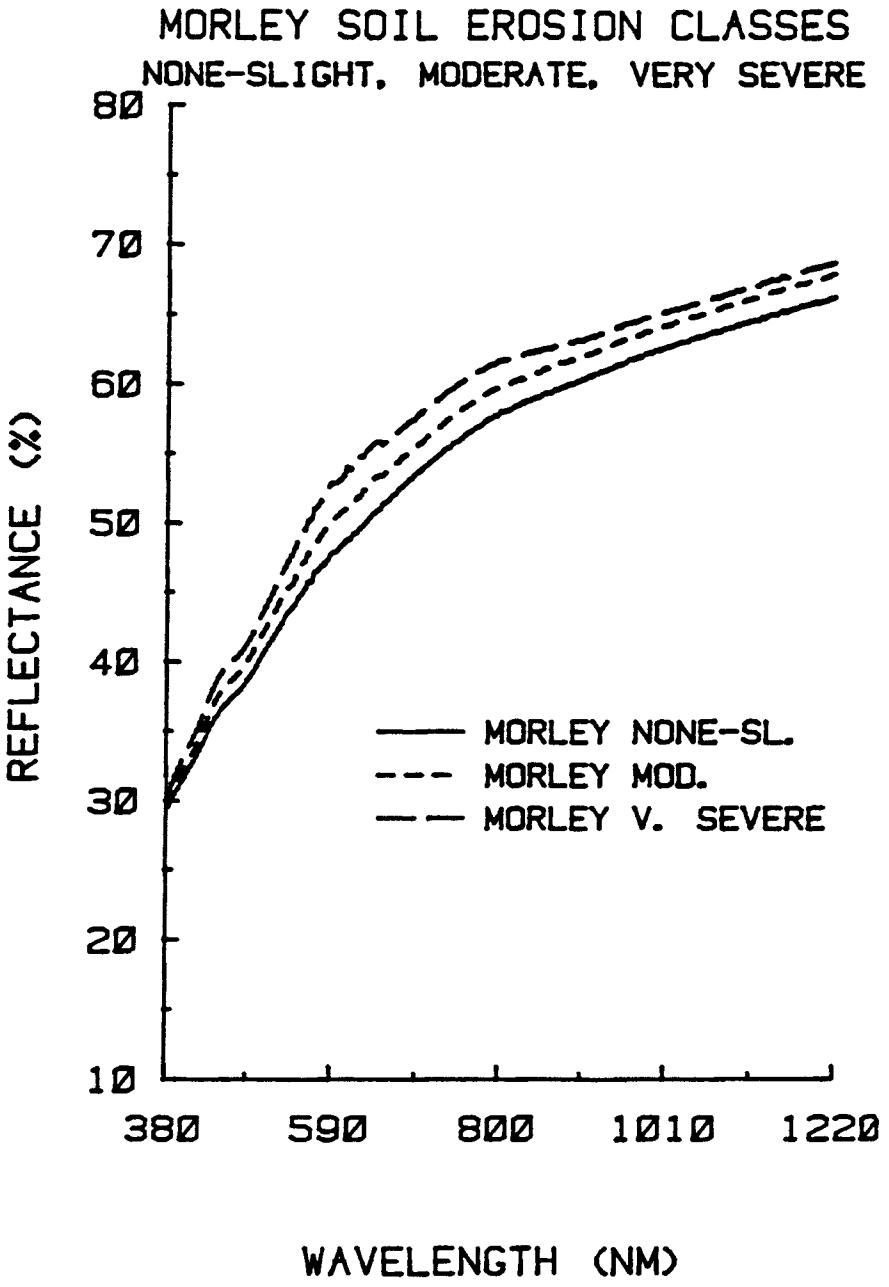

Figure 29. Reflectance spectra for the Morley soil erosion classes: none-slight, moderate, very severe.

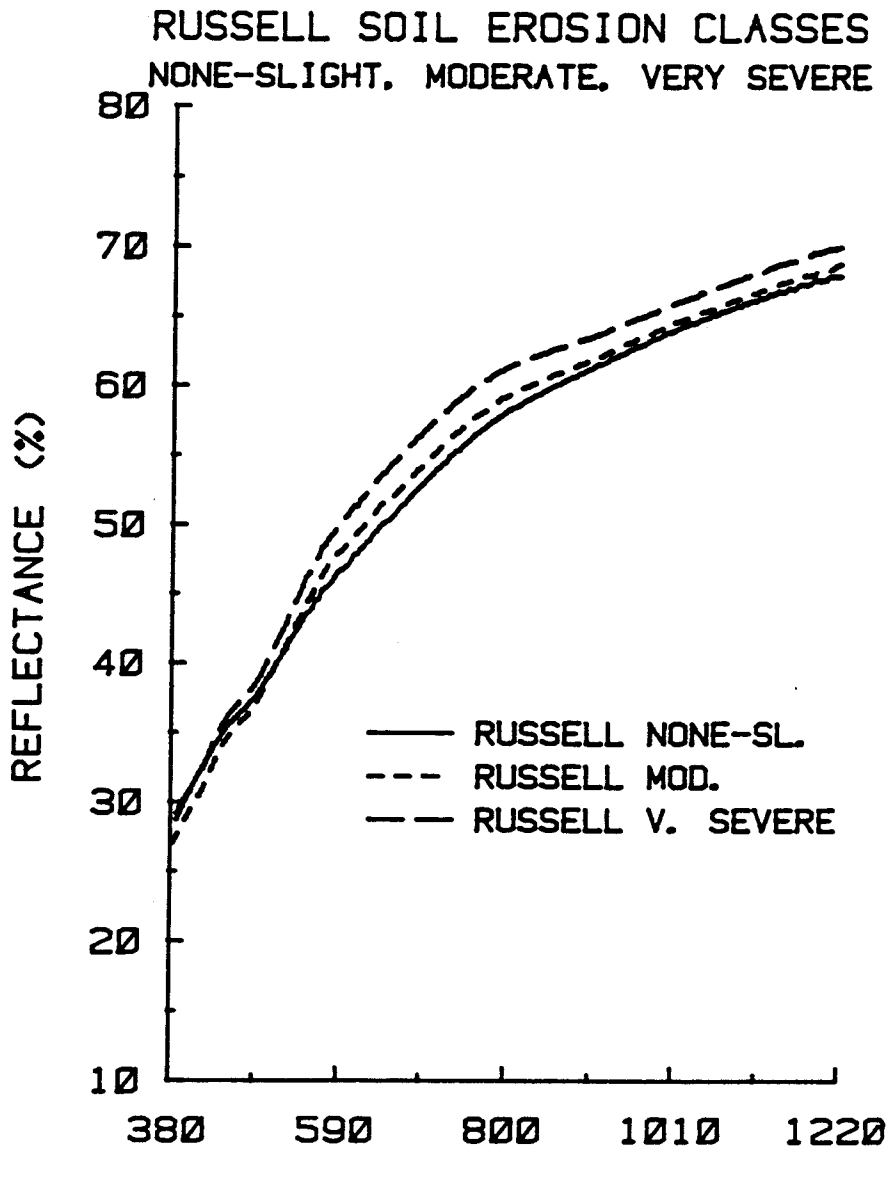

Figure 30. Reflectance spectra for the Russell soil erosion classes: none-slight, moderate, very severe.

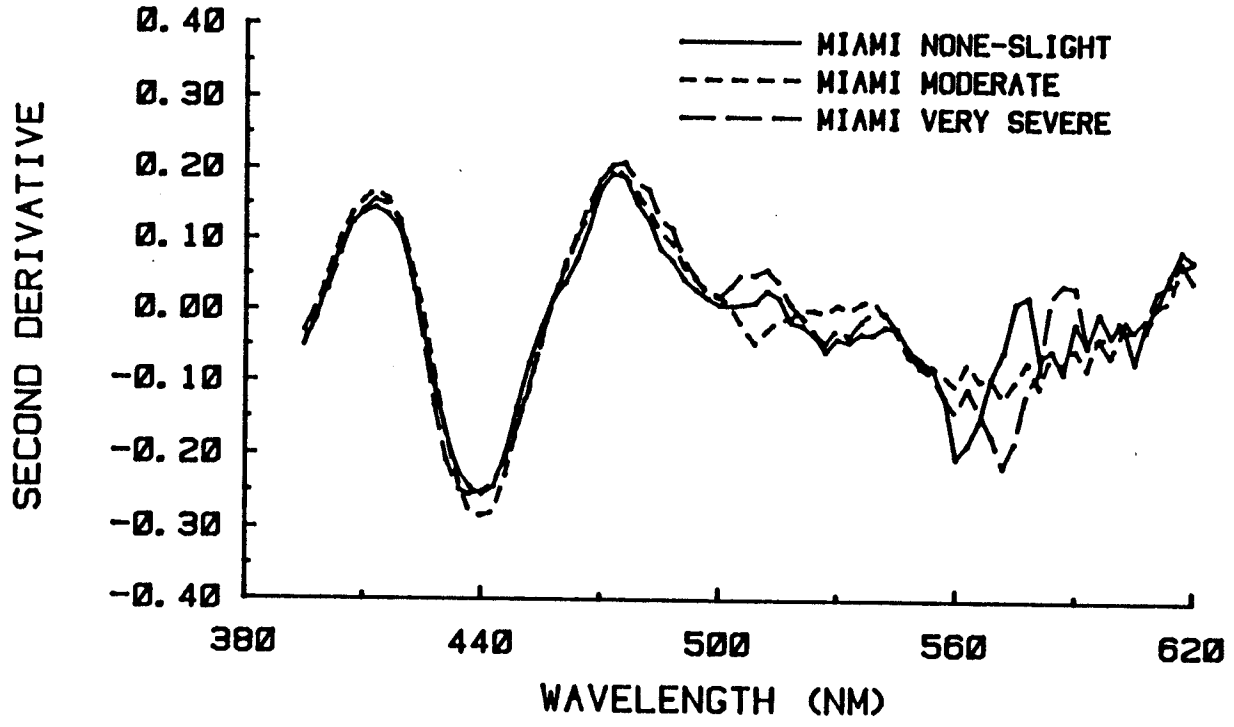

Figure 31. Second derivatives (380-620 nm) of the reflectance spectra of the Miami soil erosion classes: none-slight, moderate, very severe.

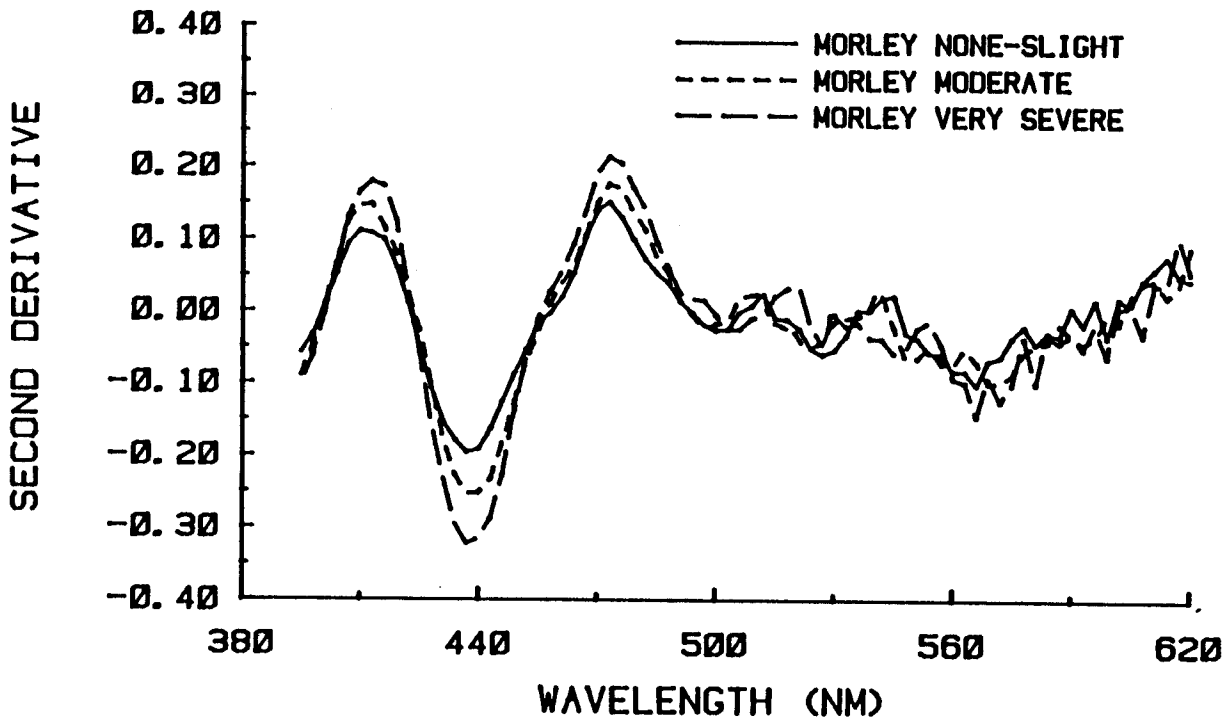

Figure 32. Second derivatives (380-620 nm) of the reflectance spectra of the Morley soil erosion classes: none-slight, moderate, very severe.

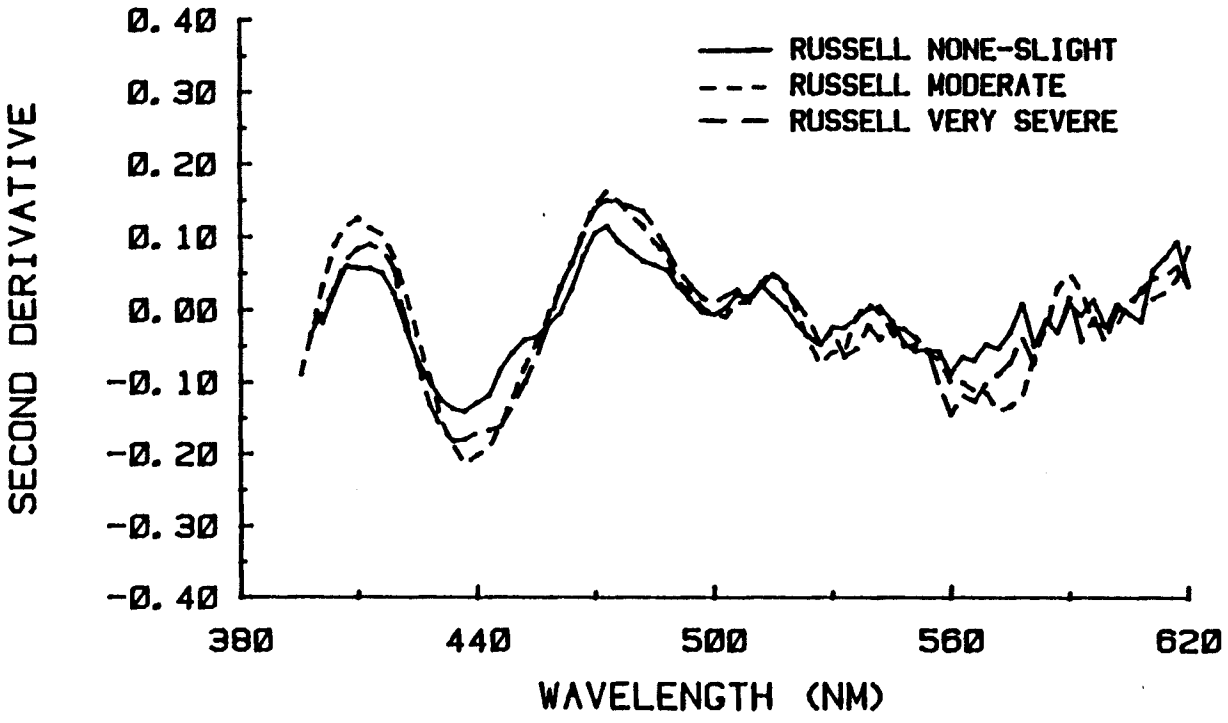

Figure 33. Second derivatives (380-620 nm) of the reflectance spectra of the Russell soil erosion classes: none-slight, moderate, very severe.

shape of the spectra when its content in soils reaches approximately 2.5%. This result is very close to the 2.0% level which was proposed by Baumgardner et al. (1970) as the point at which organic matter begins to mask the influence of other soil constituents, such as iron oxides.

A measure of the shape, or more specifically the slope, of the spectrum from 485 to 560 nm was found to be directly related to the content of iron oxide in these soil samples. The difference between the reflectance values (R_{560}-R_{485}) for all fifteen soil samples resulted in a coefficient of determination (r^2) of 0.73. Adding this value (R_{560}-R_{485}) to the percent reflectance at 660 nm produced the best predictor of iron oxide content (r^2=0.91).

$$\%Fe_2O_3 = R_{660} + (R_{560} - R_{485})$$

The reflectance at 660 nm was also the best predictor of organic matter content. The coefficient of determination (r^2) for organic matter content prediction at 660 nm was 0.94. The fact that the percent reflectance at 660 nm was an aid in predicting both organic matter and iron oxide contents is a function of the inverse relationship within the simulated erosion sequences. However, prediction of organic matter at 660 nm is justified by the lack of strong iron absorption bands in this region. Also, the high level of reflectance in this region enhances the separation of soils with different organic matter contents. This is illustrated with the Brookston soil samples (Figure 23).

The use of reflectance values at 485, 560, and 660 nm corresponded with the first three spectral bands of the Landsat D MSS, and provided an accurate prediction of % iron oxide, % organic matter, and the OM/Fe oxide ratio calculated from chemical data resulted in a coefficient of determination (r^2) of 0.95. These predicted ratios (solid symbols) are plotted with the ratios determined from chemical analysis (open symbols) in Figure 34. The accuracy of this prediction suggests that the classification of eroded soils is possible if prior knowledge of the specific soil series being classified is available. This site specific information is required because the range and variation in the OM/Fe oxide ratio is unique for each soil series.

Given this restraint the model developed above was tested on ten Morley soil samples which were collected and classified in the field with respect to their degree of erosion by the Soil Conservation Service. Chemical analyses for the ten samples show that the OM/Fe oxide ratio is an excellent predictor of erosion class when referenced to the simulated Morley erosion sequence (Table 5). The consistency of this classification was enhanced by the fact that the Morley field samples were all located in Whitley County. This was the same county sampled to provide data for the Morley simulated erosion sequence.

The application of the model developed for obtaining the OM/Fe oxide ratio from spectral reflectance data of the simulated soil erosion sequences did not result in the accurate classification of erosion for the ten Morley field samples (Table 5). Organic matter was generally overestimated in the high iron oxide soils

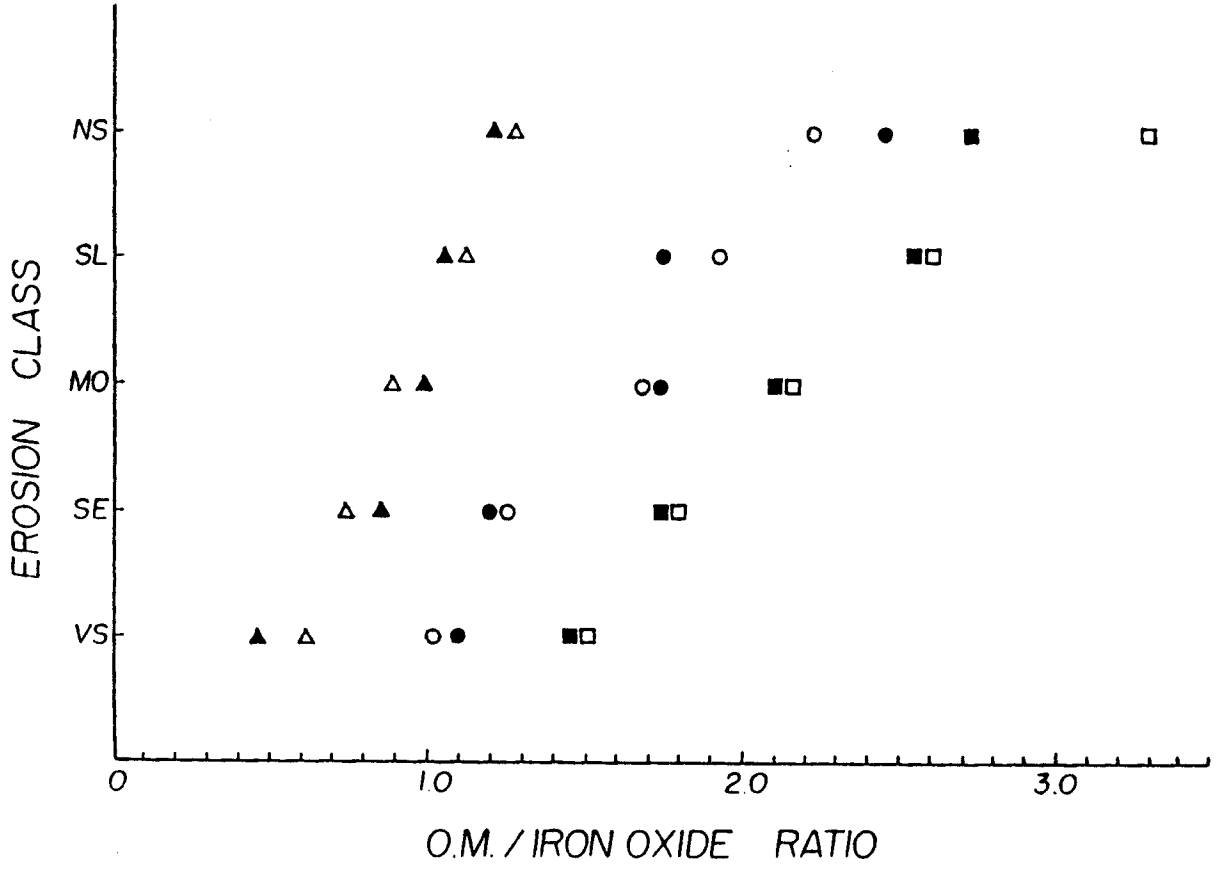

Figure 34. Erosion class for simulated erosion samples vs. OM/Fe oxide ratio: chemical data (open), reflectance data (solid); Δ Miami, O Morley, □ Russell.

Table 5. Erosion classification for Morley field samples using chemical and reflectance data.

Soil No.	Erosion Class	Chemical			Chemically Predicted Erosion Class from Ratio	Predicted from Reflectance			Reflectance Predicted Erosion Class from Ratio
		%OM	$\%Fe_2O_3$	OM/Fe ratio		%OM	$\%Fe_2O_3$	OM/Fe ratio	
1	NS(1)	2.44	1.08	2.26	NS	0.63	1.50	0.42	VS
2	NS(1)	2.34	1.25	1.87	SL	2.21	1.12	1.97	SL
3	NS(1)	2.99	1.23	2.43	NS	2.03	1.16	1.75	MO
4	M(2)	1.91	1.43	1.33	SE	1.71	1.32	1.29	SE
5	M(2)	1.31	1.55	0.84	VS	1.04	1.51	0.69	VS
6	M(2)	1.94	1.38	1.40	SE	1.39	1.39	1.00	VS
7	M(2)	2.03	1.85	1.10	SE	1.14	1.48	0.77	VS
8	S(3)	1.39	2.20	0.63	VS	2.08	1.29	1.61	MO
9	S(3)	1.29	1.79	0.72	VS	2.44	1.19	2.05	SL
10	VS(4)	1.50	1.89	0.79	VS	2.32	1.23	1.89	MO

which resulted in high OM/Fe oxide ratios for the severely eroded soils. The explanation for this poor classification is related to the inability of the simulation to account for the effects of high iron oxide contents on the percent reflectance at 660 nm (Note Morley samples 8, 9 and 10). This result can be explained in that both iron oxide and organic matter cause a decrease in total soil reflectance in this region of the spectrum. Since the simulated samples did not contain very high (>1.6%) amounts of iron oxide, the equation for predicting iron oxide content failed when applied to field samples with higher iron oxide contents. In essence most of the reflectance changes observed at 660 nm in the simulated samples were due to decreases in organic matter content.

Since the ten Morley field samples provide a wider range of chemical properties than the simulated samples, a model was developed with the Morley field samples as the data base. Given the results of the previous analysis, a predictor of iron oxide may be more useful if it is determined from the reflectance at only two wavelengths, 485 nm and 560 nm. The 485 to 560 nm region appears to be essentially an independent predictor of iron oxide content. The following equation is proposed to predict iron oxide content:

$$\%Fe_2O_3 = b_1(R_{560}) + b_2(R_{485})$$

Computer analysis using the ten Morley samples yielded an r^2 of 0.98 between chemical and predicted iron oxide contents. The final form of the equation contains the parameters $b_1 = 0.2690$ and $b_2 = -0.2924$.

The next step in the analysis involved using the prediction of iron oxide to help predict organic matter content at 660 nm. In the previous mathematical approach organic matter was over predicted at high concentrations of iron oxide. With this in mind the equation below was developed to predict organic matter at 660 nm more accurately by taking advantage of our ability to predict iron oxide from another wavelength region.

$$\%OM = b_3(R_{660}) + [b_4(b_1(R_{560}) + b_2(R_{485})]$$

or

$$\%OM = b_3(R_{660}) + [b_4(\text{Equation for predicting \% } Fe_2O_3)]$$

The final form of the equation contains the parameters b_3 = 0.0768 and b_4 = -1.4786. The r^2 between chemical and predicted organic matter contents of the ten Morley samples used as the data base is 0.98.

This model was tested on the entire set of simulated samples. The results of the predictions are presented in Table 6 and provide both promise and insight into our ability to classify eroded soils. Several trends are apparent when the data set is analyzed as a whole. One very significant result is that the OM/Fe oxide ratio (r^2 = 0.91) generally decreases with increased erosion. This trend, which is proposed as a predictor of erosion class, was not well estimated with the simplified model using the simulated erosion samples which was previously presented. Also, the prediction of the

Table 6. Comparison of chemically determined and predicted organic matter and iron oxide contents for the simulated erosion samples using reflectance data.

Soil Sample	Erosion Class	Chemical			Predicted from Reflectance		
		%OM	$\%Fe_2O_3$	OM/Fe ratio	%OM	$\%Fe_2O_3$	OM/Fe ratio
Russell	NS	3.17	0.96	3.30	2.40	1.01	2.37
	SL	2.71	1.04	2.61	2.02	1.26	1.61
	MO	2.36	1.10	2.15	1.92	1.41	1.37
	SE	2.09	1.17	1.79	1.79	1.55	1.54
	VS	1.82	1.22	1.49	1.98	1.49	1.33
Morley	NS	2.47	1.11	2.23	2.47	1.01	2.44
	SL	2.20	1.14	1.93	2.59	1.04	2.49
	MO	2.03	1.21	1.68	2.43	1.15	2.12
	SE	1.63	1.30	1.25	2.27	1.35	1.68
	VS	1.44	1.43	1.00	2.21	1.41	1.57
Miami	NS	1.60	1.25	1.28	1.78	1.70	1.05
	SL	1.50	1.34	1.12	1.66	1.74	0.95
	MO	1.30	1.44	0.90	1.66	1.80	0.92
	SE	1.11	1.51	0.74	1.55	1.90	0.82
	VS	0.97	1.59	0.61	1.70	1.91	0.89

iron oxide content is very good with some estimates extremely accurate. The prediction of organic matter content (r^2 = 0.93), although not as accurate as those for iron oxide (r^2 = 0.95), are much improved over the previous attempt. In summary, the results of this model tested on all three soil series provide an optimistic view of our ability to accurately classify erosion in the field.

Particular attention should be given to the Morley simulated samples. Since the equations were constructed with data from ten Morley field samples, one would expect that if any samples would classify accurately it would be the Morley simulated samples. In fact this is the case in that the OM/Fe oxide ratio yielded a range which could be used to classify erosion. In addition it is important to remember that the simulated samples represent a narrower range of properties than is found in the Morley field samples. Thus, it is proposed that field samples at either end of the range would be even easier to classify than the simulated samples.

To test this hypothesis a group of fourteen field samples were analyzed both chemically and spectrally (Table 7). The samples represent Russell, Morley, and Miami soils from various regions of Indiana. They were collected by the Soil Conservation Service for description and study by the Purdue University Soil Characterization Laboratory. Note that the range of properties is very similar to those of the Morley field samples used to develop the equations. However, the geographic distribution of these samples introduces variability in climatic and other soil forming factors beyond those present in the ten Morley field samples which are the base for the

Table 7. Erosion classification for selected field soils using chemical and reflectance data.

Soil Sample	Erosion Class	Chemical			Chemically Predicted Erosion Class from Ratio	Predicted from Reflectance			Reflectance Predicted Erosion Class from Ratio
		%OM	$\%Fe_2O_3$	OM/Fe ratio		%OM	$\%Fe_2O_3$	OM/Fe ratio	
Russell	11 NS	2.05	1.01	2.03	NS	2.59	1.19	2.17	NS
	12 NS	2.89	0.93	3.10	NS	2.56	1.11	2.32	NS
	13 NS	2.15	0.81	2.65	NS	2.93	0.81	3.60	NS
	21 MO	1.16	1.74	0.66	SE	1.40	1.98	0.70	SE
	22 MO	2.80	1.17	2.39	NS	2.38	1.33	1.79	MO
Morley	21 MO	2.27	1.35	1.68	MO	2.43	1.17	2.08	NS
	22 MO	2.49	1.22	2.04	NS	2.41	1.18	2.04	NS
	23 MO	2.33	1.38	1.69	MO	1.92	1.52	1.26	MO
	31 SE	2.99	2.08	1.44	MO	1.26	1.71	0.74	SE
Miami	11 NS	3.08	1.15	2.68	NS	2.81	0.75	3.75	NS
	21 MO	2.78	1.18	2.36	NS	2.44	1.14	2.14	NS
	22 MO	1.96	1.25	1.57	MO	2.05	1.48	1.38	MO
	23 MO	1.86	1.46	1.27	MO	1.32	1.89	0.70	SE
	24 MO	1.37	1.64	0.84	SE	1.02	2.16	0.47	SE

equations. Spectral analysis of these soils helps determine the extendability of a model developed from Morley field samples to other very similar Alfisols (Table 7). The results are promising with an $r^2 = 0.94$ for the prediction of organic matter, $r^2 = 0.96$ for prediction of iron oxide, and $r^2 = 0.92$ for the prediction of the OM/Fe oxide ratio. Closer examination of the data verifies their significance. All four soils classified in the field by the Soil Conservation Service as none-slightly eroded have very high OM/Fe oxide ratios. The one soil classified as severely eroded has a very low OM/Fe oxide ratio. Also of interest is the observation that some soils classified by the Soil Conservation Service as moderately eroded have chemical and spectral properties which would indicate that they may be either none-slightly or severely eroded. One possible explanation for this is that soil surveyors in the field have a tendency to classify those soils which are not near the extremes of the scale as moderately eroded. This illustrates the fact that field classification of erosion is a difficult and often subjective task. The surveyor is asked to map soil which is no longer present. This human judgment is eliminated with spectral classification once the class limits have been assigned.

These results also suggest that the narrower range of properties found in the "simulated erosion" samples are a function of our inability to simulate biological, chemical, and other soil forming factors through a laboratory mixing procedure.

General Comments

Throughout this study the accuracy and consistency of the spectral data are testimony to the viability of the method of study and procedures used in this research. The ability of the Cary spectrophotometer and accompanying instrumentation to perform high quality soil reflectance research is unquestioned. Indeed the applications of the knowledge gained through this type of research approach are unlimited with respect to many soil mapping procedures and problems, not just soil erosion mapping.

In most research projects questions arise from resultant data and interpretations which the experiment was neither designed nor intended to answer. This study is no exception in that the data presented invite discussion of issues unanticipated at its outset. These issues relate not only to the mapping of soil erosion but also to the process and study of soil erosion itself.

The results of this study should be viewed in perspective, with the objectives of the experiment held as a guide to ascertain their validity. We began by asking "Can remote sensing technology provide the researcher and land manager with quantitative information on soil erosion?" More specifically, our objective was to assess "the ultimate goal of accurately delineating, monitoring, and quantifying soil erosion with remote sensing techniques." In assessing this goal the initial question regarding the degree of spectral separability of soil erosion classes was given highest priority.

Viewed in this light the results indicate that classes of soil erosion are spectrally separable, and that the degree of this separability is significant for those soils examined. The proposed

use of the OM/Fe oxide ratio as a quantitative method of classification is justified by the results of chemical and spectral analyses. However, when this information is used to assess "the ultimate goal of accurately delineating, monitoring, and quantifying soil erosion with remote sensing techniques", it must again be viewed in perspective. This is not to say that the conclusions will necessarily be negative, but rather to promote examination of the data in a detailed and constructive manner. Thus the applicability of the results of this study must be tested in the field in order to truly assess their significance.

It is clear that the study of erosion as a "localized phenomenon" offers great opportunities to learn more about the natural dynamics of the soil erosion problem and its solutions. There is every reason to believe that remote sensing technology can provide quantitative information on soil erosion to aid in the control of this worldwide crisis.

SUMMARY AND CONCLUSIONS

The analysis of goethite and hematite spectra with respect to their chemical composition and absorptive properties provides insight into how these iron oxides influence soil color. The basic difference in the color of the two iron oxides is determined by the position and intensity of iron absorption bands in the visible region. Goethite has a strong absorption band at 520 nm while hematite's is at a slightly higher wavelength (560 nm). When even small amounts of hematite are present in the soil the green, and to a lesser degree, yellow, wavelengths are absorbed very strongly. Thus the presence of goethite is masked by hematite because of hematite's strong absorptive capacity in the green region of the spectrum. Also, water absorption bands at 940 and 1130 nm may have a dramatic effect on the shape and magnitude of the reflectance spectra of iron oxides in the near-infrared wavelength region.

The use of the computer-interfaced Cary 17D spectrophotometer for soil reflectance studies exceeded expectations. This timely method of data collection consistently provided high quality results in a digital form ready for manipulation. The second derivative of the spectral response aided in quantifying the micro-structure of a soil's reflectance. Subtle changes in a soil's reflectance characteristics are quickly identified with this technique.

The characterization of how chemical and physical properties change as erosion progresses is essential for accurate assessment of soil erosion. The chemical analyses of simulated erosion sequences show that two important factors are related to the degree of soil erosion. Organic matter content decreases as the severity of erosion increases while the iron oxide content increases as the severity of erosion increases. These two soil components are also the major factors influencing the spectral reflectance of the eroded Alfisols used in this study.

Since these two factors, organic matter and iron oxide, are inversely related with respect to the degree of soil erosion, the ratio of organic matter/iron oxide content is proposed as an aid in the classification of these eroded soils. This ratio helps to accentuate the differences between erosion classes and should provide for a more accurate classification.

A measure of the shape, or more specifically the slope, of the spectrum from 485 to 560 nm is directly related to the iron oxide content in the soils studied. The reflectance at 660 nm is the best predictor of organic matter when adjusted for iron oxide content by use of the bonds at 485 and 560 nm. These wavelengths correspond to the first three spectral bands of the Landsat D MSS. The following equations are proposed to predict iron oxide and organic matter contents from soil reflectance.

$$\%Fe_2O_3 = b_1(R_{560}) + b_2(R_{485})$$

$$\%OM = b_3(R_{660}) + [b_4(b_1(R_{560}) + b_2(R_{485})]$$

When these equations are tested with field samples, the results indicate an $r^2 = 0.94$ for organic matter, $r^2 = 0.96$ for iron oxide, and $r^2 = 0.92$ for the OM/Fe oxide ratio prediction. This degree of accuracy confirms the view that classes of soil erosion are spectrally separable, and that the separability is significant for those soils examined. To truly assess the significance and applicability of this result, it must be tested in a field mapping study of soil erosion with remote sensing techniques.

BIBLIOGRAPHY

Al-Abbas, A. H., P. H. Swain and M. F. Baumgardner. 1972. Relating organic matter and clay content to the multispectral rediance of soils. Soil Sci. 114(6):447-485.

Angstrom, A. 1925. The albedo of various surfaces of ground. Geografiska Ann. 7:323.

Bailey, P. C. 1960. Absorption and reflectivity measurements on some rare earth iron garnets and -Fe_2O_3. J. Appl. Phys. 31, 395.

Ballhausen, C. J. 1962. Introduction to Ligand Field Theory. McGraw Hill Book Co., New York.

Baumgardner, M. F., S. J. Kristof, C. J. Johannsen and A. Zachary. 1970. Effects of organic matter on the multispectral properties of soils. Proc. of the Indiana Academy of Science 79:413-422.

Beck, R. H., B. F. Robinson, W. W. McFee and J. B. Peterson. 1976. Spectral characteristics of soils related to the interaction of soil moisture, organic carbon and clay content. LARS Information Note 081176. Laboratory for Applications of Remote Sensing, Purdue University, West Lafayette, IN.

Bigham, J. M., D. C. Golden, S. W. Buol, S. B. Weed, and L. H. Bowen. 1978. Iron oxide mineralogy of well-drained ultisols and oxisols: II. Influence on color, surface area, and phosphate retention. Soil Sci. Soc. Am. J. 42:825-830.

Bowers, S. A. and R. J. Hanks. 1965. Reflection of rediant energy from soils. Soil Science 100(2):130-138.

Brady, N. C. 1974. The nature and properties of soils. MacMilliam Publishing Co., Inc., New York, New York. 303.

Bryant, R. 1981. Genesis of the Ryker and Associated Soils in Southern Indiana. Ph.D. Thesis, Purdue University, West Lafayette, Indiana.

Buol, S. W., F. D. Hole, and R. J. McCracken. 1973. Soil genesis and classification. Iowa State Univ. Press, Ames.

Burns, R. G. 1970. Mineralogical application of crystal field theory, Cambridge University Press, London.

Chen, Y., N. Senesi and M. Schnitzer. 1977. Information provided on humic substances by E_4/E_6 ratios. Soil Sci. Soc. Am. J. 41, 352-8.

Cihlar, J. and R. Protz. 1973. Surface characteristics of mapping units related to aerial imaging of soil. Can. J. of Soil Science 53:249-257.

Cipra, J. E., M. F. Baumgardner, E. R. Stoner, R. B. MacDonald. 1971. Measuring radiance characterisitcs of soil with a field spectroradiometer. Soil Science Soc. of Amer. Proc. 35:1014-1017.

Condit, H. R. 1970. The spectral reflectance of American soils. Photogrammetric Engineering 36:955-966.

Curi, N. 1983. Lithosequence and Toposequence of Oxisols from Brazil. Ph.D. Thesis, Purdue University, West Lafayette, Indiana (and personal communication).

Davey, B. G., J. D. Russell and M. J. Wilson. 1975. Iron oxide and clay minerals and their relation to colours of red and yellow podzolic soils near Sydney, Australia. Geoderma, 14:125-138.

Duchaufour, Ph. and B. Souchier. 1978. Roles of iron and clay in genesis of acid soils under a humid, temperate climate. Geoderma, 20:15-26.

FAO. 1978. Methodology for assessing soil degradation. Food and Agriculture Organization - United Nations Development Program. Rome, Italy.

FAO. 1979. A provisional methodology for soil degradation assessment. Food and Agriculture Organization - United Nations Development Program. Rome, Italy.

Faye, G. H. 1971. On the optical spectra of di and trivalent iron in corundum: a discussion. American Mineralogist, Vol. 56.

Franzmeier, D. P., G. C. Steinhardt, J. R. Crum, and L. D. Norton. 1977. Soil characterization in Indiana: I. Field and laboratory procedures. Agric. Exp. Stn. Res. Bull. No. 943. Purdue University. West Lafayette, Indiana.

Gates, D. M. 1963. The energy environment in which we live. Am. Sci. 51:327-348.

Gebermann, A. H. and D. D. Neher. 1979. Reflectance of varying mixtures of a clay soil and sand. Photogrammetric Engineering and Remote Sensing 45(8):1145-1151.

Ghosh, K. and M. Schnitzer. 1979. UV and visible absorption spectroscopic investigations in relation to macromolecular characteristics of humic substances. J. Soil Sci. 30:735-745.

Giese, A. T. and C. S. French. 1955. The analysis of overlapping spectral absorption bands by derivative spectrophotometry. Appl. Spectrosc. 9, 78.

Guruswamy, V., S. J. Kristof and M. F. Baumgardner. 1980. A case study of soil erosion detection by digital analysis of the remotely sensed multispectral Landsat scanner data of a semi-arid land in southern India. Machine Processing of Remotely Sensed Data Symp., Purdue University, West Lafayette, IN. pp. 226-271.

Hager, R. N. 1973. Derivative spectroscopy with emphasis on trace gas analysis. Analytical Chemistry. Vol. 45, No. 13.

Hayes, M.H.B. and R. S. Swift. 1978. Chemistry of soil organic colloids. In, The chemistry of soil constituents, Ed. by D. J. Greenland and M.H.B. Hayes, J. Wiley and Son, New York.

Hawthorne, A. R. and J. H. Thorngate. 1978. Improving analysis from second-derivative uv-absorption spectrometry. Applied Optics. Vol. 17, No. 5.

Hoffer, R. M. and C. J. Johannsen. 1969. Ecological potentials in spectral signature analysis. p. 1-29. in P. L. Johnson (ed.) Remote Sensing in Ecology. Univ. of Georgia Press, Athens.

Hunt, G. R. and H. P. Ross. 1967. A bidirectional reflectance accessory for spectroscopic measurements. App. Optics 6:1687-1690.

Hunt, G. R. and J. W. Salisbury. 1970. Visible and near-infrared spectra of minerals and rocks: I. Silicate minerals. Modern Geology 1:283-300.

Hunt, G. R. and J. W. Salisbury. 1971a. Visible and near-infrared spectra of minerals and rocks: II. Carbonates. Modern Geology 2:23-30.

Hunt, G. R. and J. W. Salisbury, and C. J. Lenhoff. 1971b. Visible and near-infrared spectra of minerals and rocks: III. Oxides and hydroxides. Modern Geology 2:195-205.

Hunt, G. R. and J. W. Salisbury, and C. J. Lenhoff. 1971c. Visible and near-infrared spectra of minerals and rocks: IV. Sulphides and sulphates. Modern Geology 3:1-14.

Hunt, G. R. and J. W. Salisbury, and C. J. Lenhoff. 1973a. Visible and near-infrared spectra of minerals and rocks: VI. Additional silicates. Modern Geology 4:85-106.

Hunt, G. R. and J. W. Salisbury, and C. J. Lenhoff. 1973b. Visible and near-infrared spectra of minerals and rocks: VII. Acidic igneous rocks. Modern Geology 4:217-224.

Hunt, G. R. and J. W. Salisbury, and C. J. Lenhoff. 1973c. Visible and near-infrared spectra of minerals and rocks: VIII. Intermediate igneous rocks. Modern Geology 4:237-244.

Hunt, G. R. and J. W. Salisbury, and C. J. Lenhoff. 1974. Visible and near-infrared spectra of minerals and rocks: IX. Basic and ultrabasic rocks. Modern Geology 5:15-22.

Hunt, G. R. and J. W. Salisbury. 1976a. Visible and near-infrared spectra of minerals and rocks: XI. Sedimentary rocks. Modern Geology 5:211-217.

Hunt, G. R. and J. W. Salisbury. 1976b. Visible and near-infrared spectra of minerals and rocks: XII. Metamorphic rocks. Modern Geology 5:219-228.

Jackson, M. L. 1969. Soil Chemical Analysis. Advanced Course. 2nd edition, 8th printing, 1973. Published by the author, Dept. of Soil Sci., Univ. of Wisconsin, Madison, WI.

Kaminsky, S. A., R. A. Weismiller and B. O. Blair. 1979. An investigation of analysis techniques of Landsat MSS data designed to aid te soil survey. LART Technical Report 080879. Laboratory for Applications of Remote Sensing, Purdue University, West Lafayette, IN.

Karmanov, I. I. 1970. Study of soils from the spectral composition of reflected radiation. Soviet Soil Sci. 4:226-238.

Karmanov, I. I. and V. A. Rozhkov. 1972. Experimental determination of quantitative relationships between the color characteristics of soils and soil constituents. Soviet Soil Sci. 4:666-667.

Kimberlin, L. W. 1976. Conservation treatment of erodible cropland: status and needs. in Soil Erosion: Prediction and Control. Proc. Conf. on Soil Erosion. West Lafayette, IN. pp. 339-346.

Kirschner, F. R., S. A. Kaminsky, R. A. Weismiller, H. R. Sinclair, and E. J. Hinzel. 1978. Map unit composition assessment using drainage classes defined by Landsat data. Soil Sci. Soc. Am. J. 42:768-771.

Kodama, H. and M. Schnitzer. 1977. Effect of fulvic acid on the crystallization of Fe(III) oxides. Geoderma, 19:279-291.

Kohnke, H. 1968. Soil physics. McGraw-Hill Book Company, New York.

Kononova, M. M. 1966. Soil organic matter. Pergamon Press, Oxford.

Krishna Murti, G. S. R., and K. V. S. Satyanaryana. 1971. Influence of chenmical characteristics in the development of soil colour. Geoderma 5:243-248.

Krishnan, P., J. D. Alexander, F. J. Butler and J. W. Hummel. 1980. Reflectance technique for predicting soil organic matter. Soil Sci. Soc. AM. J. 44:1282-1285.

Kristof, S. J., M. F. Baumgardner adn C. J. Johannsen. 1973. Spectral mapping of soil orgnaic matter. LARS Information Note 030773. Laboratory for Applications of Remote Sensing, Purdue University, West Lafayette, IN.

Kristof, S. J. and A. L. Zachary. 1974. Mapping soil types from multi-spectral scanner data. Photogrammetric Eng. 40(12):1427-1434.

Latz, K. 1981. A study of the spectral reflectance of selected eroded soils of Indiana in relationship to their chemical and physical properties. M.S. Thesis. Purdue University. West Lafayette, Indiana.

Leger, R. G., G.J.F. Millette and S. Chomchan. 1979. The effects of organic matter, iron oxides and moisture on the color of two agricultural soils of Quebec. Can. J. Soil Sci. 59:191-202.

Lehmann, G. 1971. On the optical spectra of di and trivalent iron in corundum: reply. American Mineralogist, Vol. 56.

Lehmann, G. and H. Harder. 1970. Optical Spectra of Di and Trivalent Iron in Corundum. American Mineralogist, Vol. 55.

Lindberg, J. D. and D. G. Snyder. 1972. Diffuse reflectance spectra of several clay minerals. American Mineralogist 57:485-493.

Lowdermilk, W. C. 1953. Conquest on the land through seven thousand years. Agric. Info. Bull. 99, U. S. Dept. Agriculture.

Marusak, L. A., R. Messier and W. B. White. 1980. Optical absorption spectrum of hematite, Fe_2O_3 Near IR to UV. J. Phys. Chem. Solids, Vol. 41:981-984.

Matthews, H. L., R. L. Cunningham and G .W. Petersen. 1973b. Spectral reflectance of selected Pennsylvania soils. Soil Sci. Soc. Am. Proc. 37:421-424.

McClure, D. S. 1959. Spectra of ions in crystals. In, Solid State Physics, Academic Press, New York, 9, 399-525.

McClure, D. S. 1962. Optical spectra of transition metal ions in corundum. Jour. Chem. Phys. 36, 2757-2779.

McKeague, J. A., J. E. Brydon and N. M. Miles. 1971. Differentiation of forms of extractable iron and aluminum in soils. Soil Sci. Soc. Am. Proc. 35:33-38.

McKeague, J. A. and J. H. Day. 1966. Dithionite- and oxalate-extractable Fe and Al as aids in differentiating various classes of soils. Can. J. Soil Sci. 46:13-22.

Mehra, O. P. and Jackson, M. L. 1960. Iron oxide removal from soils and clays by a dithionite-citrate system buffered with sodium bicarbonate. 7th Nat. Conf. on Clays and Clay Minerals. pp. 317-327.

Miller, D. M. 1981. The effect of simulated short-term weathering on the distribution of oxalate-soluble iron and aluminum in a till and a loess. M. S. Thesis. Purdue University. West Lafayette, IN.

Montgomery, O. L. and M. F. Baumgardner. 1974. The effects of the physical and chemical properties of soil on the spectral reflectance of soils. LARS Technical Report 112674. Laboratory for Applications of Remote Sensing, Purdue University, West lafayette, IN.

Montgomery, O. L. 1976. An investigation of the relationship between spectral reflectance and the chemical, physical, and genetic characteristics of soils. Ph.D. Thesis. Purdue University West Lafayette, Indiana.

Morgan, R.P.C. 1978. Evaluation of erosion risks and erosion mapping. Assessment of erosion, edited by M. de Boodt. New York: J. Wiley, c. 1980.

Morgan, R.P.C. 1980. Soil erosion, edited by M. J. Kirkby and R.P.C. Morgan. New York: J. Wiley, c. 1980.

Myers, V. I. and W. A. Allen. 1968. Electrooptical remote sensing methods as nondestructive testing and measuring techniques in agriculture. Appl. Optics 7:1819-1838.

Obukhov, A. I. and D. S. Orlov. 1964. Spectral reflectivity of major soil groups and the possibility of using diffuse reflection in soil investigation. Soviet Soil Sci. 2:174-184.

Orlov, D. S. 1966. Quantitative patterns of light reflection by soils I. Influence of particle (aggregate) size on reflectivity. Soviet Soil Sci. 13:1495-1498.

Orlov, D. S. 1972. Modern chemical and physical techniques for studying the nature and structure of soil humic substances. Soviet Soil Sci. 7:55-62.

Orlov, D. S., G. I. Glebova, and K. YE. Midakova. 1966. Analysis of the distribution of iron oxide compounds and humus in the soil profile from spectral brightness curves. Soviet Soil Sci. 13:1482-1486.

Peterson, J. B., R. H. Beck, and B. F. Robinson. 1979. Predictability of change in soil reflectance on wetting. Proc. Symp. Machine Processing of Remotely Sensed Data. 5th (West Lafayette, Indiana) I:253-263.

Planet, W. G. 1970. Some comments on reflectance measurements of wet soils. Remote Sensing of Environment 1:127-129.

Raad, A. T., R. Protz and R. L. Thomas. 1969. Determination of Na-dithionite and NH-oxalate extractable Fe, Al, and Mn in soils by atomic absorption spectroscopy. can. J. Soil Sci. 49:89-94.

Resende, M. 1976. Mineralogy, chemistry, morphology and geomorphology of some soils of the Central Plateau of Brazil. Ph.D. Thesis. Purdue University, Univ. Microfilms. Ann Arbor, Mich. (Mic. No. 77-7519).

Robinson, A. R. and L. D. Meyer. 1976. The Agricultural Research Service national research program on soil erosion by water. in Soil Erosion: Prediction and Control. Proc. Conf. on Soil Erosion. West Lafayette, IN. pp. 90-96.

Schwertmann, U. 1964. The differentiation of iron oxide in soils by a photochemical extraction with acid ammonium oxalate. A. Pflanzenernahr. Dung. Bodenkunde 105:194-201.

Schwertmann, U. 1971. Transformation of hematite to goethite in soils. Nature (London) 232:624-625.

Schwertmann, U. and W. R. Fischer. 1973. Natural "amorphous" ferric hydroxide. Geoderma Intl. J. Soil Sci. 10:237-247.

Schwertmann, U. and Taylor, R. M. 1977. Iron oxides. In: J. B. Dixon and S. B. Weed (Editors), Minerals in Soil Environments. Soil Sci. Soc. Am., Madison, Wisc., pp. 145-180.

SCS-USDA. 1972. Soil survey investigations report no. 1, "Soil survey laboratory methods and procedures for collecting soil samples." U.S. Govt. Printing Office. Washington, D.C.

Seubert, C. E., M. F. Baumgardner, R. A. Weismiller and F .R. Kirschner. 1979. Mapping and estimating areal extent of severely eroded soils of selected sites in northern Indiana. 1979 Machine Processing of Remotely Sensed Data Symp. Purdue University, West Lafayette, IN.

Shields, J. A., E. A. Paul, R. J. St. Arnaud, and W. K. Head. 1968. Spectrophotometric measurement of soil color and its relationship to moisture and organic matter. Can. J. Soil Sci. 48:271-280.

Soileau, J. M. and R. J. McCracken. 1967. Free iron and coloration in certain well-drained coastal plain soils in relation to their other properties and classification. Soil Sci. Soc. Am. Proc. 31:248-255.

Soil Erosion: Prediction and Control. 1976. Proc. Conf. on soil erosion. Purdue University, West Lafayette, IN. Soil conservation Society of America. Special publication #21.

Soil Survey Staff. 1951. Soil sruvey manual. U.S. Dept. of Agriculture Handbook 18. U.S. Govt. Printing office. Washington, D.C.

Soil Survey Staff. 1975. Soil taxonomy - a basic system of soil classification for making and interpreting soil survey. Soil Conservation Service. U.S. Dept. of Agric. Agriculture Handbook No. 436. Washington, D.C.

Stoner, E. R. 1979. Atlas of soil reflectance properties. Agric. Exp. Stn. Res. Bull. #962. Purdue University. West Lafayette, Indiana.

Stoner, E. R. and M. F. Baumgardner. 1980. Physiochemical, site, and bidirectional reflectance factor characteristics of uniformly moist soils. LARS Technical Report 111679. Laboratory for Applications of Remote Sensing, Purdue University, West Lafayette, IN.

Stoner, E. R., M. F. Baumgardner, and P. H. Swain. 1976. Determining density of maize canopy form digitized photographic data. Agron. J. 68:55-59.

Stoner, E. R., M. F. Baumgardner, R. A. Weismiller, L. L. Biegl, and B. F. Robinson. 1979. Extension of laboratory-measured soil spectra to field conditions. Proc. Symp. Machine Processing of Remotely Sensed Data. 5th (West Lafayette, Indiana) I:253-263.

Stoner, E. R. and E. H. Horvath. 1971. The effect of cultural practices on multispectral response from surface soil. Proc. Intern. Symp. on Remote Sensing of Environment. 7th (Ann Arbor, Michigan) III:2109-2113.

Tandon, S. P. and J. P. Gupta. 1970. Diffuse reflectance spectrum of ferric oxide. Spectroscopy Letters 3 (11 and 12).

Torrent, J., U. Schwertmann and D. G. Schulze. 1980. Iron oxide mineralogy of some soils of two river terrace sequences in Spain. Geoderma, 23:191-208.

Tossell, J. A, Vaughan, D. J. and Johnson, K. H. 1973. Nature 244, 42.

Walker, T. R. 1967. Formation of red beds in modern and ancient deserts. Bull. Geol. Soc. Am., 78: 353-368.

Weismiller, R. A. and S. A. Kaminsky. 1978. Application of remote sensing technology to soil survey research. J. Soil Water Conserv. 33:287-289.

Weismiller, R. A., F. R. Kirschner, S. A. Kaminsky, and E. J. Hinzel. 1979. Spectral classification of soil characteristics to aid the soil survey of Jasper County, Indiana. LARS Technical Report 040179. Laboratory for Applications of Remote Sensing. Purdue University. West Lafayette, Indiana.

Westin, F. C. and C. J. Frazee. 1976. Landsat data, its use in a soil survey program. Soil Sci. Soc. Am. J. 40:81-89.

Westin, F. C. and G. D. Lemme. 1978. Landsat spectral signatures: studies with soil associations and vegetation. Photogram. Eng. and Remote Sensing 44:315-325.

Whitbeck, M. R. 1981. Second derivative Infrared Spectroscopy. Applied Spectroscopy. 35:1.

White, W. B. and K. L. Keester. 1966. Optical absorption spectra of iron in the rock-forming silicates. Amer. Mineral. 51, 774-791.

White, W. B. and K. L. Keester. 1967. Spectral rules and assignments for the spectra of ferrous iron in pyroxenes. American Mineralogist, Vol. 52.

Young, A. 1978. Evaluation of erosion risks and erosion mapping. Assessment of erosion, edited by M. de Boodt. New York: J. Wiley, c. 1980.

Appendix A

Physical and chemical data for the soil samples presented.

- Simulated erosion samples

Soil	% Sand	% Silt	% Clay	Texture	% OM	% Fe_2O_3	% Amor. Fe_2O_3
RUNS	12.6	70.8	16.6	SI.	3.17	0.96	0.53
RUSL	12.3	68.7	19.0	SIL	2.71	1.04	0.52
RUMO	11.5	66.0	22.5	SIL	2.36	1.10	0.53
RUSE	11.1	67.2	21.7	SIL	2.09	1.17	0.54
RUVS	11.0	66.0	23.0	SIL	1.82	1.22	0.55
MINS	17.8	61.2	21.0	SIL	1.60	1.25	0.55
MISL	16.3	60.9	22.8	SIL	1.50	1.34	0.58
MIMO	15.4	59.5	25.1	SIL	1.30	1.44	0.61
MISE	16.0	57.1	26.9	SIL	1.11	1.51	0.64
MIVS	17.8	54.1	28.1	SICL	0.97	1.59	0.67
MONS	32.8	49.4	17.8	L	2.47	1.11	0.36
MOSL	31.8	50.1	18.1	SIL	2.20	1.14	0.36
MOMO	29.5	49.1	21.4	L	2.03	1.21	0.36
MOSE	28.1	47.3	24.6	L	1.63	1.30	0.37
MOSV	26.3	45.6	28.1	CL	1.44	1.43	0.39

- National Soil Erosion Laboratory samples (Morley soil)

Soil #	% Sand	% Silt	% Clay	Texture	% OM	% Fe_2O_3
1	31.3	50.5	18.2	L	2.44	1.08
2	28.9	45.3	25.8	L	2.34	1.25
3	31.7	46.6	21.8	L	2.99	1.23
4	26.7	49.2	24.1	SIL	1.91	1.43
5	33.8	41.0	25.2	L	1.31	1.55
6	38.9	37.8	23.3	L	1.94	1.38
7	9.2	71.6	19.2	SIL	2.03	1.85
8	22.7	46.1	31.2	L	1.39	2.20
9	34.1	46.7	19.2	L	1.29	1.79
10	26.1	37.9	36.0	CL	1.50	1.89

-- Characterization Laboratory samples

Soil	Erosion Class	% Sand	% Silt	% Clay	Texture	% OM	% Fe_2O_3	% Amor. Fe_2O_3*
RU11	NS	12.3	71.8	15.9	SIL	2.05	1.01	0.29
RU12	NS	11.1	74.3	14.6	SIL	2.89	0.93	0.36
RU13	NS	12.0	74.0	14.0	SIL	2.15	0.81	0.44
RU21	MO	11.2	65.1	23.7	SIL	1.16	1.74	0.64
RU22	MO	7.1	76.2	16.7	SIL	2.80	1.17	0.44
MI11	NS	10.8	77.3	19.9	SIL	3.08	1.15	0.49
MI21	MO	19.0	66.6	14.4	SIL	2.78	1.18	0.40
MI22	MO	14.4	68.1	17.5	SIL	1.96	1.25	0.42
MI23	MO	20.7	56.7	22.6	SIL	1.86	1.46	0.37
MI24	MO	14.4	62.0	23.6	SIL	1.37	1.64	0.58
MO21	MO	18.0	51.2	30.8	SICL	2.27	1.35	0.43
MO22	MO	48.3	35.2	16.5	L	2.49	1.22	0.31
MO23	MO	31.4	45.1	23.5	L	2.33	1.38	0.32
MO31	SE	27.0	42.4	30.6	CL	2.99	2.08	0.41

Soil Key -- RU = Russell MI = Miami MO = Morley

Erosion Key -- NS = none-to-slight; SL = slight; MO = moderate; SE = severe; VS = very severe.

*Road, A. T., R. Protz and R. L. Thomas. 1969. Determination of Na-dithionite and NH_4-oxalate extractable Fe, Al and Mn in soils by atomic adsorption spectroscopy. Can. J. Soil. Sci. 49:89-94.

Appendix B

Location and field information for naturally eroded soil sites.

Morley soils from the National Soil Erosion Laboratory are listed first (p93-102), followed by eroded soils collected by the Soil Conservation Service for analysis by the Purdue University Soil Characterization Laboratory (p105-106).

DEPARTMENT OF AGRICULTURE
Soil Conservation Service

SCS-SOI-1
4-81

SOIL-CROP YIELD DATA

Morley #1

	SAMPLE NUMBER ST	CO	ID	KIND OF PLOT	SIZE OF PLOT	LOCATION X COORD.	Y COORD.	OTHER DESCRIPTION	AGENCY	DATE MO	DY	YR
1	2N	183	331		.001	41-05-45	85-33-00	NE ¼ SEC. 31, T 31 N, R 9 E	SCS	07	08	81

	SOIL IDENT SOIL SYMBOL	SOIL NAME	SOIL IDENT. AT SITE Y/N
2	MuB	Morley Silt Loam 3-7% slope	Y

	SOIL INFO INTERP RECORD NUMBER	USDA TEXTURE	SLOPE (PCT)	FLOODING	OTHER PHASE CRITERIA
3	IL0017	SiL	2	NONE	

	OTHER SOIL INFO EROSION	A HORIZON COLOR	A HORIZON THICKNESS (IN)	ORGANIC MATTER (PCT)	PH	ROOTING DEPTH (IN)	SLOPE LENGTH THRU SITE (FT)	SLOPE LENGTH ABOVE SITE (FT)	SLOPE KIND	SLOPE SHAPE	ASPECT	K FACTOR
4	1	10YR 4/1	9	1.5	5.6	35			1		W	.43

	WEATHER MOISTURE RESERVE AT PLANTING	AT START OF GROW SEAS	PRECIPITATION DURING GROWING SEASON QUAL	BY MONTH 1	2	3	4	5	6	7	8	9	10	11	12	DROUGHT DAMAGE	WATER DAMAGE	T FACTOR
5	1	1	2													0	0	160

	CROP DATA MULTI CROPPED N-Y	CURRENT CROP	CURRENT CULTIVAR (Variety)	FIRST PREVIOUS CROP	SECOND PREVIOUS CROP	THIRD PREVIOUS CROP
6	N	CORN	DEKALB SSA	CORN	CORN	CORN

	CROP DATA (Cont) PLANTING INFORMATION DATE MO	DY	YR	TIMING	RATE LB/AC	ROW SPAC	HARVEST INFORMATION DATE MO	DY	YR	TIMING	CROP YIELD	UNIT MEAS	RESIDUE T/AC
7	05	25	81	3	26800	30	10	13	81	1	91	bu/ac	

	CROP MGT. COMMERICAL FERTILIZER LB/AC N	P	K	OTHER KIND	OTHER LB/AC	ORGANIC MATERIALS MANURE T/AC	MANURE KIND	CROP Y-N	TILLAGE	WEED CONTROL CHEM Y-N	NUM CULT	CROP DAMAGE	INSECT/DISEASE CONTROL CHEM Y-N	KIND TREAT	NUM APPLIC	CROP DAMAGE
8	177	55	3/3					Y	3	Y	0	0	Y	3		0

	CROP MGT. (Cont) OTHER DAMAGE	CONS PRACT	IRRIGATION Y-N	IRRIGATION TYPE	IRRIGATION ADEQUACY	DRAINAGE Y-N	DRAINAGE CROP DAMAGE	C FACTOR	NAME OF RECORDER
9	0	0	N			N	0	.29	

KEYING INSTRUCTIONS: DUPLICATE SAMPLE NUMBER ON ALL LINES

DEPARTMENT OF AGRICULTURE
Conservation Service

SCS-SOI-1
4-81

Morley #2

SOIL-CROP YIELD DATA

	SAMPLE NUMBER ST	CO	IC	KIND OF PLOT	SIZE OF PLOT	LOCATION X COORD.	Y COORD.	OTHER DESCRIPTION	AGENCY	DATE MO	DY	YR
1	18	183	531	4	.001	41-13-05	85-25-45	NE ¼ SEC 24 T32N R9E	16	06	30	81

	SOIL IDENT SOIL SYMBOL	SOIL NAME	SOIL IDENT AT SITE Y/N
2	MuB1	Morley Silt Loam 3-7% slope	Y

	SOIL INFO INTERP RECORD NUMBER	USDA TEXTURE	SLOPE (PCT)	FLOODING	OTHER PHASE CRITERIA
3		SiL	2	NONE	

	OTHER SOIL INFO EROSION	A HORIZON COLOR	A HORIZON THICKNESS (IN)	ORGANIC MATTER (PCT)	PH	ROOTING DEPTH (IN)	SLOPE LENGTH THRU SITE (FT)	SLOPE LENGTH ABOVE SITE (FT)	SLOPE KIND	SLOPE SHAPE	ASPECT	K FACTOR
4	1	10YR 4/3	10	1.5	6.0	41			1		F	.43

	WEATHER MOISTURE RESERVE AT PLANTING	AT START OF GROW SEAS	DUAL	PRECIPITATION DURING GROWING SEASON BY MONTH 1	2	3	4	5	6	7	8	9	10	11	12	DROUGHT DAMAGE	WATER DAMAGE	R FACTOR
5	1	1	1													0	1	160

	CROP DATA MULTI CROPPED Y/N	CURRENT CROP	CURRENT CULTIVAR (Variety)	FIRST PREVIOUS CROP	SECOND PREVIOUS CROP	THIRD PREVIOUS CROP
6	M	CORN	PAG 397	CORN	CORN	HAY

	CROP DATA (Cont) PLANTING INFORMATION DATE MO	DY	YR	TIMING	RATE LB/AC	ROW SPAC	HARVEST INFORMATION DATE MO	DY	YR	TIMING	CROP YIELD	UNIT MEAS	RESIDUE PAC
7	05	05	81	2	23500	30	10	13	81	1	119	bu/ac	

	CROP MGT. COMMERCIAL FERTILIZER LB/AC N	P	K	OTHER KIND	OTHER LB/AC	ORGANIC MATERIALS MANURE T/AC	MANURE KIND	CROP Y/N	TILLAGE	WEED CONTROL CHEM Y/N	NUM CULT	CROP DAMAGE	INSECT/DISEASE CONTROL CHEM Y/N	KIND TREAT	NUM APPLIC	CROP DAMAGE
8	195	172	106			0	0	Y	4	Y	0	0	Y	3		

	CROP MGT. (Cont) OTHER DAMAGE	CONS PRACT	IRRIGATION Y/N	TYPE	ADEQUACY	DRAINAGE Y/N	CROP DAMAGE	C FACTOR	NAME OF RECORDER
9		0						.36	

KEYING INSTRUCTIONS: DUPLICATE SAMPLE NUMBER ON ALL LINES

. DEPARTMENT OF AGRICULTURE
...il Conservation Service

SCS-SOI-1
1-81

SOIL-CROP YIELD DATA

Morley #3

	SAMPLE NUMBER ST	CO	ID	KIND OF PLOT	SIZE OF PLOT	LOCATION X COORD.	Y COORD.	OTHER DESCRIPTION	AGENCY	DATE MO	DY	YR
1	IN	183	111		.001	41-6-35	85-32-30	NW 1/4, SEC. 29, T31N R9E	SCS	10	20	81

	SOIL IDENT SOIL SYMBOL	SOIL NAME	SOIL IDENT. AT SITE Y/N
2	MxB	Morley Silt Loam 3-7% SLOPES	Y

	SOIL INFO INTERP RECORD NUMBER	USDA TEXTURE	SLOPE (PCT)	FLOODING	OTHER PHASE CRITERIA
3	IL0017	SIL	3	NONE	

	OTHER SOIL INFO EROSION	A HORIZON COLOR	A HORIZON THICKNESS (IN)	ORGANIC MATTER (PCT)	pH	ROOTING DEPTH (IN)	SLOPE LENGTH THRU SITE (FT)	SLOPE LENGTH ABOVE SITE (FT)	SLOPE KIND	SLOPE SHAPE	ASPECT	K FACTOR
4	1	10YR 4/3	8	1.5	6.2	33			1		VE	.43

	WEATHER MOISTURE RESERVE AT PLANTING	AT START OF GROW SEAS	QUAL	PRECIPITATION DURING GROWING SEASON BY MONTH	DROUGHT DAMAGE	WATER DAMAGE	R FACTOR
5	2	1	1		0	1	160

	CROP DATA MULTI CROPPED Y/N	CURRENT CROP	CURRENT CULTIVAR (Variety)	FIRST PREVIOUS CROP	SECOND PREVIOUS CROP	THIRD PREVIOUS CROP
6	M	CORN	DEKALB XL 55A	CORN	BEANS	CORN

	CROP DATA (Cont) PLANTING INFORMATION DATE MO	DY	YR	TIMING	RATE LB/AC	ROW SPAC	HARVEST INFORMATION DATE MO	DY	YR	TIMING	CROP YIELD	UNIT MEAS	RESIDUE T/AC
7	05	22	81	3	26000	30	10	14	81	1	147	bu/ac	

	CROP MGT. COMMERICAL FERTILIZER LB/AC N	P	K	OTHER KIND	OTHER LB/AC	ORGANIC MATERIALS MANURE T/AC	MANURE KIND	CROP Y/N	TILLAGE	WEED CONTROL CHEM Y/N	NUM CULT	CROP DAMAGE	INSECT/DISEASE CONTROL CHEM Y/N	KIND TREAT	NUM APPLIC	CROP DAMAGE
8	214	96	173			-		M	3	M	0	1	M	3		0

	CROP MGT. (Cont) OTHER DAMAGE	CONS PRACT	IRRIGATION Y/N	IRRIGATION TYPE	IRRIGATION ADEQUACY	DRAINAGE Y/N	DRAINAGE CROP DAMAGE	C FACTOR	NAME OF RECORDER
9	0	0	N	-	-	M	0	.32 .29	

*KEYING INSTRUCTIONS: DUPLICATE SAMPLE NUMBER ON ALL LINES

...incl cover after Planting

DEPARTMENT OF AGRICULTURE
Soil Conservation Service

SCS-SOI-1
4-81

SOIL-CROP YIELD DATA

Morley #4

	SAMPLE NUMBER ST	CO	ID	KIND OF PLOT	SIZE OF PLOT	LOCATION X COORD.	Y COORD.	OTHER DESCRIPTION	AGENCY	DATE MO	DY	YR
1	IN	133	02		.001	41-6-35	85-32-30	NW 1/4, SEC. 29, T31N, R9E	SCS	10	20	81

	SOIL IDENT SOIL SYMBOL	SOIL NAME	SOIL IDENT AT SITE Y-N
2	MvB2	Morley Silt Loam 3-7% slopes eroded	Y

	SOIL INFO INTERP RECORD NUMBER	USDA TEXTURE	SLOPE (PCT)	FLOODING	OTHER PHASE CRITERIA
3	IL0017	Sil	4	NONE	

	OTHER SOIL INFO EROSION	A HORIZON COLOR	A HORIZON THICKNESS (IN)	ORGANIC MATTER (PCT)	pH	ROOTING DEPTH (IN)	SLOPE LENGTH THRU SITE (FT)	SLOPE LENGTH ABOVE SITE (FT)	SLOPE KIND	SLOPE SHAPE	ASPECT	K FACTOR
4	2	10YR 4/3	8	1.0	5.6	28			3		E	.43

	WEATHER MOISTURE RESERVE AT PLANTING	AT START OF GROW SEAS	PRECIPITATION DURING GROWING SEASON QUAL	BY MONTH 1	2	3	4	5	6	7	8	9	10	11	12	DROUGHT DAMAGE	WATER DAMAGE	R FACTOR
5	2	1	1													01	1	160

	CROP DATA MULTI CROPPED Y-N	CURRENT CROP	CURRENT CULTIVAR (Variety)	FIRST PREVIOUS CROP	SECOND PREVIOUS CROP	THIRD PREVIOUS CROP
6	N	CORN	DEKALB XL 55A	CORN	BEANS	CORN

	CROP DATA (Cont) PLANTING INFORMATION DATE MO	DY	YR	TIMING	RATE LB/AC	ROW SPAC	HARVEST INFORMATION DATE MO	DY	YR	TIMING	CROP YIELD	UNIT MEAS	RESIDUE T/AC
7	05	22	81	3	26000	30	10	14	81	1	155	bu	DC

	CROP MGT. COMMERCIAL FERTILIZER LB/AC N	P	K	OTHER KIND	OTHER LB/AC	ORGANIC MATERIALS MANURE T/AC	MANURE KIND	CROP Y-N	TILLAGE	WEED CONTROL CHEM Y-N	NUM CULT	CROP DAMAGE	INSECT/DISEASE CONTROL CHEM Y-N	KIND TREAT	NUM APPLIC	CROP DAMAGE
8	214	96	173					M	3	Y	0	1	M	3		0

	CROP MGT. (Cont) OTHER DAMAGE	CONS PRACT	IRRIGATION Y-N	IRRIGATION TYPE	IRRIGATION ADEQUACY	DRAINAGE Y-N	DRAINAGE CROP DAMAGE	C FACTOR	NAME OF RECORDER
9	0	0	N	-	-	M	0	.32 .34	

KEYING INSTRUCTIONS: DUPLICATE SAMPLE NUMBER ON ALL LINES

U.S. DEPARTMENT OF AGRICULTURE
Soil Conservation Service

SCS-SOI-1
4-81

SOIL-CROP YIELD DATA

Morley #5

KEYING INSTRUCTIONS: DUPLICATE SAMPLE NUMBER ON ALL LINES

	SAMPLE NUMBER ST	CO	IC	KIND OF PLOT	SIZE OF PLOT	LOCATION X COORD.	Y COORD.	OTHER DESCRIPTION	AGENCY	DATE MO	DY	YR
1	IN	183	422		.001	41-B-25	85-34-55	NE ¼ SW ¼ SEC. 13, T 31 N RBE	SCS	10	20	81

	SOIL IDENT SOIL SYMBOL	SOIL NAME	SOIL IDENT. AT SITE Y/N
2	MxB	MORLEY LOAM 3-7% SLOPE ERODED	Y

	SOIL INFO INTERP RECORD NUMBER	USDA TEXTURE	SLOPE (PCT)	FLOODING	OTHER PHASE CRITERIA
3	IL0017	L	4	NONE	

	OTHER SOIL INFO EROSION	A HORIZON COLOR	A HORIZON THICKNESS (IN)	ORGANIC MATTER (PCT)	PH	ROOTING DEPTH (IN)	SLOPE LENGTH THRU SITE (FT)	SLOPE LENGTH ABOVE SITE (FT)	SLOPE KIND	SLOPE SHAPE	ASPECT	K FACTOR
4	2	10YR 4/3	9	1.0	6.2	28			1		NW	.43

	WEATHER MOISTURE RESERVE AT PLANTING	AT START OF GROW SEAS	QUAL	PRECIPITATION DURING GROWING SEASON BY MONTH 1	2	3	4	5	6	7	8	9	10	11	12	DROUGHT DAMAGE	WATER DAMAGE	T FACTOR
5	1	1	1													0	1	160

	CROP DATA MULTI CROPPED Y/N	CURRENT CROP	CURRENT CULTIVAR (Variety)	FIRST PREVIOUS CROP	SECOND PREVIOUS CROP	THIRD PREVIOUS CROP
6	N	CORN	CO-OP C-43	WHEAT	BEANS	BEANS

	CROP DATA (Cont) PLANTING INFORMATION DATE MO	DY	YR	TIMING	RATE LB/AC	ROW SPAC	HARVEST INFORMATION DATE MO	DY	YR	TIMING	CROP YIELD	UNIT MEAS	RESIDUE T/AC
7	05	28	81	3	25000	30	10	14	81	1	147	bu/ac	

	CROP MGT. COMMERCIAL FERTILIZER LB/AC N	P	K	OTHER KIND	OTHER LB/AC	ORGANIC MATERIALS MANURE T/AC	MANURE KIND	CROP Y/N	TILLAGE	WEED CONTROL CHEM Y/N	NUM CULT	CROP DAMAGE	INSECT/DISEASE CONTROL CHEM Y/N	KIND TREAT	NUM APPLIC	CROP DAMAGE
8	150	84	198			2	3	Y	4	Y	0	0	Y	3		0

	CROP MGT. (Cont) OTHER DAMAGE	CONS PRACT	IRRIGATION Y/N	IRRIGATION TYPE	IRRIGATION ADEQUACY	DRAINAGE Y/N	DRAINAGE CROP DAMAGE	C FACTOR	NAME OF RECORDER
9	0	0	N			N	1	.36	

DEPARTMENT OF AGRICULTURE
Soil Conservation Service

SCS-SOI-1

SOIL-CROP YIELD DATA

Morley #6

	SAMPLE NUMBER ST	CO	ID	KIND OF PLOT	SIZE OF PLOT	LOCATION X COORD.	Y COORD.	OTHER DESCRIPTION	AGENCY	DATE MO	DY	YR
1	IN	183	312	M	.001							

	SOIL IDENT	SOIL SYMBOL	SOIL NAME	SOIL IDENT. AT SITE Y-N
2		MrB2	Morley Silt Loam 3-7% slopes eroded	M

	SOIL INFO	INTERP RECORD NUMBER	USDA TEXTURE	SLOPE (PCT)	FLOODING	OTHER PHASE CRITERIA
3		IL0017	SiL	4	NONE	Er.

	OTHER SOIL INFO	EROSION	A HORIZON COLOR	A HORIZON THICKNESS (IN)	ORGANIC MATTER (PCT)	pH	ROOTING DEPTH (IN)	SLOPE LENGTH THRU SITE (FT)	SLOPE LENGTH ABOVE SITE (FT)	SLOPE KIND	SLOPE SHAPE	ASPECT	K FACTOR
4		2	10YR 4/3	7	1.0	5.8	26			2		SW	.43

	WEATHER	MOISTURE RESERVE AT PLANTING	MOISTURE RESERVE AT START OF GROW SEAS	QUAL	PRECIPITATION DURING GROWING SEASON BY MONTH 1	2	3	4	5	6	7	8	9	10	11	12	DROUGHT DAMAGE	WATER DAMAGE	T FACTOR
5		1	1	2													0	0	

	CROP DATA	MULTI CROPPED N-Y	CURRENT CROP	CURRENT CULTIVAR (Variety)	FIRST PREVIOUS CROP	SECOND PREVIOUS CROP	THIRD PREVIOUS CROP
6		N	CORN	DEKALB SSA	CORN	CORN	CORN

	CROP DATA (Cont)	PLANTING INFORMATION DATE MO	DY	YR	TIMING	RATE LB/AC	ROW SPAC	HARVEST INFORMATION DATE MO	DY	YR	TIMING	CROP YIELD	UNIT MEAS	RESIDUE T/AC
7		05	25	81	3	26800	30	10	13	81	1	73	bu/ac	

	CROP MGT.	COMMERCIAL FERTILIZER LB/AC N	P	K	OTHER KIND	OTHER LB/AC	ORGANIC MATERIALS MANURE T/AC	MANURE KIND	CROP Y-N	TILLAGE	WEED CONTROL CHEM Y-N	NUM CULT	CROP DAMAGE	INSECT/DISEASE CONTROL CHEM Y-N	KIND TREAT	NUM APPLIC	CROP DAMAGE
8		177	55	313					M	3	M	0	0	M	3		0

	CROP MGT. (Cont)	OTHER DAMAGE	CONS PRACT	IRRIGATION Y-N	IRRIGATION TYPE	IRRIGATION ADEQUACY	DRAINAGE Y-N	DRAINAGE CROP DAMAGE	C FACTOR	NAME OF RECORDER
9		0	0	N			N	0	.29	

KEYING INSTRUCTIONS: DUPLICATE SAMPLE NUMBER ON ALL LINES

DEPARTMENT OF AGRICULTURE
Soil Conservation Service

SCS-SOI-1
4-81

SOIL-CROP YIELD DATA

Morley #7

	SAMPLE NUMBER ST	CO	ID	KIND OF PLOT	SIZE OF PLOT	LOCATION X COORD.	Y COORD.	OTHER DESCRIPTION	AGENCY	DATE MO	DY	YR
1	18	183	211		.001	41-09-15	85-34-55	S ½ SW ¼ SEC. 7 T 31 N R 9 E	16	10	15	81

	SOIL IDENT	SOIL SYMBOL	SOIL NAME	SOIL IDENT. AT SITE Y/N
2		MxB2	MORLEY SILT LOAM 3-7% SLOPES ERODED	Y

	SOIL INFO	INTERP RECORD NUMBER	USDA TEXTURE	SLOPE (PCT)	FLOODING	OTHER PHASE CRITERIA
3		IL0017	SIL	3	NONE	

	OTHER SOIL INFO	EROSION	A HORIZON COLOR	A HORIZON THICKNESS (IN)	ORGANIC MATTER (PCT)	pH	ROOTING DEPTH (IN)	SLOPE LENGTH THRU SITE (FT)	SLOPE LENGTH ABOVE SITE (FT)	SLOPE KIND	SLOPE SHAPE	ASPECT	K FACTOR
4		2	10YR 4/3	9	1.0	6.4	27			1		5	.43

	WEATHER	MOISTURE RESERVE AT PLANTING	AT START OF GROW SEAS	QUAL	PRECIPITATION DURING GROWING SEASON BY MONTH 1	2	3	4	5	6	7	8	9	10	11	12	DROUGHT DAMAGE	WATER DAMAGE	I FACTOR
5		1	1	1													0	1	160

	CROP DATA	MULTI CROPPED Y/N	CURRENT CROP	CURRENT CULTIVAR (Variety)	FIRST PREVIOUS CROP	SECOND PREVIOUS CROP	THIRD PREVIOUS CROP
6		N	CORN	PIONEER 3518	CORN	WHEAT	BEANS

	CROP DATA (Cont)	PLANTING INFORMATION DATE MO	DY	YR	TIMING	RATE LB/AC	ROW SPAC	HARVEST INFORMATION DATE MO	DY	YR	TIMING	CROP YIELD	UNIT MEAS	RESIDUE T/AC
7		06	02	81	3	24600	30	10	14	81	1	96	bu/ac	

	CROP ACT.	COMMERCIAL FERTILIZER LB/AC N	P	K	OTHER KIND	OTHER LB/AC	ORGANIC MATERIALS MANURE T/AC	MANURE KIND	CROP Y/N	TILLAGE	WEED CONTROL CHEM Y/N	NUM CULT	CROP DAMAGE	INSECT/DISEASE CONTROL CHEM Y/N	KIND TREAT	N/A APPLIC	CROP DAMAGE
8		177	55	313					Y	4	1	0	0	Y	3		1

	CROP ACT. (Cont)	OTHER DAMAGE	CONS PRACT	IRRIGATION Y/N	TYPE	ADEQUACY	DRAINAGE Y/N	CROP DAMAGE	C FACTOR	NAME OF RECORDER
9		0	0	N			N	2	.33	

KEYING INSTRUCTIONS: DUPLICATE SAMPLE NUMBER ON ALL LINES

DEPARTMENT OF AGRICULTURE
Conservation Service

SOIL-CROP YIELD DATA

Morley #8

	SAMPLE NUMBER ST	CO	IC	KIND OF PLOT	SIZE OF PLOT	LOCATION X COORD.	Y COORD.	OTHER DESCRIPTION	AGENCY	DATE MO	DY	YR
1	18	183	233		.001	41 09 15	85 34 55	S½ SW¼ SEC. 7 T3N R9E	16	10	15	81

	SOIL IDENT	SOIL SYMBOL	SOIL NAME	SOIL IDENT. AT SITE Y-N
2		MxB3	Morley Clay Loam 3-7% slope severely eroded	Y

	SOIL INFO	INTERP RECORD NUMBER	USDA TEXTURE	SLOPE (PCT)	FLOODING	OTHER PHASE CRITERIA
3		ILD017	CL	6	NONE	

	OTHER SOIL INFO	EROSION	A HORIZON COLOR	A HORIZON THICKNESS (IN)	ORGANIC MATTER (PCT)	pH	ROOTING DEPTH (IN)	SLOPE LENGTH THRU SITE (FT)	SLOPE LENGTH ABOVE SITE (FT)	SLOPE KIND	SLOPE SHAPE	ASPECT	K FACTOR
4		3	10YR 4/3	9	0.5	6.2	24			3		5	.43

	WEATHER	MOISTURE RESERVE AT PLANTING	MOISTURE RESERVE AT START OF GROW SEAS	QUAL	PRECIPITATION DURING GROWING SEASON BY MONTH 1	2	3	4	5	6	7	8	9	10	11	12	DROUGHT DAMAGE	WATER DAMAGE	R FACTOR
5		1	1	1													0	1	160

	CROP DATA	MULT CROPPED Y-N	CURRENT CROP	CURRENT CULTIVAR (Variety)	FIRST PREVIOUS CROP	SECOND PREVIOUS CROP	THIRD PREVIOUS CROP
6		M	CORN	Pioneer 3518	CORN	WHEAT	BEANS

	CROP DATA (Cont)	PLANTING INFORMATION DATE MO	DY	YR	TIMING	RATE LB/AC	ROW SPAC	HARVEST INFORMATION DATE MO	DY	YR	TIMING	CROP YIELD	UNIT MEAS	RESIDUE T/AC
7		06	02	81	3	24600	30	10	14	81	1	66	bu/ac	

	CROP MGT.	COMMERCIAL FERTILIZER LB/AC N	P	K	OTHER KIND	OTHER LB/AC	ORGANIC MATERIALS MANURE T/AC	MANURE KIND	CROP Y-N	TILLAGE	WEED CONTROL CHEM Y-N	MECH CULT	CROP DAMAGE	INSECT DISEASE CONTROL CHEM Y-N	KIND TREAT	NUM APPLIC	CROP DAMAGE
8		177	55	313					M	1	M	0	0	Y	3		1

	CROP MGT. (Cont)	OTHER DAMAGE	CONS PRACT	IRRIGATION Y-N	IRRIGATION TYPE	IRRIGATION ADEQUACY	DRAINAGE Y-N	DRAINAGE CROP DAMAGE	C FACTOR	NAME OF RECORDER
9		0	0	N			N	2	.33	

BEING INSTRUCTIONS: DUPLICATE SAMPLE NUMBER ON ALL LINES

DEPARTMENT OF AGRICULTURE
Soil Conservation Service

SOIL-CROP YIELD DATA

Morley #9

KEYING INSTRUCTIONS: DUPLICATE SAMPLE NUMBER ON ALL LINES

Line	Sample Number ST	CO	ID	Kind of Plot	Size of Plot	X Coord.	Y Coord.	Other Description	Agency	Date MO	DY	YR
1	18	183	513	4	.001	41-13-05	85-25-45	NE 1/4 SEC. 24 T32N R9E	16	06	30	81

Line	Soil Ident: Soil Symbol	Soil Name	Soil Ident at Site Y/N
2	MxB3	Morley Clay Loam 3-7% Slope Severely eroded	Y

Line	Soil Info: Interp Record Number	USDA Texture	Slope (PCT)	Flooding	Other Phase Criteria
3		CL	6	NONE	Severely Eroded

Line	Other Soil Info: Erosion	A Horizon Color	A Horizon Thickness (IN)	Organic Matter (PCT)	pH	Rooting Depth (IN)	Slope Length Thru Site (FT)	Slope Length Above Site (FT)	Slope Kind	Slope Shape	Aspect	K Factor
4	3	10YR 4/3	9	0.5	6.2	23			2		S	.43

Line	Weather: Moisture Reserve at Planting	At Start of Grow Seas	Qual	Precipitation During Growing Season by Month 1	2	3	4	5	6	7	8	9	10	11	12	Drought Damage	Water Damage	R Factor
5	/	/	/													d	/	160

Line	Crop Data: Multi Cropped Y/N	Current Crop	Current Cultivar (Variety)	First Previous Crop	Second Previous Crop	Third Previous Crop
6	N	CORN	PAG 397	CORN	CORN	Hay

Line	Crop Data (Cont): Planting Date MO	DY	YR	Timing	Rate LB/AC	Row Spac	Harvest Date MO	DY	YR	Timing	Crop Yield	Unit Meas	Residue T/AC
7	05	05	81	2	23500	30	10	13	81	1	110	bu/ac	

Line	Crop Mgt.: Commercial Fertilizer LB/AC N	P	K	Other Kind	Other LB/AC	Organic Materials Manure T/AC	Manure Kind	Crop Y/N	Tillage	Weed Control Chem Y/N	Num Cult	Crop Damage	Insect-Disease Control Chem Y/N	Kind Treat	Num Applic	Crop Damage
8	195	172	106			0	0	N	4	Y	0	d	Y	3		

Line	Crop Mgt. (Cont): Other Damage	Cons Pract	Irrigation Y/N	Irrigation Type	Irrigation Adequacy	Drainage Y/N	Drainage Crop Damage	C Factor	Name of Recorder
9		0						.36	

PARTMENT OF AGRICULTURE
onservation Service

SCS-SOI-1
8-81

SOIL-CROP YIELD DATA

Morley #10

	SAMPLE NUMBER ST	CO	IC	KIND OF PLOT	SIZE OF PLOT	LOCATION X COORD.	Y COORD.	OTHER DESCRIPTION	AGENCY	DATE MO	DY	YR
1	IN	193	124		.001	41-6-35	85-32-30	NW¼ SEC. 29, T31N, R7E	SCS	10	20	81

	SOIL IDENT SOIL SYMBOL	SOIL NAME	SOIL IDENT AT SITE Y-N
2	MxC4	Morley Silty Clay Loam 7-12% slope very severely eroded	M

	SOIL INFO INTERP RECORD NUMBER	USDA TEXTURE	SLOPE (PCT)	FLOODING	OTHER PHASE CRITERIA
3	IL0017	SI CL	8	NONE	

	OTHER SOIL INFO EROSION	A HORIZON COLOR	A HORIZON THICKNESS (IN)	ORGANIC MATTER (PCT)	pH	ROOTING DEPTH (IN)	SLOPE LENGTH THRU SITE (FT)	SLOPE LENGTH ABOVE SITE (FT)	SLOPE KIND	SLOPE SHAPE	ASPECT	K FACTOR
4	4	10YR 4/4	6	0.3	6.4	15			2		W	.43

	WEATHER MOISTURE RESERVE AT PLANTING	AT START OF GROW SEAS	QUAL	PRECIPITATION DURING GROWING SEASON BY MONTH 1	2	3	4	5	6	7	8	9	10	11	12	DROUGHT DAMAGE	WATER DAMAGE	R FACTOR
5	2	1	1													0	1	160

	CROP DATA MULTI CROPPED Y-N	CURRENT CROP	CURRENT CULTIVAR (Variety)	FIRST PREVIOUS CROP	SECOND PREVIOUS CROP	THIRD PREVIOUS CROP
6	M	CORN	DEKALB XL55A	CORN	BEANS	CORN

	CROP DATA (Cont) PLANTING INFORMATION DATE MO	DY	YR	TIMING	RATE LB/AC	ROW SPAC	HARVEST INFORMATION DATE MO	DY	YR	TIMING	CROP YIELD	UNIT MEAS	RESIDUE T/AC
7	05	22	81	3	26000	30	10	18	81	1	118	bu/ac	

	CROP MGT. COMMERCIAL FERTILIZER LB/AC N	P	K	OTHER KIND	OTHER LB/AC	ORGANIC MATERIALS MANURE T/AC	MANURE KIND	CROP Y-N	TILLAGE	WEED CONTROL CHEM Y-N	NUM CULT	CROP DAMAGE	INSECT/DISEASE CONTROL CHEM Y-N	KIND TREAT	NUM APPLIC	CROP DAMAGE
8	214	96	173		—	-		M	3	M	0	1	M	3		9

	CROP MGT. (Cont) OTHER DAMAGE	CONS PRACT	IRRIGATION Y-N	IRRIGATION TYPE	IRRIGATION ADEQUACY	DRAINAGE Y-N	DRAINAGE CROP DAMAGE	C FACTOR	NAME OF RECORDER
9	0	0	N	-	-	N	0	.32	

KEYING INSTRUCTIONS: DUPLICATE SAMPLE NUMBER ON ALL LINES

Soil Series: Russell (Code: RU21)
County: Wayne
Location: 2200' S & 260' W of NE corner of the Sec.22 T15N R13E
Landform: Moraine, shoulder
Parent Material: Loess Wisconsinan (2) Till Wisconsinan
Slope: 4
Erosion: Moderate
Drainage: Well
Vegetation: Corn

Soil Series: Russell (Code: RU22)
County: Franklin
Location: 1056' S & 300' W of the center of Sec.24 T.ION R1W
Landform: Head slope, backslope
Parent Material: Till Wisconsinan
Slope: 2
Erosion: B
Drainage: Well
Vegetation: Corn Stubble

Soil Series: Miami (Code: MI11)
County: Randolph
Location: 200' W & 2800' S of the NE corner of Sec.27 T20N R13E
Landform: Till Plain, Swell
Parent Material: Till Wisconsinan
Slope: 0
Erosion: None to Slight
Drainage: Well
Vegetation: Soybeans

Soil Series: Miami (Code: MI21)
County: Randolph
Location: 1100' W & 300' S of the NE corner of Sec.1 T16N R1W
Landform: Side slope, backslope
Parent Material: Till Wisconsinan
Slope: 3
Erosion: Moderate
Drainage: Well
Vegetation: Corn

Soil Series: Miami (Code: MI22)
County: Rush
Location: 1400' E & 500' N of the SW corner of Sec.8 T13N R11E
Landform: Sideslope, backslope
Parent Material: Loess, Wisconsinan (2) Till Wisconsinan
Slope: 3
Erosion: Moderate
Drainage: Well
Vegetation: Corn

Soil Series: Miami (Code: MI23)
County: Franklin
Location: 800' W & 200' S of the NE corner of Sec.22 T8N R1W
Landform: Head slope, backslope
Parent Material: Till Wisconsinan
Slope: 2
Erosion: B
Drainage: Well
Vegetation: Corn Stubble

Soil Series: Miami (Code: MI24)
County: Montgomery
Location: 2112' W & 600' S of the NE corner of Sec.35 T17 R6W
Landform: Till Plain, Swell
Parent Material: Till Wisconsinan
Slope: 9
Erosion: Moderate
Drainage: Well
Vegetation: Corn

Soil Series: Morley (Code: MO21)
County: Adams
Location: 1580' W & 1360' S of the NE ¼ Sec.15 T25N R14E
Landform: Till Plain Swell
Parent Material: Till Wisconsinan
Slope: C
Erosion: Moderate
Drainage: Moderately Well
Vegetation: Hay

Soil Series: Morley (Code: MO22)
County: Fulton
Location: 1760' E & 2060' N of the SW corner of Sec.22 T30N R5E
Landform: Till Plain, swell
Parent Material: Till Wisconsinan
Slope: 4
Erosion: Moderate
Drainage: Well
Vegetation: Corn Stubble

Soil Series: Morley (Code: MO23)
County: Whitley
Location: 2425' W & 2375' N of the SE corner of Sec.8 T3IN R9E
Landform: Convex Moraine
Parent Material: Till Wisconsinan
Slope: B
Erosion: Moderate
Drainage: Well
Vegetation:

Soil Series: Morley (Code: M031)
County: Randolph
Location: 1200' S & 2000' W of the NE corner of Sec.9 T21N R13E
Landform: Till Plain, swell
Parent Material: Till Wisconsinan
Slope: 10
Erosion: Severe
Drainage: Well
Vegetation: Hay

Soil Series: Brookston (Code: BR11)
County: Henry
Location: 90' N & 660' W of the SE corner of Sec.27 T18N R9E
Landform: Till Plain, Swale
Parent Material: Loess, Wisconsinan
Slope: 0
Erosion: None to Slight
Drainage: Very Poorly
Vegetation: Plowed

Soil Series: Brookston (Code: BR12)
County: Jasper
Location: 1000' W & 1300' N of the SE corner of Sec.11 T29N R7W
Landform: Convex Moraine
Parent Material: Till Wisconsinan
Slope: 1
Erosion: None to Slight
Drainage: Very Poorly
Vegetation: Soybean

Soil Series: Brookston (Code: BR13)
County: Fulton
Location: 120' E & 980' N of the SW corner of Sec.24 T31N R3E
Landform: Till Plain, Swale
Parent Material: Till Wisconsinan
Slope: 0
Erosion: None to Slight
Drainage: Very Poorly
Vegetation: Plowed

Soil Series: Frederick (Code: FR21)
County: Washington
Location: 2500' S & 2000' W of the NE corner of Sec.4 T1S R3E
Parent Material: Loess Wisconsinan (2) Limestone
Slope: 15
Erosion: Moderate
Drainage: Well
Vegetation: Pasture

Soil Series: Frederick (Code: FR22)
County: Jackson
Location: 590' W & 860' S of the NE corner of Sec.26 T5N R2E
Landform: Side Slope, Shoulder
Parent Material: Limestone
Slope: 8
Erosion: Moderate
Drainage: Well
Vegetation: Hay

Appendix C

Reflectance data at 485, 560, and 660 nm for the soil samples presented.

- Simulated erosion samples

Soil	R_{485}	R_{560}	R_{660}
RUNS	37.50	44.52	50.70
RUSL	36.12	43.93	50.53
RUMO	36.94	45.38	52.08
RUSE	37.18	46.18	53.17
RUVS	38.47	47.35	54.50
MINS	30.71	48.38	55.78
MISL	38.23	48.04	55.15
MIMO	38.39	48.42	56.27
MISE	38.73	49.17	56.82
MIVS	39.86	50.44	58.96
MONS	38.64	45.76	51.65
MOSL	40.37	47.75	53.73
MOMO	40.00	47.74	53.71
MOSE	40.72	49.28	55.55
MOVS	41.28	50.12	56.02

- National Soil Erosion Laboratory samples (Morley soil)

Soil #	R_{485}	R_{560}	R_{660}
1	44.78	53.43	59.38
2	39.93	47.32	53.04
3	41.29	48.71	53.77
4	40.28	49.66	53.03
5	41.22	51.62	57.73
6	41.27	50.68	56.33
7	41.08	51.35	57.33
8	37.66	47.90	53.55
9	37.09	46.86	52.13
10	36.98	46.94	52.58

- Soil Characterization Laboratory samples

Soil	Erosion Class	R_{485}	R_{560}	R_{660}
RU11	NS	41.91	49.99	56.67
RU12	NS	41.16	48.85	54.66
RU13	NS	40.91	47.49	53.75
RU21	MO	37.21	47.82	56.38
RU22	MO	41.07	49.57	56.46
MI11	NS	38.93	45.11	51.12
MI21	MO	39.41	47.07	53.67
MI22	MO	39.25	48.16	55.11
MI23	MO	36.85	47.08	53.57
MI24	MO	35.93	47.10	54.89
MO21	MO	40.29	48.14	54.19
MO22	MO	40.88	48.83	54.10
MO23	MO	39.46	48.55	54.36
MO31	SE	33.58	42.84	49.20

Soil Key - RU = Russell MI = Miami MO = Morley

Erosion Key - NS = none-to-slight; SL = slight; MO = moderate;
SE = severe; VS = very severe